ALMA MATER STUDIORUM
UNIVERSITÀ DI BOLOGNA

ALMA MATER STUDIORUM UNIVERSTY OF BOLOGNA

D.I.C.A.M
Department of Civil, Chemical, Environmental and Materials Engineering.

MASTER IN INDUSTRIAL ENGINEERING

EXPERIMENTAL TEST ON THE LONG TERM BEHAVIOUR OF CRACKED FRC ELEMENTS

PRUEBAS EXPERIMENTALES SOBRE EL COMPORAMIENTO A LARGO PLAZO DE ELEMENTOS DE HORMIGON FIBRO-REFORZADO EN ELEMENTOS AGRIETADOS

Miss MORÍS HERNANDEZ, Carmen
TUTOR: Mr. BURATTI, Nicola
TUTORA: Mrs. LAMELA REY, María Jesús

DATA: 19 of July 2018

0. Resumen

1. Introducción

El hormigón es un material frágil, su resistencia a tracción es baja en relación con la resistencia a compresión. Hoy en día las políticas que se siguen en materia de infraestructuras tienen un componente importante en la conservación, mantenimiento y refuerzo de las mismas. El agrietamiento del hormigón es un fenómeno indeseable cuya causa va desde variaciones de la composición del material hasta los efectos de los cambios térmicos. Para poder compensar su fragilidad se utilizan refuerzos. Durante el siglo pasado, el refuerzo consistió típicamente en barras de acero, colocadas en el encofrado antes del vaciado del hormigón. Debido a los avances en la tecnología de materiales, ha sido posible reemplazarlas o añadirles nuevos materiales, este es el caso del hormigón reforzado con fibras.

El hormigón fibro-reforzado (FRC) es hormigón que contiene material fibroso, lo que aumenta su integridad estructural. La fibra es una pequeña pieza de material de refuerzo que posee ciertas propiedades características. La fibra, a menudo, se describe mediante un parámetro llamado "relación de aspecto". La relación de aspecto de la fibra es la relación entre su longitud y su diámetro, esta varía de 30 a 150. Las fibras se clasifican en:

- Fibras de acero.
- Fibras de vidrio.
- Fibras sintéticas.
- Fibras naturales.

La necesidad del hormigón fibro-refozado se debe a que:

- Incrementa la resistencia a la tracción del hormigón.
- Reduce el aire y agua.
- Incrementa la durabilidad del hormigón.
- Las fibras como el grafito y el vidrio tienen una excelente resistencia a la fluencia.

2. Objetivos

Los materiales nuevos requieren investigación, el objetivo de esta tesis es caracterizar los métodos para evaluar el efecto del hormigón fibro-reforzado en fluencia. Dado que hoy en día, no existe ningún modelo o regulación que informe sobre cuál es el efecto del FRC en la fluencia. Para caracterizar estos métodos, se realizarán las siguientes pruebas:

- Prueba de fluencia a compresión en especímenes cilíndricos.
- Prueba de fluencia a flexión en especímenes prismáticos con entalla.
- Prueba de fluencia a tracción en especímenes con el núcleo entallado.
- Prueba de fluencia a tracción en fibras.

Estas pruebas a diferentes escalas facilitan una mejor comprensión de los fenómenos mecánicos que controlan el comportamiento de fluencia de la sección transversal agrietada del hormigón fibro-reforzado. Además, se investigará el efecto de las variaciones moderadas de temperatura, al aumentar la temperatura ambiental durante la prueba a largo plazo.

3. Materiales

Para esta investigación se ha usado un solo tipo de hormigón, cuya mezcla se compone de:

- Arena natural, S 0-5
- Arena natural, S 0-1
- Grava, P 5-15
- Cemento Portland
- Superfluidificante *Glenim Sky 542*
- Fibras poliméricas *BASF 254*

Con él se han rellenado los siguientes moldes para obtener 6 cubos, 13 prismas y 6 cilindros.

Figura 1-Moldes de hormigón

Durante la primera semana se introducen en un tanque con agua a 20ºC, trascurrida esta semana se realizan las entallas de los especímenes y se vuelven a introducir en agua hasta completar los 28 días.

Prueba de compresión

Para la realización de esta prueba se utilizan los cubos, se seleccionaran dos cubos de cada mezcla de hormigón.

Figura 2- Especímenes antes y después de la prueba de compresión

	Resistencia a compresión [MPa]
G3_254_8_C4	57.31
G3_254_8_C5	52.47
G3_254_8_C1	55.64
G3_254_8_C2	53.39

Tabla 1-Resultados de las pruebas de compresión

Módulo elástico

Para la realización del módulo elástico se utilizan los especímenes cilíndricos. Estos tienen un diámetro de 100 mm, para llevar acabo la prueba es necesario regularizar las superficies, por lo que su altura final es de 150 mm.

Figura 3-Especímen cilíndrico siendo regularizado

Los resultados del ensayo para la obtención del módulo elástico se muestran en el figura 4.

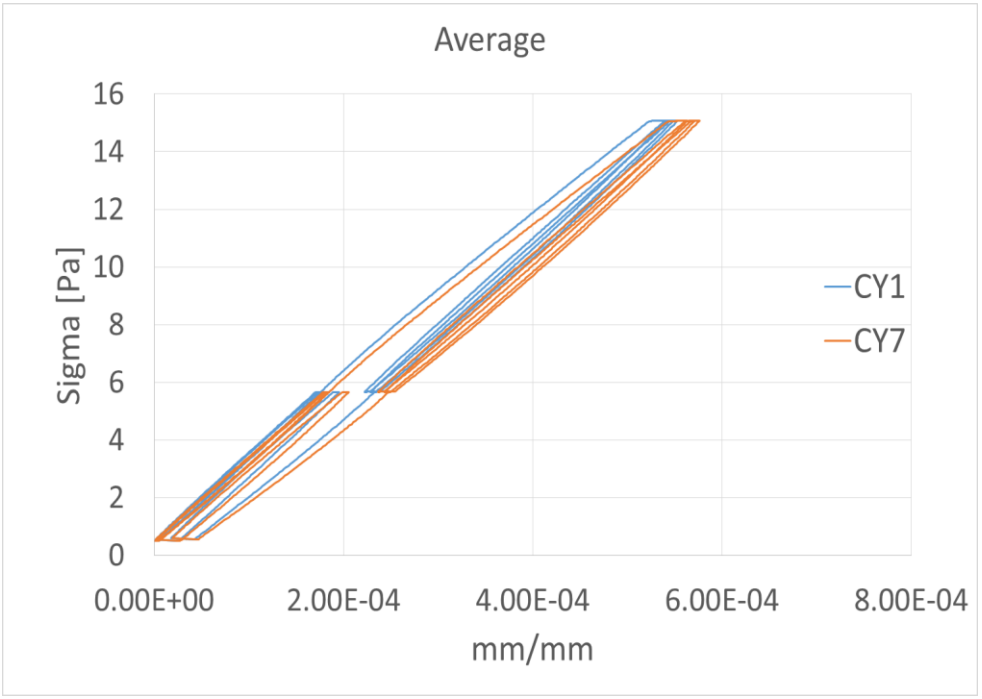

Figura 4-Módulo elástico de cilindros CY1 y CY7

El ciclo de carga que se ha utilizado se muestra en la figura 5 con el valor medio del módulo elástico.

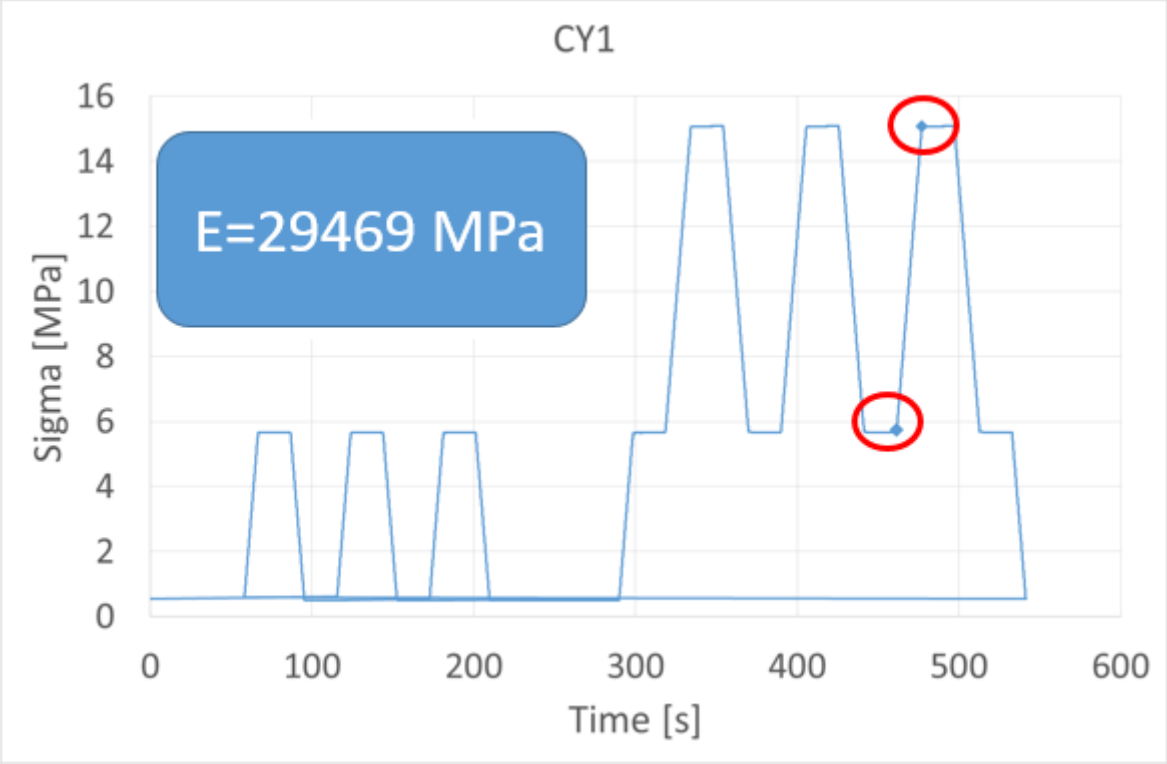

Figura 5-Ciclo de carga para la obtención del módulo elástico.

Especímenes prismáticos

Son utilizados como especímenes prismáticos entallados figura 6 izquierda o para la creación de cilindros como se puede ver en la figura 6 derecha.

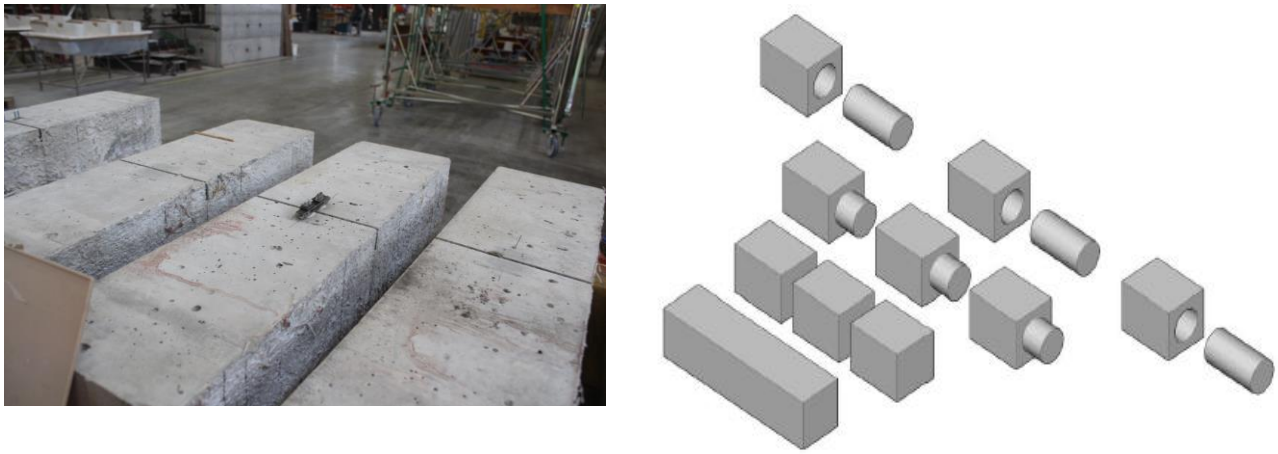

Figura 6-Especímenes prismáticos

4. Prueba de fluencia a compresión en especímenes cilíndricos

En la prueba de compresión se mide la deformación que viene de dos fenómenos, la viscosidad y el proceso de retracción plástica del hormigón. Para la prueba de fluencia se utilizaran dos galgas extensiométricas separadas entre sí 180º y se dispondrán dos cilindros en la forma que muestra la figura 8.

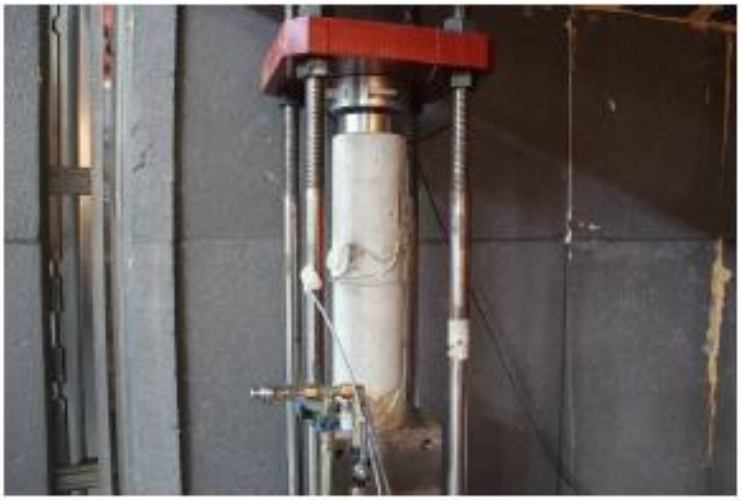

Figura 7-Prueba de fluencia a compresión en especímenes cilíndricos

Para la realización de esta prueba es necesario examinar cilindros aislados para poder evaluar el proceso de retracción plástica del hormigón. Este fenómeno produce daños volumétricos en el hormigón debido a los cambios del agua. Es independiente de la carga y está influenciado por la geometría de la muestra y las condiciones ambientales del entorno en el que se encuentra. Para ello, y para las demás pruebas, se introducen los especímenes en una sala donde se puede controlar la temperatura y la humedad relativa figura 7.

Durante los primeros 50 días la temperatura será 20ºC con una humedad relativa del 55%. Después se incrementara a 30º, durante los próximos seis meses se seguirá incrementado esta temperatura pero los datos ya no están recogidos en esta tesis.

Figura 8-Sala de control de condiciones ambientales

5. Prueba de fluencia a flexión en especímenes prismáticos con entalla.

Para esta prueba se necesitan dos procedimientos, el primero es un pre-agrietamiento de la zona entallada mediante una prueba de flexión a tres puntos, mostrada en la figura 8.

Figura 9-Prueba de flexión a tres puntos

En esta prueba se mide la apertura de la entalla hasta llegar a 0.5 mm para simular las condiciones de uso. Se ensayan 8 especímenes de los cuales es necesario seleccionar tres para la prueba a largo plazo. Se seleccionaran los que mayor tensión tengan. En la figura 10 se puede ver el cuadro de carga que se utiliza para la prueba a largo plazo.

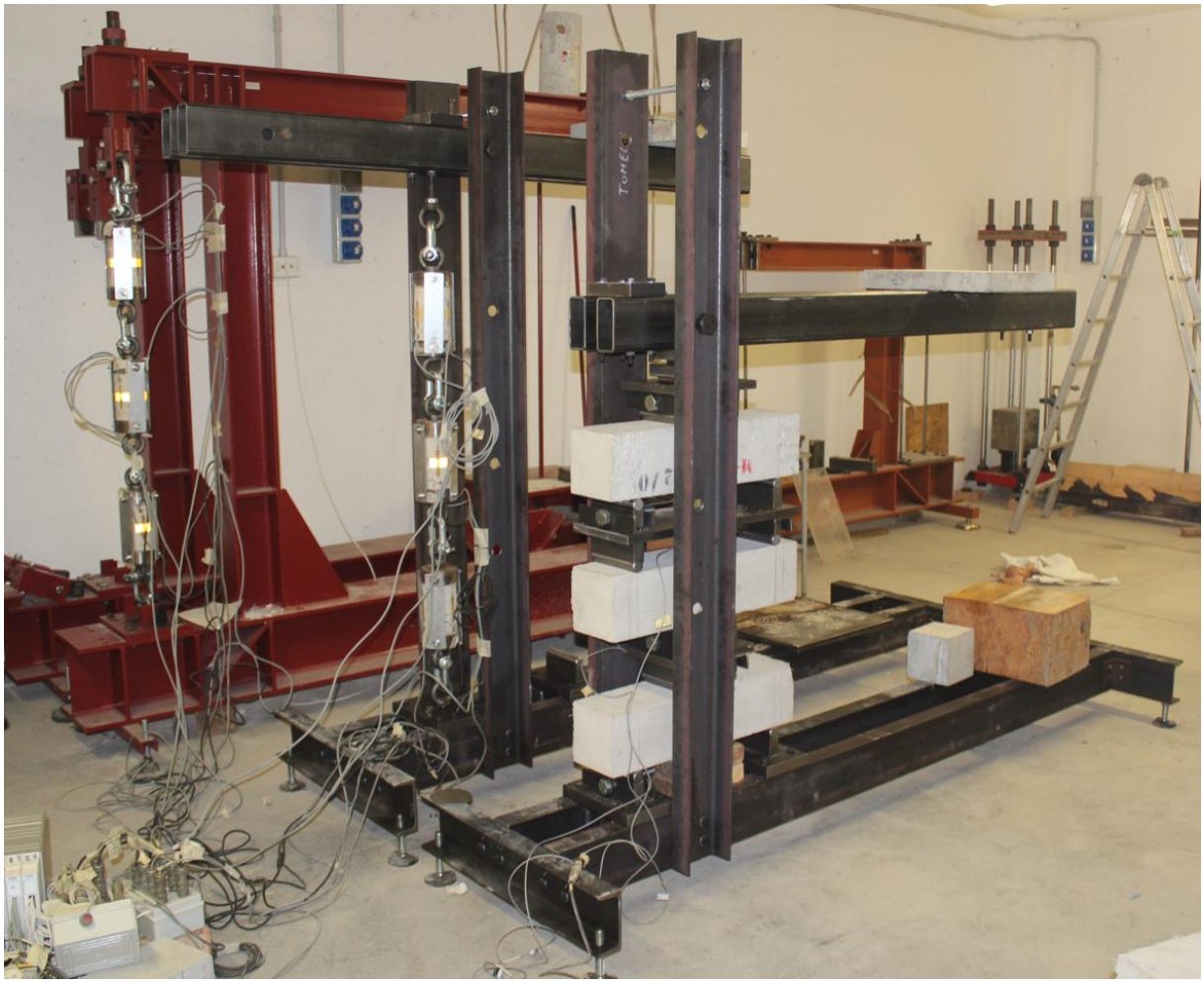

Figura 10-Prueba a largo plazo para los especímenes prismáticos

De esta prueba se realizan tres gráficos diversos.

CMOD-tiempo

Donde se ve el crecimiento de la apertura de entalla, CMOD (Crack Mouth Opening Displacement), crecer a lo largo del tiempo.

Coeficiente de viscosidad-tiempo

El coeficiente de viscosidad se calcula de la siguiente manera;

$$\varphi = \frac{CMODt - CMOD_0}{CMOD_0}$$

Donde;

- CMODt es la apertura de la entalla en tiempo t.
- $CMOD_0$ es la apertura de la entalla en el tiempo inicial.

Tasa de aumento de viscosidad-tiempo

La tasa de aumento de la viscosidad se calcula como la pendiente entre dos puntos, se calculará cada 6 horas para el primer día, cada 12 horas para los primeros 7 días y, una vez pasado este tiempo, para cada semana.

6. Prueba de fluencia a tracción en especímenes con el núcleo entallado.

Al igual que anteriormente se llevarán a cabo dos fases, una de apertura de la fisura y una a largo tiempo. Para la apertura de la fisura se realiza una prueba de tracción, donde se medirá la apertura de la entalla, el control se realiza en dos fases la primera mide el COD máximo hasta alcanzar 0.05 mm y luego mide la media de los tres transductores hasta 0.2 mm.

Figura 11-Prueba de tracción

Se ensayaron 12 cilindros, de los cuales 6 tuvieron una apertura de la entalla uniforme. De esos 6, han de seleccionarse 3 para la prueba a largo plazo, el criterio a seguir es aquellos que tengan un comportamiento a tracción más puro.

Figura 12-Prueba a largo plazo para especímenes cilíndricos entallados.

Para estos ensayos se realizan los mismos gráficos que para los especímenes prismáticos.

7. Prueba de fluencia a tracción en fibras.

La prueba de fluencia en fibras se divide en dos, a corto y a largo plazo. Para la prueba a corto plazo los extremos de las fibras se sujetan mecánicamente en las placas de aluminio y se cargan al 30%. Como se puede ver en la figura 13.

Figura 13-Prueba a corto plazo para fibras.

Para la prueba a largo plazo se utiliza el cuadro de la figura 14, la fibra se carga al 20% y se mide el alargamiento de la fibra mediante dos LVDT.

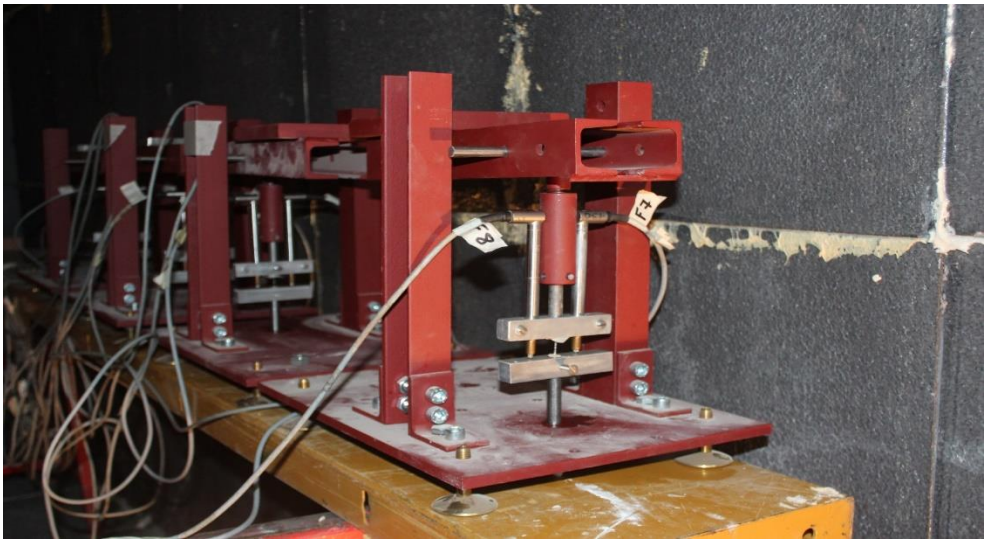

Figura 14-Prueba a largo plazo para fibras.

Al igual que los dos últimos ensayos a largo plazo, las gráficas serán las mismas.

8. Conclusiones

- La fluencia puede ser visible tanto en todo el material, como en las fibras individuales como polímeros.
- Al analizar el coeficiente de fluencia es posible decir que aumenta con el tiempo y tiene un aumento significativo cuando la temperatura es más alta.
- Los protocolos de las pruebas y la relación entre los principales parámetros de deformación deben desarrollarse para permitir una comparación más fácil de los resultados y facilitar la discusión entre los investigadores.
- Los parámetros tales como la apertura de grietas al comienzo de la prueba a largo plazo, la temperatura y la humedad relativa aún no se ha definido del todo.
- Los fenómenos químicos, físicos y mecánicos que regulan la fluencia de los FRC en condiciones agrietadas aún no se han entendido completamente.
- Es probable que se requieran procedimientos de análisis inversos para la interpretación de las pruebas de flexión a largo plazo.
- Los modelos de predicción para la fluencia FRC en condiciones agrietadas y, en particular, para la fluencia de tracción aún no están disponibles, pero son necesarios sí estos fenómenos deben incluirse en el diseño.
- Para incluir la caracterización del FRC en la norma, se debe realizar un mayor número de pruebas.

Index

1. Introduction

1.1 THE PROBLEM

Concrete is a brittle material; is tensile strength is low in relation to the compressive strength. To compensate this lack, reinforcement is normally used in load carrying structures. During the past century, reinforcement has typically consisted of steel bars, placed in the formwork prior to the casting of the concrete. Advances in material technology has made it possible to replace or to add to the conventional steel bars.

Nowadays the policies that are followed in matter of infrastructures have an important component in the conservation, maintenance and reinforcement of the same. Cracking of concrete is an undesirable phenomenon whose cause range from variations of the composition of the material to the effects of thermal changes. To reduce the cracking of the concrete, fibres can be used.

Fibre reinforced concrete (FRC) is concrete containing fibrous material, which increases its structural integrity. Fibre is a small piece of reinforcing material possessing certain characteristics properties. They can be circular or flat. The fibre is often described by a convenient parameter called “aspect ratio”. The aspect ratio of the fibre is the ratio of its length to its diameter. Typical aspect ratio ranges from 30 to 150. It contains short discrete fibres that are uniformly distributed and randomly oriented. Fibres include steel fibres, glass fibres, synthetic fibres and natural fibres. Within these different fibres that character of fibre reinforced concrete changes with varying concretes, fibre materials, geometries, distribution, orientation and densities. (Parveen, 2013)

The necessity of the Fibre Reinforced Concrete is due to:

- Increases the tensile strength of the concrete.
- Reduces the air and water void in the inherent porosity of gel.
- Increase the durability of the concreate.
- Fibres such as graphite and glass have excellent resistance to creep, while the same is not true for most resins.

1.2 GOALS

New materials require a researcher and characterization, the goal of this thesis is to characterize the methods to quantify fibro reinforced concrete in creep. Given that nowadays, there is no model or any regulation to report on what is the effect of the FRC in creep.

In order to characterize the methods, the following test will be carried out.

- Compression creep test on cylindrical specimens
- Bending creep test on cracked notched beams
- Uniaxial tensile creep tests on cracked cores
- Pull–out test and tensile tests single fibres

These tests at different scales aim at better understanding the mechanical phenomena controlling the creep behaviour of cracked FRC cross section. Furthermore, the effect of moderate temperature variations will be investigated, by increasing the environmental temperature during the long-term test.

1.3 STRUCTURE

Once exposed in this chapter 1, Introduction, the problem and the goals that are pursued, the structure that follows this work is briefly described below:

- In the chapter 2, *Background,* FRC and fibres are described in a general way in term of these characteristics. After this, the theoretical information necessary to understand the subsequent tests and analyzes carried out is included. At the end, the main applications are shown.
- In the chapter 3, *Materials used and their preparation,* will be described all the stages of preparation of the specimens. The casting steps of the fibre-reinforced concrete used in the present study will be described. Finally, all the work performed on the specimens that are necessary before the execution of each single test, will be described.
- In the chapter 4, *Used measuring instruments and machines*, will be dedicated to the description of the characteristics and the operation of the servohydraulic machine used for the test campaign object of the present elaborate and present in the *CIRI laboratory (Centro Interdipartimentale per l'Ricerca Industriale - Edilizia e Costruzioni)*.

As well as all the measuring elements and other instruments used in the realization of the thesis, are described.

- In the chapters 5, 6, 7 and 8 *Compression creep test on cylindrical specimens*, *Bending creep test on cracked notched beams, uniaxial tensile creep test on cracked cores, pull-out test on single fibres,* The development of the tests are described as well as the results obtained.
- In the chapter 9, *Conclusions,* main conclusions that derive from the work carried out are presented.

2. Background

2.1 GENERAL CHARACTERISTICS

Fibre Reinforced concrete, indicated by the abbreviation FRC, is a composite material obtained from the addition of discrete fibres in the cement conglomerate. Due to this addition, the cement-based matrix (concrete or mortar) is reinforced and the mechanical properties of the material are improved. The ordinary concrete is characterized by being brittle material.

The fibres in the concrete could be different in material and geometry, the most known are fibres of steel, polymer, organic material, such as carbon or glass and of natural origin.

To obtain a concrete with guaranteed performance is important a designation of a good mix. The composite mixture must be appropriated designed, combining the different components in order to obtain good properties with the performance that is required. Moreover, the properties of the composite are related to the characteristics and dosages of the constituent materials, to the characteristics of the matrix, to the geometric and the mechanical characteristic of the fibres, to their volumetric percentage used and to the adhesion that is developed between matrix and fibres.

One of the greatest benefits of using fibre is the improvement of the behaviour in the serviceability limit state, understood as the capacity of a structure, or part of it, maintain its resistance and integrity to crack propagation.

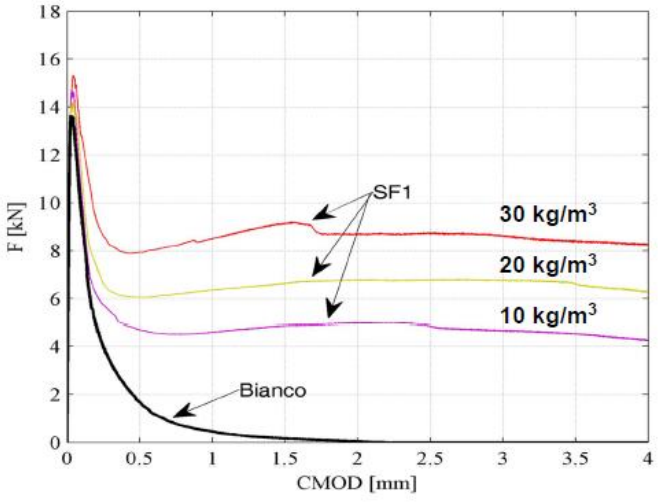

Figure 2.1-Tension-CMOD curve

The addition of fibres allows the composite material to have one significant post-cracking residual tensile strength, defined as toughness, due to the ability of the fibres to connect the surfaces of the cracks once cracking has occurred. Therefore, the matrix without fibres regulates the behaviour before cracking and the fibres regulates and modify the post-cracking behaviour of the system. Furthermore, given that the fibres can be considered as a reinforcement dispersed in the conglomerate, the concrete fibre-reinforced can be properly used to ensure better distribution of cracks and limit the opening width of these.

The use of fibres can also improve other properties:

- Resistence to impact
- Fatigue
- Fire resistance

In addition, in some cases, the tensile and flexural strength.

The presence of fibres substantially changes the behaviour of the concreate from brittle to ductile for this reason is suitable for hyperstatic structures, as the residual traction effort can increase the overall load-bearing capacity of the structure and improve its ductility. From this point of view, the addition of short fibres in high concretes resistance, particularly fragile in the absence of fibres, increases the toughness and the ductility.

There are many areas of employment in the building industry that take advantage from the using of fibre-reinforced concrete. The field of applications of FRCs can concern:

- Facing panels
- Paving plates
- Prefabricated floors and final coatings of tunnels and mines
- Beams
- Joints or structural nodes, for the advantage offered to reduce the usual high percentages of armor present there
- Roofing elements, for the possibility of creating small thicknesses without of the usual armor placed in the middle floor;
- Structures designed to absorb shocks and / or to resist fatigue, such as collectors or pipes for high pressures, railway sleepers, poles of high resistance…

2.2 THE FIBRES

In recent years, the use of fibre reinforced concrete (FRC) has increased. By dispersing discontinuous fibres of variable size and material, into the fresh concrete, ductile structural members can be produced in a labor efficient manner (Fall, 2014). The concept of using discrete fibres to improve the performance of brittle materials has existed since ancient times, with evidence showing that the ancient Egyptians used straw to improve the cracking behaviour of sun-dried mud bricks used in construction (Mansour, Srebic, & and Burley, 2007).

Fibres can be classified according to their size. Löfgren describes an approach whereby the fibres are classified as macro-fibres when they are longer than the maximum aggregate size of the concrete, when their diameter is much greater than the cement grain size, and when the aspect ratio (length to diameter ratio) is less than 100. Fibres with a cross-section diameter of the same order as the cement grains and a length less than the maximum aggregate size are classified as micro-fibres. Basically, macro-fibres increase the composite toughness by bridging macro-cracks, whereas micro-fibres increase resistance to micro-cracking prior to the formation of macro-cracks. (Löfgren, 2005)

Nowadays, there are many types of reinforcing fibres, with different characteristics. The fibres are characterized by the following parameters:

- Length of the fibre (lf), or the distance between the ends of the fibre, and the length in development of the fibre (ld), that is the length of the fibre axis line.
- The equivalent diameter (df), the diameter of a circle with a area equal to the average area of the fibre cross-secction.
- The aspect ratio, defined as a quotient between the length, lf, and the equivalent diameter, df, of the fibre;
- The shape, that is the geometry of the axis line and any variation of their cross-section; fibres can be divided into fibres smooth, hooked, wavy, ribbed, etc.

With the same composition and dosage, the fibres are more effective if the aspect ratio and if the shape assumes an irregular contour that favors adhesion to the cement matrix.

2.2.1 Steel fibres

Steel fibres have proven to provide significant post-crack ductility to the otherwise brittle concrete. Steel fibres can be used as primary reinforcement, in some applications, and evidence good resistance to corrosion. (Bentur & Mindess, 2007) review several investigations of the durability of steel fibre reinforcement (SFRC). The results of these studies generally show that SFRC does not suffer any degradation due to corrosion. This improvement of the corrosion resistance, compared with conventional steel reinforcement bars, is likely because of the reduced crack width and the lack of electrical conductivity (short and discontinuous fibres). Furthermore, the spalling of concrete, caused by rust, is avoided as the small diameter of the fibres generates only a minor amount of corrosion product.

Following the CNR-DT 204/2006 the steel fibres have a length between 6 and 70 mm and the equivalent diameter, df, between 0.15 and 1.2 mm. These can be classified according to the production process, to the shape and to the type of the material.

Figure 2.2-Steel fibres

Production process:

- From drawn wire (Type A)
- From cut sheet metal (Type B)
- From other manufactures (Type C)

Material:

- Low carbon steel (C ≤ 0.20, type 1)
- High carbon steel (C>0.2, type 2)
- Stainless steel

Shape:

- Rectilinear
- Shaped (hooked,wavy,etc)

2.2.2 Glass fibres

Glass fibres are most commonly used in thin, non-structural, concrete elements, e.g. facade elements. The tensile strength of glass fibres is very high; however, it may be heavily influenced by deterioration. According to Bentur and Mindess (2007), the strength of a fully aged glass fibre reinforced concrete, if exposed to an outdoor environment, is reduced to 40% of the initial strength, whereas the strain capacity is reduced to about 20% of the initial capacity. The two main mechanisms responsible for this deterioration are chemical attack and the formation of hydration products (mainly calcium hydroxide) between the filaments; these mechanisms lead to a reduction in strength and embrittlement, respectively. (Fall, 2014).

Figure 2.3-Glass fibres

2.2.3 Natural fibres

Natural fibres are interesting mainly due to their low cost. Cellulose fibres from bamboo or sugar cane can be used as well as other such as jute, sisal or coconut fires (coir). As the organic fibres in their natural form, contrary to many synthetic fibres, are hygroscopic, the fibre properties are more widely affected by changes in moisture content than fibres of any other material, which may cause swelling, shrinkage or rot. Depending on the fibre material, the exposure to alkali environments causes varying amounts of strength degradation, ranging from 16% of the initial tensile strength (sisal) up to 50% (coir) (Ramakrishna & Sundararajan, 2005).

Figure 2.4-Natural fibres

2.2.4 Synthetic fibres

According to CNR-DT 204/2006, polymeric fibres of acrylic, aramide, nylon, polyester, polyethylene and polypropylene, and carbon fibres are commercially available. The fibres can be distinguished in microfibres, with lengths contained in the order of millimeters, and macrofibres with lengths up to 80 mm. Typical values of the aspect ratio are between 100 and 500. The main characteristic of commercially available polymeric and carbon fibres are shown in the figure 2.5.

Tipo di fibra	Diametro equivalente [10^{-3} mm]	Densità [g/mm^3]	Resistenza a trazione [MPa]	Modulo di elasticità normale [MPa]	Deformazione ultima [%]	Temperatura di ignizione (accensione) [°C]	Temperatura di fusione,ossidazione /decomposizione [°C]	Assorbimento d'acqua * [% in peso]
Acrilica	12.7-104.14	1.16-1.18	269-1000	13790-19306	7.5-50	-	221-235	1.0-2.5
Arammide I	11.94	1.44	2930	62055	4.4	Alta	482	4.3
Arammide II	10.16	1.44	2344	117215	2.5	Alta	482	1.2
Carbonio, PAN HM	7.62	1.6-1.7	2482-3034	379914	0.6-0.7	Alta	400	Nil
Carbonio, PAN HT	8.89	1.6-1.7	3447-3999	230293	1.0-1.5	Alta	400	Nil
Carbonio, pitch GP	9.91-12.95	1.6-1.7	483-793	27580-34475	2.0-2.4	Alta	400	3-7
Carbonio, pitch HP	8.89-17.78	1.80-2.15	1517-3103	151690-482650	0.5-1.1	Alta	500	Nil
Nylon	22.86	1.14	965	5171	20	-	200-221	2.8-5.0
Poliestere	19.81	1.34-1.39	227-1103	17237	12-150	593	257	0.4
Polietilene	25.4-1016	0.92-0.96	76-586	4999	3-80	-	134	Nil
Polipropilene	-	0.90-0.91	138-689	3447-4826	15	593	165	Nil
Polivinilalcol	14-600	1.30	880-1600	25000-40000	6-10			4.0

* in accordo con lo standard ASRM D570.

Figure 2.5-Properties of synthetic fibres

For such applications, fibres with a relatively low modulus, such as polypropylene and polyethylene, are used and the fibre volume content would typically be only about 0.1% by volume. Fibres added for controlling plastic cracking are normally designated micro-fibres, with a diameter of around 40 to 100 μm. Smaller diameters yield better performance (Naaman, Wongtanakitcharoen, & Hauser, 2005).

2.3 MECANICHAL CHARACTERISTIC OF FIBRE-REINFORCED CONCRETES

The knowledge of the physical nature of the fracture process of cement composites plays a central role in the design of structures and in the development of new high-performance materials. The verification of the mechanical characteristics can only be performed thanks to appropriate tests on samples extracted from the already prepared material; some of these tests are similar to those used for simple concrete, others have been designed specifically for fibre-reinforced concrete. The most significant difference between normal concrete and fibre-reinforced concrete is the ability to absorb energy.

2.3.1 Tensile behaviour of FRCs in post-cracking phase

The addition of fibres improves the tensile behaviour of the plain concrete of the cementitious matrix by contrasting the progressive opening of the cracks. Once the matrix cracked, the fibres are able to show their own contribution, giving the composite a post-cracking resistance absent in the concrete without fibres, characterized by a brittle failure. The strongly degrading behaviour, typical of a monoaxial traction test on the concrete, can be significantly modified by the addition of fibres, as the growth of the volumetric percentage, Vf, of them. For small volumetric percentages of fibres (about 0.2-2%) the tensile load-displacement bond of a FRC still has a descending branch (degrading behaviour), but is characterized from a residual strength and a higher toughness. For volumetric percentages of higher fibres (about 2-8%), the behaviour can become hardening, thanks to the appearance of a multi-crack. (Istruzioni per la Progettazione, l'Esecuzione ed il Controllo di Strutture di Calcestruzzo Fibrorinforzato, 2008)

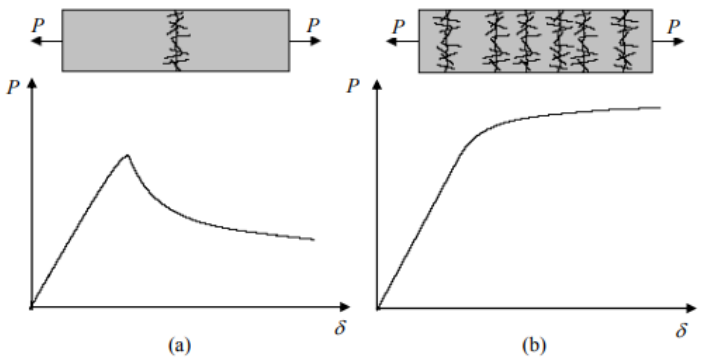

Figure 2.6-Load curve P vs displacement δ for FRC a) low percentage of fibres b) high percentage

However, uniaxial tensile tests are generally difficult to perform. For this reason, the standardized methods are based on bending test on notched prismatic samples. Because flexural behaviour is markedly different from uniaxial traction behaviour, it may occur that composites with degrading behaviour in traction exhibit a work-hardening behaviour at bending. In fact, in the flexural tests, the linearity of the deformation profile on the non-cracked section makes possible a more stable propagation of the cracks and there is a significant flexural hardening, even if the material showed a degrading post-cracking behaviour at pure traction. (di Prisco, Plizzari, & Vandewalle, 2009)

2.3.2 Tensile strength: design indications

The fibres improve the tensile behaviour of the cracked matrix, as shown the figure 2.7. For non-high fibre contents, with volumetric percentage indicatively less than 2%, the behaviour is degrading. In case of high fibre contents, the resistance may be higher than the matrix due to the effect of a hardening behaviour.

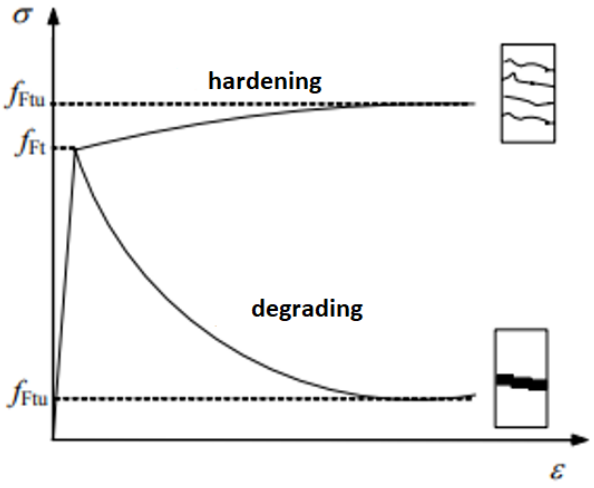

Figure 2.7-Traction behaviour

In both cases, degrading or hardening behaviour, the ultimate residual uniaxial tensile strength of the material is significantly influenced by the volumetric fraction of fibres, Vf, from the aspect ratio, lf/df, and adherence between matrix and fibre. This circumstance can be easily deduced from the equilibrium in the normal direction to the fracture surface, assuming the fibres parallel to that direction and evaluating the specific extraction force Q.

$$Q = n_f * \pi * d_f * l_b * \tau_m = \omega * \frac{V_f}{A_f} * \pi * d_f * l_b * \tau_m = \omega * V_f * \frac{l_f}{d_f} * \tau_m$$

Where

- n_f is the number of fibres present on the area unit of the breaking surface.
- d_f is the equivalent diameter of the fibre
- $l_b = l_f/4$ is the conventional anchorage length of each fibre
- τ_m is the average tangential stress of adhesion
- ω is a coefficient that takes into account the actual orientation of the fibre
- V_f is the volumetric fraction of the fibres
- A_f is the area of the straight section of the single fibre

This equation gives an approximate value not taking into account other factors, such as the shape of the fibre, the fibre-matrix interface, the direction of the jet, the mixing and compacting modes of the fresh concrete that influence the dispersion of the fibres in the matrix and their orientation

Therefore, a performance approach is suggested that identifies experimentally the traction constitutive curve through appropriate test on samples of fibre reinforced concrete. The tension can be determined by uniaxial or flexural tensile test. The uniaxial traction test directly provides the σ-w can be performed according to UNI U73041440. In case of material with degrading behaviour, this test is not easy to perform. Alternatively, the bending test performed according to UNI 11039 can be used.

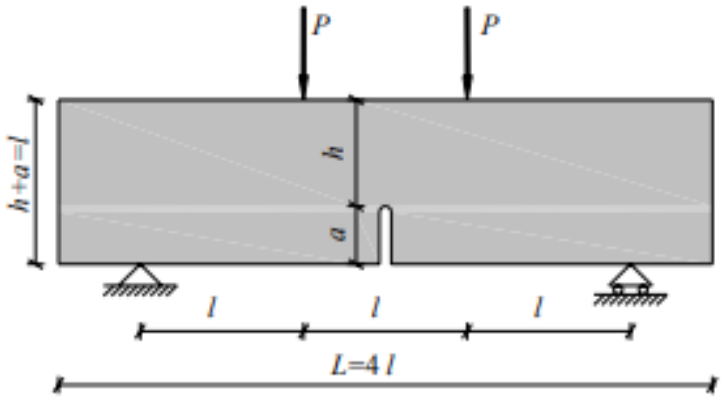

Figure 2.8- Bending test on four load points UNI 11039

The post-crack resistance can be defined based on punctual values, fi, corresponding to assigned nominal opening values of the crack, or average, feqi, calculated values on an assigned slot opening interval. In the case of carved specimen, the opening of the slot can be assumed conventionally equal to the displacement between two points places at the top of the notch, CTOD (Crack Tip Opening Displacement).

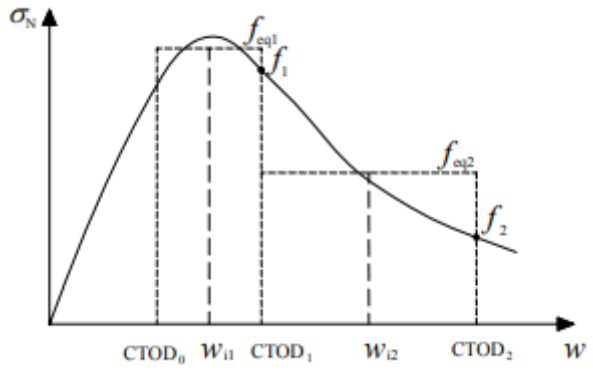

Figure 2.9-Definition of punctual and average residual resistance

On the basis of the data deduced from the bending test, two different simplification of the constitutive behavior can be defined:rigid plastic or linear post-cracking behavior, hardening or degrading.

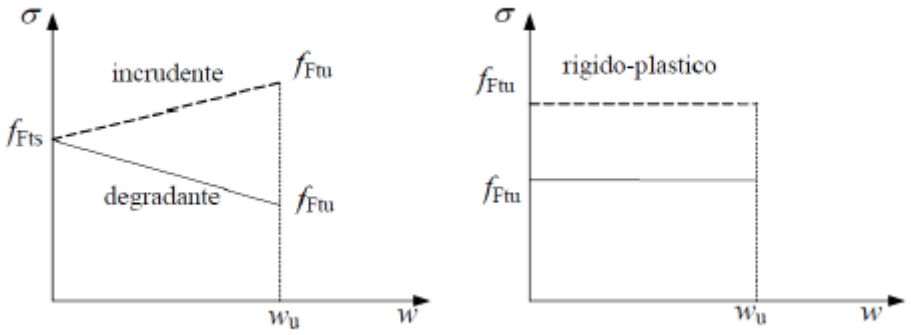

Figure 2.10-Simplified constitutive ties for tension-opening of the slit

For the purposes of defining the constitutive bond, for materials with degrading behaviour the ultimate value of the crack opening, wu, can not exceed the maximum value of 3 mm, in the case of inflected elements, and of 1.5 mm in the case of tense elements.

For materials with work-hardening behaviour, therefore in the presence of multi-setting, it is not necessary to determine the opening of the slots, as it is possible to operate directly in terms of stresses and deformations as specified below. Alternatively, more complex models can be used in the literature.

2.3.3 Compressive behaviour of FRC

The compressive behaviour of FRCs, as well as that of ordinary concretes, is influenced by the presence of small discontinuities and micro-cracks which, under the action of compression, propagate until the concrete breaks. This propagation process should be stopped by the fibres, thanks to their "sewing" function, leading to an increase in compressive strength. However, the growth of the cracks does not stop due to the lack of perfect adherence between the fibres and the matrix. The consequence is that the fibres can not influence the compressive behaviour of concrete and its compressive strength, regardless of the nature of the fibres. In compression, the ultimate strength is only slightly affected by the presence of fibres, with observed increases ranging from 0 to 15 percent for up to 1.5 percent by volume of fibres. (544.1R, 1996). From a designation point of view, the compression resistance can be assimilated to unreinforced material.

2.3.4 Modulus of elasticity and Poisson's ratio

In practice, when the volume percentage of fibres is less than 2 percent, the modulus of elasticity and Poisson's ratio of SFRC are generally taken as equal to those of a similar non-fibrous concrete or mortar.

2.3.5 Fatigue strength and endurance limit

One of the important attributes of FRC is the enhancement of fatigue strength compared to plain concrete. Failure strength is defined as the maximum flexural fatigue stress at which the beam can withstand two million cycles of non-reversed fatigue loading. In many applications, particularly in pavements and bridge deck overlays, full depth pavements and industrial floors, and offshore structures, flexural fatigue strength and endurance limit are important design parameters mainly because these structures are subjected to fatigue load cycles. The endurance limit of concrete is defined as the flexural fatigue stress at which the beam could withstand two million cycles of non-reversed fatigue loading, expressed as a percentage of the modulus of rupture of plain concrete (544.1R, 1996). The addition of polypropylene fibres, even in small amounts, has increased the flexural fatigue strength. Using the same basic

mixture proportions, the flexural fatigue strength was determined for three fibre contents (0.1, 0.2, and 0.3 percent by volume) and it was shown that the endurance limit for two million cycles had increased by 15 to 18 percent. (Ramakrishnan, Gollapudi, & and Zellers, 1987).

2.4 RHEOLOGICAL PROPERTIES OF FRC

The study of rheology of concrete provides information on properties of fresh concrete such as deformation, behaviour of mix, and placement of mixed concrete. Rheology is a term that is mainly used for fluids whose flow properties are complicated in nature, other than fluids like liquids or gases. The term rheology may be defined as the study of the science of the flow and deformation of materials (The constructor , 2018). The characteristics of FRC in a fresh state can be described using rheological parameters that characterize flow, or deformation, under stress. These parameters enable workability, flow, pumping ability, placement, compaction, and finishing characteristics to be quantitatively monitored and used during the construction phase. (544, 2010)

2.4.1 Workability of concrete

Workability of concrete is the property of freshly mixed concrete which determines the ease and homogeneity with which it can be mixed, placed, consolidated and finished' as defined by ACI Standard 116R-90. (116R-90: Cement and Concrete Terminology, 2000).

The UNI EN 206-1 standard allows to classify the workability of concrete through different methods. Every modes are associated with consistency classes, among which: classes of lowering to the cone (slump test), Vebè classes, classes of compatibility and spreading classes. The most commonly performed test to determine consistency is the lowering test at the cone. It consists of filling concrete with a truncated-conical container (Abrams cone) which is subsequently lifted and then measures the lowering (slump) that the concrete undergoes; the lowering is greater the smaller the material consistency. This test is carried out in both concreate, ordinary and with fibres, however it is suitable for a quality control of the conglomerate coming from the same processing, rather than to compare concretes packed with different materials. In particular, the slump test can be used to determine the workability of concretes before adding the fibres, show a lowering of the cone than 100 mm.

Figure 2.11-Abrams cone

When the height of the cone is reduced, it is preferable to resort to the use of the Vebè, for a correct measure of the workability of a fibre reinforced concrete. The Vebè test is considered the most representative of the workability of fibre-reinforced concrete, as it simulates the compaction and the treatment that the fibrous material (and more generally the ordinary concrete) undergoes during the vibration in place. The test provides first that the mixture in the fresh state is compacted within a standard cone located in a cylinder rigidly connected to a vibrating table; the cone is lifted and, subsequently, a transparent disc is placed on the top of the concrete. At this point, the vibrating table starts working and the time taken by the concrete is measured to completely cover the transparent disk; this time is defined as Vebè time and is considered a measure of workability as it is linked to the energy required for concrete compaction. According to the UNI EN 206-1 it is possible to identify 5 Vebè consistency classes indicated by a letter "V" followed by a number from 0 to 4 according to the compaction time ($V0 \geq 31$ sec., $V1 = 30 \div 21$ sec. , $V2 = 20 \div 11$,sec., $V3 = 10 \div 6$ sec., $V4 = 5 \div 3$ sec.). The Vebè time is influenced by:

- The shape
- Volume of the inters
- The air content
- The presence of additives
- Surface friction of the fibres

The Vebè test makes it possible to identify that volume of fibres, for a certain type of fibres and for a given matrix, beyond which complete compaction can not be achieved using compaction techniques present on site.

Researchers found that the key factors affecting rheology were the fibre volume, aspect ratio, type, and geometry. Workability decreases proportionately with (l/d) 1/2 × Vf (Hughes & Fattuhi, 1976). The fresh-state properties worsen as the fibre reinforcement index increases, and that the rate of change is directly related to the fibre type. Varying steel fibre geometries were evaluated, including straight-round, hooked-end, and crimped, deformed continuously along the length, fibres (Mangat & Swamy, 1974). Generally, crimped fibres were shown to have slightly higher workability than the other geometries. Figure 2.13 and 2.14 show the effects of fibre reinforcement index on the slump and inverted cone time, respectively (Bayasi & Soroushian, 1992).

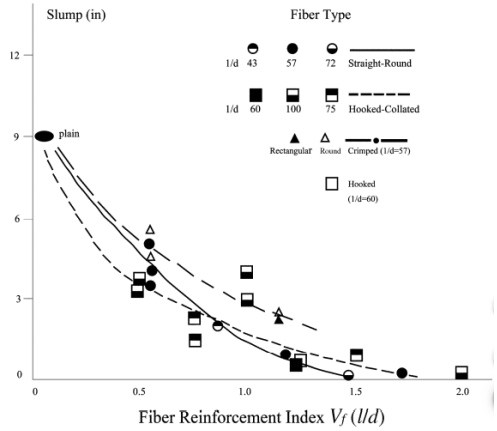

Figure 2.12-Effect of fibre reinforcement index and type on slump

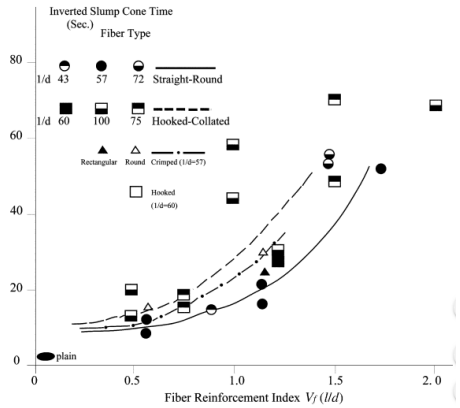

Figure 2.13-Effect of fibre reinforcement index and type on inverted slump cone time.

Another important factor, which affect the workability, is the size of the aggregates. In fact, the fibres are separated by granules, which have dimensions greater than the average spacing of the fibres and this entails a grouping and therefore a lack of uniformity in the dispersion of the fibres. The uniformity in the dispersion is all the more difficult to obtain as the maximum diameter of the aggregate increases. (Collepardi & Coppola, 1996)

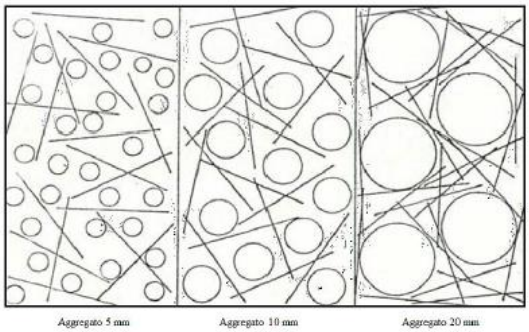

Figure 2.14-Effect of the diameter of the aggregate on the dispersion of fibres

Workability can be improved through appropriate interventions on the composition:

- Increasing the fraction e/o or reduction he maximum diameter of the aggregate.
- Using fly ash in order to obtain plastic or semi-fluid concretes (slump 50-150 mm) also using relative large fibres.
- Selection fluidifying additives in a manner to compensate the workability.

2.4.2 Stability and segregation of fibre-reinforced concretes

In general, the segregation index decreased when the carbon fibres content increased. This is because the increased volume of carbon fibres decreased the fluidity of concrete mixture. SCC is more prone to segregation due to higher fluidity. This segregation tendency is reduced in the presence of fibres. (EFNARC, 2002).

The tendency to segregate a concrete, ordinary or fibre-reinforced concrete, can be evaluated through a test that consists in letting a volume of concrete on a cone-shaped base fall from a fixed height in order to favor the separation of large aggregates from the rest of the mixture. This determines the degree of stability (which is the opposite of segregation), which is expressed by the ratio between the weight of the aggregates that remain in the mixture after and before the execution of the test. In general, the addition of polymeric fibres allows for greater stability of the concrete.

2.4.3 Plastic shrinkage

The width of the shrinkage slots in the plastic phase is reduced by the presence of the fibres. The fibres that best meet this requirement are polymeric microfibres (polypropylene).

2.5 FIRE BEHAVIOUR

The experience gained on the fire behaviour of concretes reinforced with steel fibres made it possible to formulate the following considerations.

- Low percentages of fibres (up to 1%) do not significantly alter diffusivity thermal, which therefore remains calculable based on the data available for the matrix.
- The damage caused in the material by a thermal cycle pushed up to 800 ° C results predominantly related to the maximum temperature reached in the cycle and produces an effect irreversible on the matrix. This behaviour, mainly found in the presence of limited volumetric fractions of metal fibres, suggests, once the ambient temperature, to appreciate the degradation induced through the evaluation of the residual strength.
- When the maximum exposure temperature changes, the first cracking resistance it is aligned with that of the matrix. For temperatures above 600 C, the fibres improve the behaviour of the matrix.
- When the maximum exposure temperature changes, the modulus of elasticity of the concretes.

Fibre-reinforced is not significantly affected by the presence of limited fractions volumetric ($\leq$ 1%) of fibres and, therefore, can be assimilated to that of the matrix. The presence of polypropylene fibres is effective to limit the effects of spalling destructive. In particular, these fibres partially sublimate at a temperature of 170 ° C leaving free cavities in the array. A volumetric fraction of fibres between 0.1% and 0.25% is unable to significantly mitigate or eliminate the phenomenon.

2.6 FCR AND THE EFFECT OF TEMPERATURE

Possibly the most beneficial effect of fibre additions in concrete is the ability to absorb energy this is the main reason for the use of fibre reinforcements within floor slabs. If toughness is reduced with an increase in temperature, this could be considered a major disadvantage when designing structural elements for hot climates. The effect on the temperature of a FRC depends on the characteristics of the fibres that are used. There is a huge difference between steel fibres and polymer fibres.

Polypropylene has a high resistance to the flow of electrons, leading to a low rate of heat transfer within the material. At ambient to high temperatures, polypropylene is a ductile material and shows qualities of a plastic/elastic nature. At temperatures below freezing, polypropylene tends to become brittle. The brittle nature of polypropylene is a serious disadvantage and can become problematic, especially in certain applications when mechanical performance is concerned. (Richardson & Ovington, 2017)

Research carried out by Lau et al investigated the effect that elevated temperature had on steel fibre concrete. The steel fibre concrete was subject to temperatures ranging between 105°C and 1200°C. These temperatures are extreme and beyond maximum air temperature, but they do provide an understanding of the performance of steel fibre concrete under high temperatures. The research reported a decrease in elastic modulus as the temperature increased as well as a small, but not significant, reduction in strength at temperatures below 400°C. It was concluded that the use of steel fibres in concrete continues to be beneficial even at temperatures of 1200°C and that steel fibre concrete can provide a greater resistance to the effects of heating. (Lau & Anson, 2006)

The study carried out by Lau and Anson performed two different test flexural strength table 2.1 and pull out table 2.2. It is possible to see how the polymeric fibres are much more sensitive to temperature changes

Concrete Type	Average Flexural Strength (N/mm^2)		
	-20°C	Ambient	60°C
Plain	11.63	5.84	3.78
Polypropylene fibre	11.47	4.58	4.01
Steel fibre	11.74	6.29	3.85

Table 2.1-The average flexural strength for each beam classification and temperature

Type of Fibre	Average Pull Out Force (N)	
	-20°C	60°C
Polypropylene	196.6	131.0
Steel	768.9	841.4

Table 2.2-The average pull out force of each fibre type

2.7 MAIN FRC EXPERIMENTAL TEST

The behaviour of FRCs over time is not yet well known and is still the objective of numerous researches. The experimental tests carried out did not limit themselves to studying the creep of the non-cracked fibre-reinforced concrete; they tried to simulate the conditions that the FRC is in operation. The studies on creep response of FRCs were generally conducted on previously cracked specimens by direct tensile test or flexural tests, to study mainly the post-cracking behaviour as the FRC cracked state is regulated mainly by the fibres contribution. The pre-cracking of the specimens is also useful because it allows studying the contribution and the long-term effects of the fibres alone, separating them from those linked to the concrete.

The research in this field show some limitations. One of the main problems is the absence of the standardized test methods for quantifying viscosity in fibre-reinforced products. Various researches were conducted following different procedures and led to results and conclusions that are often difficult to compare and generalize.

2.7.1 Compression creep test

Fibres, in general, are not consider particularly effective to counteract the creep of the concrete under compression loading, because these will be mainly compressed and the cracks formed are parallel to the applied load. However, they can offer a contrasting action to the viscous sliding of the concrete. Studies on creep of FRC in compression indicate that fibres restrain creep strains when compared to plain mortar and concrete. (PS & M, 1986)

An experimental investigation in order to determine the influence of steel fibre reinforcement on the creep of cement matrices under compression, was carried out by creep test, appling stress-strength ratios ranging between 0.3 to 0.9. Melt extract and hooked steel fibres were used at volume fractions ranging between 0 and 3% by volume of a mix. Three types of cement matrices were used namely cement paste, mortar and two mix proportions of concrete. The results indicate that steel fibres restrain the creep of cement matrices at all stress strength ratios, the restraint being greater at lower stresses and at higher fibre contents. Steel fibres are effective in restraining only the flow component of creep of cement matrices, the delayed elastic component being unaffected. The reduction in creep of cement pastes, due to fibre reinforcement, is much greater than that for mortar or concrete matrices. (Mangat & Azari, Compression creep behaviour of steel fibre reinforced cement composites)

Taking into account other research, the influence of fibres on the creep of concrete have a significant influence. It is visible especially in the early-age and hardened concrete. The use of fibres can decrease the number of matrix defects in concrete and limit the development of cracks. However, the positive influence of fibres is insignificant under load lower than the destructive load. The stress analysis of elements with dispersed reinforcement, especially those loaded at an early age or under indirect forces need to be done for different model than the one provided by the Code. The tests were performed for two levels of applied load: 40% and 80% of the destructive load at the load time, respectively, at 1, 4, 7 and 28 days. The resulting creep strain was compared with the calculating method from Eurocode 2, and Pre-norm Fib 2010 (Báyszko, 2017).

2.7.2 Bending creep test

The analysis of flexural creep behaviour of cracked FRC elements is a relatively new topic, which has not been entirely researched yet. There is no standardized method to assess such behaviour at this time. Several serious differences are observed between such studies that compromise the possibility of considering their results as comparable: different methodologies and test setups, different concrete and fibre types, fibre contents, crack openings or deflections considered, load levels, test specimen, standards, and procedures. As a result, some attempt to establish a methodology and a convenient test setup to study the flexural creep behaviour of pre-cracked FRC specimens was necessary (Arango, Serna, Martí-Vargas, & García-Taengua, 2011).

Bending tests are by far the most widely used in order to evaluate creep deformations in cracked conditions (Buratti & Mazzoti, 2016). Experimental setup used for long-term bending test is shown in the figure 2.26, is derived from adapted a hydraulic loading frame for creep tests in order to perform long-term bending tests used a setup in which clamped specimens are loaded by a lever in a cantilever behaviour. In this case the load on the specimens is obviously larger at the bottom of the pile, but often specimens can be ordered in such a way that the ratio of applied force versus residual strength at pre-cracking is constant. This is typically easier on MSFRC specimens because of smaller variability in the post peak behaviour

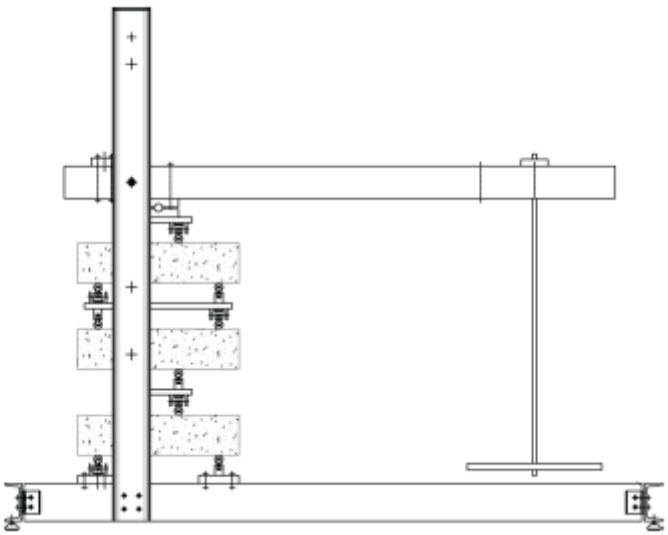

Figure 2.15-Experimental setup used for long-term bending test

The most common in published test are notched specimens (MacKay & Trottier) but examples of tests on un-notched specimens can be found in the literature (Kurtz & Balaguru). The most typical setup adopted while testing staked specimens is four-point bending, for obvious stability advantages. However, research showed that use of three or four-point loading configuration in bending does not affect creep tests results in terms of the COD rate or the stress levels where a stable creep behaviour takes place. (Zerbino, Monetti, & Giaccio).

In the literature, concerning long-term bending test there is not yet agreement on the extent to which some parameters might influence the test results. However, the following can be differentiated.

- The Creep load ratio
- Crack opening
- Environmental conditions; temperature and relative humidity.
- Minimum test duration
- Deformation parameters

2.7.3 Uniaxial tensile creep test

The experience of uniaxial tension tests on FRCs is in general limited. The heterogeneity of these materials leads to various issues such as the need of large specimens, and the development of secondary flexural moments, causing redistribution of stresses. (van Mier & van Vliet, 2002). Buratti and Mazzotti proposed a test procedure on notched cylinders on which the specimen ends are allowed to rotate, both in the pre-cracking and in the long-term test phase, by means of a spherical joint. During the pre-cracking phase, the authors identified specimens with anomalous rotations, e.g. parts in compression, which were then not used for long-term tests. (Buratti & Mazzotti, 2016). Long-term tests were then carried out on a chain of three specimens loaded using a lever frame, figure 2.27.

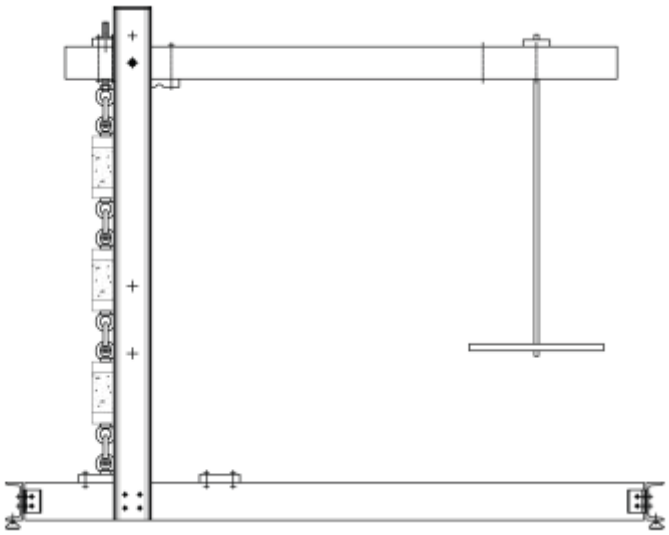

Figure 2.16-Exprimental setup for long-term uniaxial tension test.

Testing procedure can be summarized. The specimen is firstly pre-cracked up to a defined crack-opening (O-A) at which the residual strength f_R is measured. The average crack opening is normally considered to quantify the crack opening. Then the specimen it is unloaded (A-B) and transferred to the long-term testing frame. Since pre-cracking is normally carried out at very low crack opening rates, and therefore creep deformations develop during this stage, delayed deformations are in part recovered in the unloaded state (B-C). There is yet no agreement in the scientific community on the significance of these deformations and on whether they should be monitored. The specimen is then reloaded up to a fraction of the residual stress measured during pre-cracking (C-D), where indicates the creep load ratio. The time t_L in Figure 2.28 indicates the reloading time which should be as short as possible, in order to limit the interference between instantaneous and creep deformations. During the long-term tests, deformations will increase at a constant load (D-E). At the end of the long term test the specimen is unloaded (E-F) and part of the long-term deformation is recovered (F-G). Finally, the specimen might be reloaded to failure in a short term test (G-H). It is worth noticing that tertiary creep (leading to failure) might be observed during the long-term tests. These tests are normally carried out in controlled environmental conditions. (Buratti & Mazzoti, 2016)

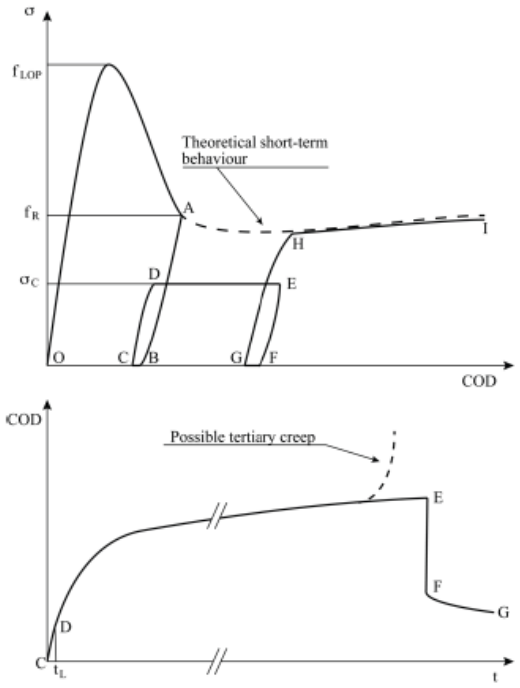

Figure 2.17-Typical behaviour observed, in a softening FRC, in long-term tests in cracked conditions, in terms of nominal-stress vs crack opening (top panel) and crack opening vs time.

2.7.4 Pull-out test on single fibres

The mechanism responsible for the enhancement in performance of macro synthetic FRC at both macro and structural levels is rooted in the understanding of the micro level phenomenon. The micromechanical observation of FRC has to do with the response at the single fibre level and its pullout performance from a cementitious matrix. An understanding of the pullout mechanism of single fibres is paramount to designing structural elements for their desired mechanical performance. (Babafemi A. J., 2015)

Pull-out tests might allow a better understanding of the bond behaviour, even though using information on the long-term behaviour obtained from these tests in order to predict the behaviour of cross sections might be complicated by random fibre orientation and anchorage lengths. (Buratti & Mazzotti, 2016). Single fibre long-term pull-out tests observing that specimens loaded at 50% of the quasi-static capacity pulled out over time. Time-dependent crack widening under sustained loading was identified to be caused by two mechanisms: time-dependent fibre pull-out and time-dependent fibre creep. (Babafemi & Boshoff, 2015).

2.8 FRC APPLICATIONS

The uniform dispersion of fibres throughout the concrete mix provides isotropic properties not common to conventionally reinforced concrete. The applications of fibres in concrete industries depend on the designer and builder in taking advantage of the static and dynamic characteristics of this new material. (Wafa, 1990). Fibre reinforced concrete can be used for a variety of applications shown below. It is ideally suited for concrete applications that require protection from plastic and drying shrinkage, improved durability, increased service life and reduced construction costs (Fiber Reinforced Concrete Asociation, 2018). The main area of FRC applications are:

- **Agricultural.** Farm and animal storage structures, wall, silos, paving, etc.

Figure 2.18-FRC Agricultural application

- **Commercial**: Exterior and interior floors, polished concrete, slabs, parking areas and roadways.

Figure 2.19-FRC Commerical application

- **Elevated Decks**: Commercial and industrial composite steel deck construction and elevated formwork at airports, commercial buildings, shopping centers, etc.

Figure 2.20-FRC Elevate Desk application

- **Highways, Roadways & Bridges:** Conventional concrete paving, SCC, white-toppings, barrier rails, curb and gutter work, pervious concrete, sound attenuation barriers, etc.

Figure 2.21-FRC Bridge application

- **Mining & Tunneling:** Precast segments and shotcrete, which may include tunnel lining, shafts, slope stabilization, sewer work, etc.

Figure 2.22-FRC Tunneling application

- **Ports & Airports:** Runways, taxiways, aprons, seawalls, dock areas, packing and loading ramps.

Figure 2.23-FRC Port application

- **Precast Concrete & Products**: Architectural panels, tilt-up construction, walls, fencing, septic tanks, burial vaults, grease trap structures, bank vaults and sculptures.

Figure 2.24-FRC Precast Concrete application

- **Residential:** Driveways, sidewalks, pool construction with shotcrete, basements, colored concrete, foundations, drainage, etc.

Figure 2.25-FRC Residential application

- **Warehouse & Industrial:** Light- to heavy-duty loaded floors and roadways.

Figure 2.26-FRC Industrial application

- **Waterways:** Dams, lock structures, channel linings, ditches, storm-water structures, etc.

Figure 2.27-FRC Waterways application

- **Other Applications:** Any other FRC-related applications not specifically described above.

Figure 2.28-FRC application

3. Materials used and their preparation

In this section, are described the material used in this research. It had been used 13 long beams, 6 cubes and 6 cylinders, from 2 concrete cast. This standard prescribes the constituents and the proportions necessary to make reference concrete that can be used for the evaluation of the rest of the fibres dispersed in the concrete under standard laboratory conditions.

3.1 MIX DESIGN

In this experimental study, a concrete was used with mechanical characteristics similar to those prescribed by the standard EN 14845-1: 2006. This standard prescribes the constituents and the proportions necessary to make reference concretes that can be used for the evaluation of the rest of the fibres dispersed in the concrete under standard laboratory conditions.

The aggregates used in the construction of the reference concrete are:

- Natural sand, S 0-5, with a granulometry between 0 and 5 mm.

Figure 3.1-Natural sand S 0-5

– Natural sand, S 0-1, with a granulometry between 0 and 1 mm.

Figure 3.2-Natural sand, S 0-1.

– Crushed stone, P 5-15, with a granulometry between 5 and 15 mm.

Figure 3.3-Crushed stone, P 5-15

In the following table 3.1 are shown the mix design.

Litres of concrete casting	1000	0.02	Absorption	Water ass	Dry weigth
S 0-5	20	kg	1.66%	0.242186549	14.34736459
S 0-1	172	kg	1.13%	0.038813443	3.396004479
P 5-15	837	kg	1.91%	0.319657377	16.41633092
Cement	400	kg			
Water	184	L			
Superplasticizer	2	L			
Water ass	Total H2o ass: 18.25 Kg				

Table 3.1-Mix design

The relationship w/c is 0.46. The amount of fibres is 8 kg with a density of 900 kg/m^3.

Figure 3.4 shown the curves of each individual aggregate and the Bolomey curves.

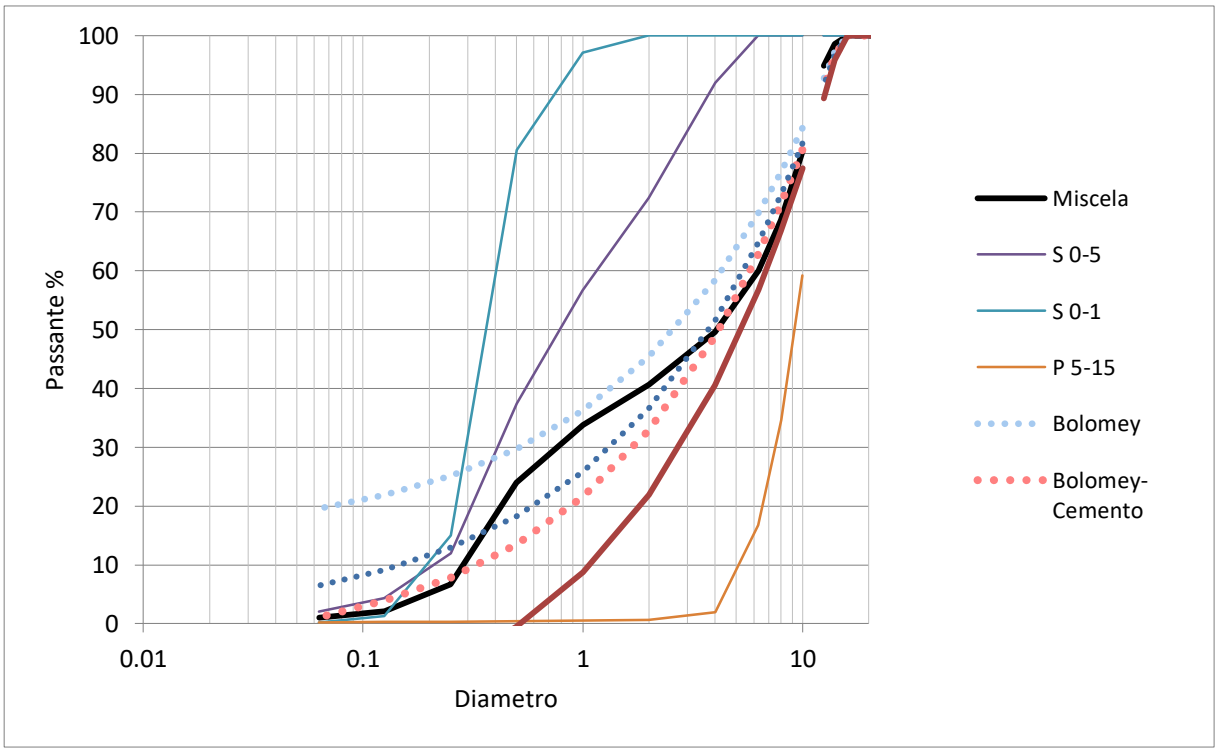

Figure 3.4-Granulometric curve of the aggregates of the reference concrete

The cement used in the reference concrete is a Portland 42.5 class R cement. Table 3.2 shows the characteristics.

Portland limestone cement	
Identification	CEM II/a-LL 42.5 R
Mechanical requirement (2 days)	Compressive strength ≥ 20 MPa
Mechanical requirement (28 days)	Compressive strength ≥ 42.5 MPa

Table 3.2-Characteristics of the cement used

The mixing water comes from the laboratory's drinking water supply. The water - cement ratio, is set at 0.46. Considering that the same standard also specifies the cement content that must be equal to 400 kg / m^3, it follows that the amount of water per cubic meter of composite is 184 liters/m^3.

The superfluidifier was added to the mixture in order to have a greater workability of the mixture. The characteristics of the superfluidificant are reported in the table 3.3.

Glenium Sky 542 (EN 934-2:2000)	
Description	Superfluidifying additive based on polycarboxylates 2nd generation
Minimum chloride content	>10 % by mass
Maximum chloride content	≤2.5% by mass
Hazardous substances	-

Table 3.3-Characteristics of the superfluidifier used.

The total volume of concrete was equal to 130 liters.

3.2 POLYMER FIBRES

The fibres with which the study has been carried out are class II polymer fibres. Provided by the company BASF Construction Solutions GmbH, whose main characteristics are shown in the following table 3.1.

Polymer type	Polypropylene	Colour	Colourless
Sectional shape	Irregular	Longitudinal Shape	Straight Crimp
Density	910 kg/m^3	Fibre length	54 mm
Eq. Diameter	0.81 mm	Aspect ratio	67
Tensile strength	552 MPa	Secant modulus	6000 MPa
Effect on strength	5 kg/m^3	Effect on consistence	11s vs 7s
Melting point	160 ºC		

Table 3.4-Fibres characteristics

3.3 FORMWORKS

The formworks used for the beams to be subjected to bending test are such as to create a prismatic samples of dimension 150x150x600 mm. The formworks used for the specimens to be tested for direct traction are cylindrical in shape with a diameter of 100 mm and a height of 200 mm. In addition, cubic formworks of 150 mm side were used which were necessary both for an estimate of the mass per cubic meter of the reinforced concrete and to evaluate the compressive strengths. In the following table 3.5 is shown the amount of volume used in each formworks.

	Liters	Number	Total
Prismatic	13.5	7	94.5
Cylindrical	1.57	6	9.42
Cube	0.3375	3	1.0125
Abrams cone	21.9911		
Total			**104.933**

Table 3.5- Volume in frameworks

Figure 3.5-Formworks used concrete casting

3.4 CONCRETE CASTING

Concrete casting was made inside the CIRI laboratory, in the date 10/04/2018. The phases of the casting were the following.

- Placing in the cement mixer the aggregates, which are dry, because they have been in an oven one day at 120 degrees, and the adsorption water. Mix about five minutes.

Figure 3.6-Aggregates in the cement mixer

- Adding all the cement, the rest of the water and the superplasticizer.

Figure 3.7-Adding superplasticizer

– Addition of BASF fibres.

Figure 3.8-Addion of BASF fibres.

The cone test is performed until the desired consistency is achieved. The achieved slump is 20 cm and the slump class S3.

Figure 3.9- Test of lowering at the cone

When the concreate has the required consistency, it is poured in the formworks. To achieve a uniform compaction, the concrete has been vibrated.

Figure 3.10- Vibration of concrete in the formwork

Once the formworks were filled and the conglomerate was suitably vibrated, the upper face was finished and the fresh concrete was protected with a film in order to avoid negative hygrometric exchanges between the concrete and the external environment.

Figure 3.11-Surface of formwork finished

Figure 3.12-Specimen coverage

The specimens are put in a tank with water at 20º during a week, then they are notched and after this again in water until completing 28 days.

3.5 COMPRESSIVE STRENGTH OF CONCRETE

For each of the cast concrete, the compressive strength at 28 days of maturation was evaluated. The compression test is was carried out on the cubic specimens using the Metro Com da test machine 400 ton (100 ton scale).

Figure 3.13-Specimen before and after the compression test

	Slump (cm)
	(cm)
G3_254_8_C4	20.00
G3_254_8_C5	20.00
G4_254_8_C1	19.00
G4_254_8_C2	19.00

Table 3.6-Slump of the cubes

	Side A	Side B	Height	h/d	Area
	(mm)	(mm)	(mm)	-	(mm2)
G3_254_8_C4	150.00	150.00	150.00	1.00	22500
G3_254_8_C5	150.00	152.00	150.00	1.00	22800
G4_254_8_C1	150.00	151.00	150.00	1.00	22650
G4_254_8_C2	149.00	151.00	150.00	1.01	22499

Table 3.7-Values of the cubes obtained from concrete cast

	Fluid	Fresh Weight	Hardened Weight	Fresh density	Density	Load	Rc	μ	σ	CoV
	(%)	(g)	(g)	(kg/m3)	(kg/m3)	(kN)	(MPa)	(MPa)	(MPa)	(%)
G3_254_8_C4	0.98	7850	7720	2325.93	2287.41	1289.57	57.31	54.89	3.42	6.23
G3_254_8_C5	0.98	7850	7740	2325.93	2263.16	1196.41	52.47	54.89	3.42	6.23
G4_254_8_C1	0.91	7700	7760	2266.37	2284.03	1260.15	55.64	54.52	1.59	2.91
G4_254_8_C2	0.91	7700	7710	2266.37	2284.55	1201.31	53.39	54.52	1.59	2.91

Table 3.8-Result of the compression test

3.6 GEOMETRIC CHARACTERISTICS AND PREPARATION OF TEST SPECIMENS

In this paragraph the geometric characteristics of the specimens will be exposed and all the steps for the preparation, in order to obtain the specimen to carrying out the test.

3.7 CYLINDRICAL SPECIMENS

The cylindrical specimens at the time of disarming, are all about 200 mm high and 100 of diameter. In order to be able to regularize the surfaces of the bases and eliminate the parts of concrete at the ends of the cylinder, considered to be of lower quality, it necessary two cuts. The final height of the cylinder is of 150 mm.

Figure 3.14- Cutting with a disk saw

These specimens will be used to obtain the elastic module.

3.7.1 Prismatic specimens for cylinders

Once obtained the prismatic specimens, it will be divide into three pieces and from each one we will obtain a cylinder. As it shown in the figure 3.15.

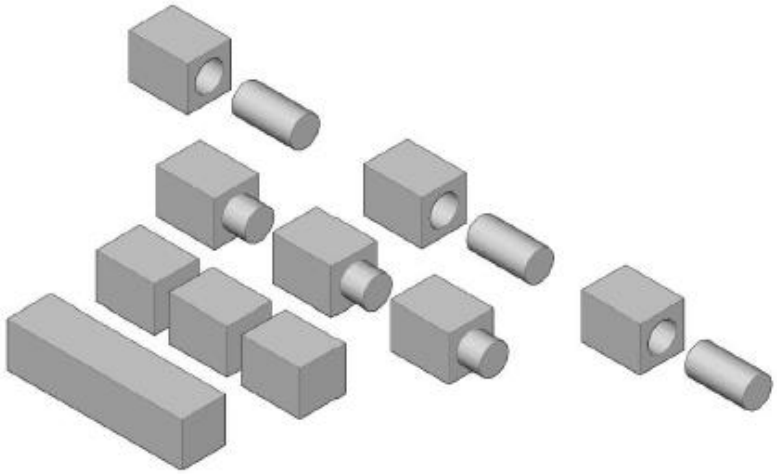

Figure 3.15-Extraction of cylindrical specimens from the prismatic.

These cylinders have a height of 200 mm and a diameter of 125 mm. The cylinders will be marked with the letters A, B, C.

Figure 3.16-Removing cylinder

Figure 3.17-Removal of the cylinder in the machine

Cutting the ends, the base surfaces of the samples were first sanded and cleaned with compressed air and alcohol, then they were glued to the circular plates, diameter 125 mm, on which the two U-shaped elements that allow the joints to be screwed grabbed by the test machine.

The gluing of the specimens with the plates was made using the glue GeoLite Gel. The steps to follow are:

– For the bonding it is necessary to clean the surface.

Figure 3.18-Specimen cleaning with industrial dryer and with alcohol

– Preparation of the glue

Figure 3.19-Preparation of the glue

– Gluing circular plate

Figure 3.20-Gluing process of circular plate

– The specimen is place

Figure 3.21- Placing the specimen in circular plate

– Gluing the top of specimen.

Figure 3.22- Gluing the top of the specimen

– Finally the upper and lower parts are joined.

Figure 3.23-Union of the lower and upper part

Once the plates have been glued to the specimen, a notch has been made at half height of the cylinder and along the entire circumference. This allows the cracking, during the tensile test, to be located in a specific section of the specimen. The carving was made through the diamond disc saw. Cylinder plates were screwed to a pin that was manually rotated. Approaching the saw and progressively rotating the cylinder around its own axis, the carving was made.

Figure 3.24-Disc saw and system for making notch

Figure 3.25-Final result of the cylinders

Once the notch has been made, the pairs of plates must be applied to the specimens, at 120 ° from each other and straddling the notch, necessary to position the transducers. For this is necessary:

- Prepare the surface with a sandpaper
- Clean it with alcohol
- Glue the base with X60
- Let dry and remove guides.

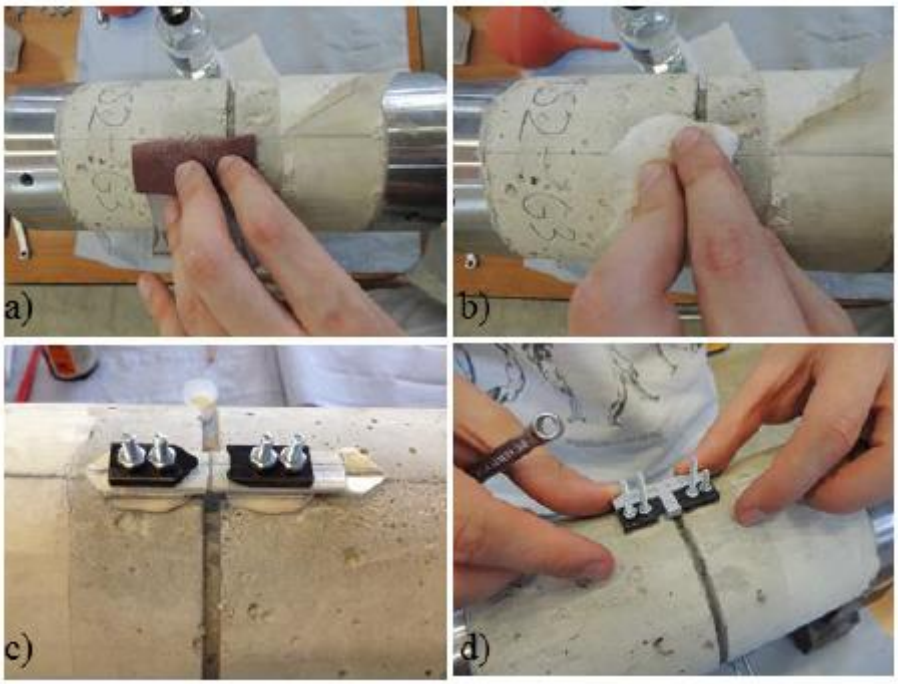

Figure 3.26-Preparation of transducer support plates

After this process, the transducer will be placed as in the following figure 3.25.

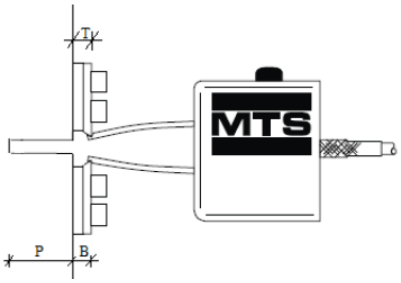

Figure 3.27-Transducer positioning diagram and distances to be measured

Once prepared the cylindrical specimens are measured, the results of these measurements are summarized in the table 3.8.

Code	Area (mm2)	Diameter (mm)	Notch				diam,int	Area,int
			h1 (mm)	h2 (mm)	h3 (mm)	hm (mm)		
G4_T2A	390	124.140856	8.07	9.81	8.4	8.76	114.94	10376.06
G4_T4A	389	123.82	9.75	9.19	8.28	9.07	114.63	10319.56
G4_T1C	389	123.82	9.45	8.11	9.28	8.95	114.75	10342.38
G4_T1A	388	123.50	7.97	10.85	9.28	9.37	114.33	10266.81
G4_T3C	390	124.14	10.64	11.85	11.8	11.43	112.27	9899.59
G4_T5B	389	123.82	8.68	8.58	9.24	8.83	114.87	10362.82
G4_T3A	390	124.14	10.44	9.84	9.39	9.89	113.81	10173.04
G4_T4C	389	123.82	12.46	11.67	11.75	11.96	111.74	9806.35
G4_T5A	390	124.14	9.2	8.02	8.5	8.57	115.13	10409.78
G4_T1B	390	124.14	10.42	9.82	10.22	10.15	113.55	10126.02
G4_T2B	389	123.82	11.41	10.5	12.26	11.39	112.31	9906.65
G4_T4B	389	123.82	11.58	10.38	12.78	11.58	112.12	9873.16

Table 3.9-Measure of the cylindrical specimens

3.7.2 Prismatic specimens

These specimens are used of the three-point bending test. Bending test is a standardized test, the preparation steps of the shutters must comply with the conditions imposed by the UNI EN 14651 standard. For this purpose a notch has been made on each joist at the center line using a diamond saw, the reference depth is 25 mm, but in making this notch there may have been variations with respect to this value.

Figure 3.28-Measure of the notch

For the realization of the test, it will be measured 250 mm from the center on both sides, for the supports.

Figure 3.29-Measures of beams

The same arrangement will be placed as in the cylinders to measure the opening of the notch as it is possible to see in the figure 3.25.

Figure 3.30- Position of the instrument

As for the cylinders, a measurement of the characteristic measurements of the prismatic specimens are made. These are shown in the tables 3.10 and 3.11

CODE	hInt1	hInt2	hInt3	H1	H2	H3	H4	B1	B2	B3	B4
	mm	mm	mm	mm	mm	mm	mm	mm	mm	mm	mm
G3_254_8_T6	25	24.54	23.69	149.89	150.22	147.05	147	149.4	150.06	150.63	150.98
G3_254_8_T4	25.63	25.42	24.7	149.74	149.56	149.1	148.7	152.2	151.05	152.19	154.241
G3_254_8_T5	25.24	25.97	26.3	150.27	150.37	149.5	149.96	151.88	150.63	151.77	148.9
G3_254_8_T1	25.67	25.56	25.57	148.36	148.68	149.44	149.56	148.91	151.88	151.28	150.31
G3_254_8_T8	25.2	25.17	25.57	149.85	149.26	149.67	149.67	153.29	152.88	152.67	148.5
G3_254_8_T3	24.36	24.94	24.91	149.67	149.55	148.02	148.05	149.29	150.76	150.63	149.53
G3_254_8_T2	25.28	25.22	24.69	149.48	149.44	148.4	148.26	150.98	150.46	150.98	150.68
G3_248_8_T7	25.23	25.8	25	149.51	150.06	150.83	148.59	152.01	153.04	152.83	151.04

Table 3.10- Measures of the prismatic specimens

CODE	hMed	Hmed	Bmed	Hnet
	mm	mm	mm	mm
G3_254_8_T6	24.41	148.54	150.27	124.13
G3_254_8_T4	25.25	149.28	152.42	124.03
G3_254_8_T5	25.84	150.03	150.80	124.19
G3_254_8_T1	25.60	149.01	150.60	123.41
G3_254_8_T8	25.31	149.61	151.84	124.30
G3_254_8_T3	24.74	148.82	150.05	124.09
G3_254_8_T2	25.06	148.90	150.78	123.83
G3_248_8_T7	25.34	149.75	152.23	124.40

Table 3.11-Measures of the prismatic specimens

3.8 ARTICULATIONS

During the direct traction test, specimen rotations may occur, especially during the cracking and the parts of the specimen outside the cracked area begin to rotate. In order to avoid bending moments that contrast these relative rotations between the parts of the test piece subjected to traction, they were used together in both the upper and lower head.

The self-lubricating rotating heads of the TESNO CFP25 series have been used according to DIN ISO 12240-4 K series (www.chiavette.com) with stainless steel couplings and wire mesh with PTFE.

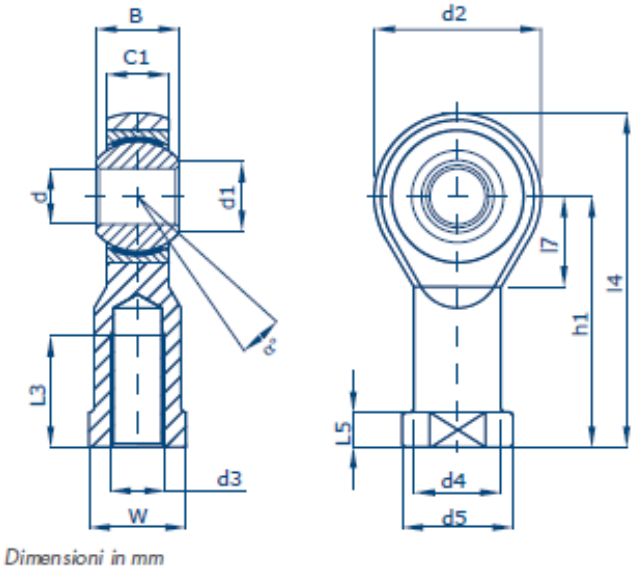

Figure 3.31-Diagram of CFP25

They must be assembled by a fork, pin and swivel head as is shown in figure 3.22.

Figure 3.32-Fork, pin and swivel head

3.9 ELASTIC MODULE

3.9.1 Preparation of the test

To obtain the elastic module, the cylinders of 150 mm in height and 100 in diameter have been used. The elastic modulus will be evaluated in two of these cylinders; these will have placed 3 strain gauge, 120 degrees apart from each other, and in the middle of the cylinder. The strain gauges are attached to the cylinders by the glue X60. The process is the following:

- Cleaning the surface with alcohol.

Figure 3.33- Cleaning the surface of the specimen

- Surface drying

Figure 3.34- Surface drying

- Placement of the strain gauges.

Figure 3.35-Placement of the strain gauges.

- Gluing the strain gauges.

Figure 3.36- Gluing the strain gauges

- Final placement of strain gauges

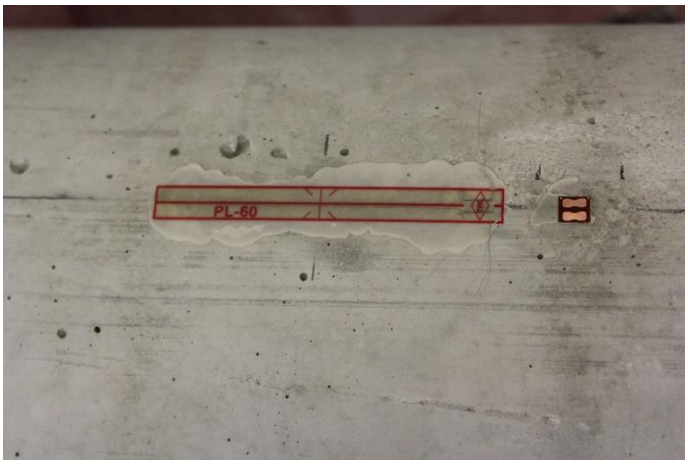

Figure 3.37-Final placement of strain gauges.

3.9.2 Test

To obtain the elastic module, EN 12390-13:2013 *"Testing hardened concrete" Part 13: Determination of secant modulus of elasticity in compression* is followed. The steps according to the standard are:

Preloading cycles

- Three preloading cycles are carried out in order to check the wiring stability (first check) and specimen positioning (second check).
- Place the test specimen, with the measuring instruments attached axially, centrally in the testing machine.
- For the first loading cycle, apply stress to the specimen at a rate of (0,6 ± 0,2) MPa/s up to the lower stress σ_b. Hold the lower stress within ± 5 % of the nominal value for a period not exceeding 20 s. Record the lower stress m b σ. Reduce the stress at a rate of (0,6 ± 0,2) MPa/s down to the preload stress σp. Hold the preload stress for a period not exceeding 20 s. At the end of this period, zero the strain measuring instruments.
- Repeat the loading cycles above for a further two times, i.e. cycles two and three. At the end of each of the second and third cycles at the lower stress level, record the strain ε_b along each measuring line.
- After the three cycles, maintain the preload stress within ± 5 % of the nominal value and perform the following consecutive checks within 60 s.
- First check
- On each measuring line, the variation of ε_b from the second cycle to the third cycle shall not be greater than 10 %. If the strain difference is greater than 10 %, stop the test; adjust the measuring instruments and restart. If it is not possible to reduce the difference below 10 % after re-starting, the test shall be stopped
- . Second check
- The strains ε_b at the third cycle on all the measuring lines shall not differ from their average by more than 20 %. If the limit is not achieved, re-centre the specimen and restart the test. If it is not possible to reduce the difference below 20 % the test shall be stopped and the specimen rejected.

Loading cycles

- Increase stress at a rate of (0,6 ± 0,2) MPa/s from the preload stress to the lower stress. Hold the lower stress within ± 5 % of the nominal value for a period not exceeding 20 s. At the end of this period, record the strain along each measuring line and calculate the average strain εb,0 at this stress level.
- Three loading cycles are carried out.
- For each cycle, increase the stress applied to the specimen at a rate of (0,6 ± 0,2) MPa/s until the upper stress, σa, is reached. Hold the upper stress within ± 5 % of the nominal value for a period not exceeding 20 s. For cycles one and two, reduce the stress at a rate of (0,6 ± 0,2) MPa/s to the lower stress. Hold the lower stress within ± 5 % of the nominal value for a period not exceeding 20 s.
- At the end of the upper stress phase of the first and third cycles and when the load is stable, record the corresponding strains along each measuring line and calculate the average strains, ε_a,1 and ε_a,3, at these stress levels.
- At the end of the lower stress phase of the second cycle and when the load is stable, record the strain along each measuring line and calculate the average strain ε_b,2 at this stress level.
- The measured value of the lower stress m b σ shall be recorded.
- The measured value of the upper stress m σ a shall be recorded.
- When all measurements are completed at the upper stress level of the third loading cycle, the compressive strength of the specimen shall be determined in accordance with the loading procedure given in EN 12390-3. Record the compressive strength to the nearest 0,1 MPa.
- In order to prevent permanent damage to the measuring gauges, it may be desirable to remove them from the specimen before the load is increased to failure. This should be performed safely.
- If the measured compressive strength differs from f_c by more than 20 %, it shall be noted in the test report.
- The test cycle for the determination of elastic modulus is given in Figure 3.37.

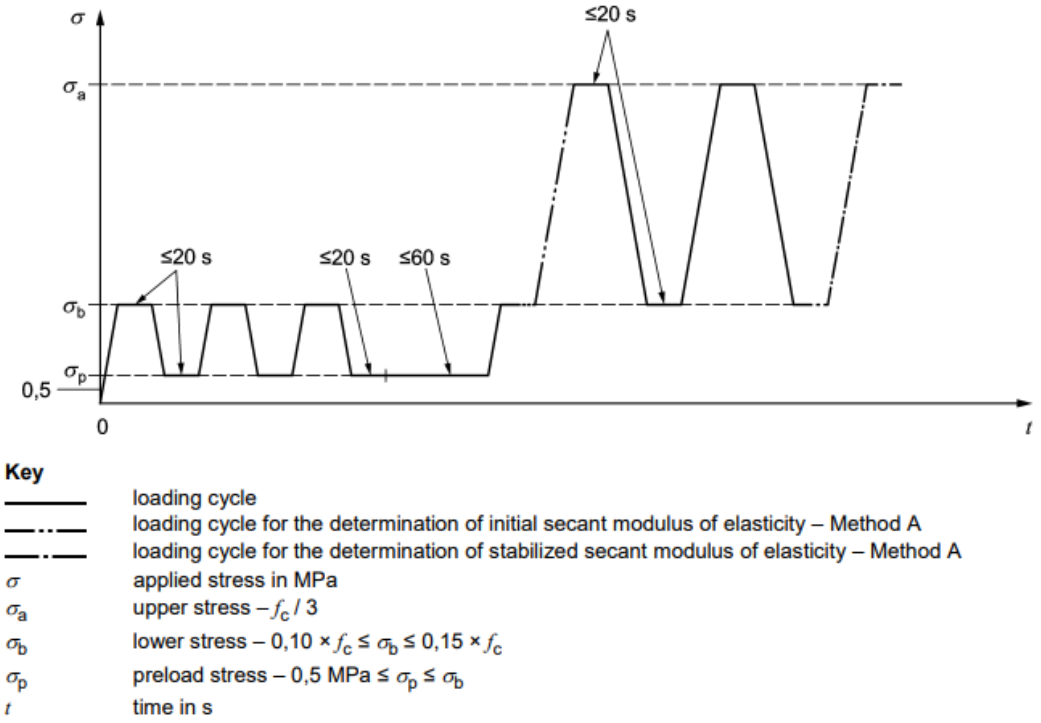

Figure 3.38-Cycle for the determination of initial and stabilized secant modulus of elasticity

3.9.3 Results

The test are carried out on two specimens *G4_245_8_GY1* and *G4_248_8_CY7* and the results are shown in the figures 3.38, 3.39 and 3.40.

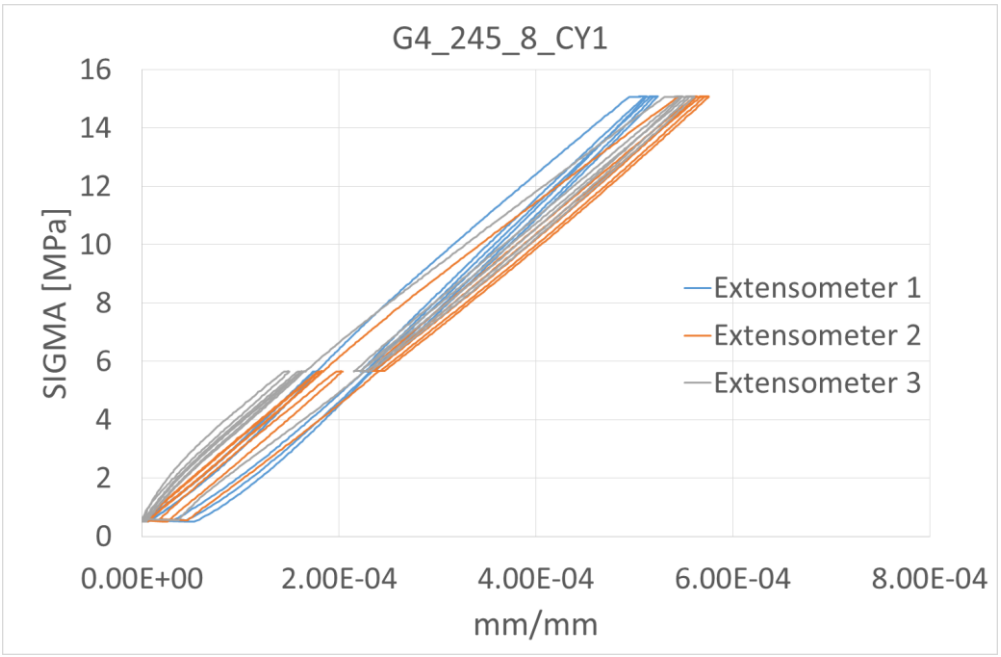

Figure 3.39- Elastic module *G4_245_8_CY1*

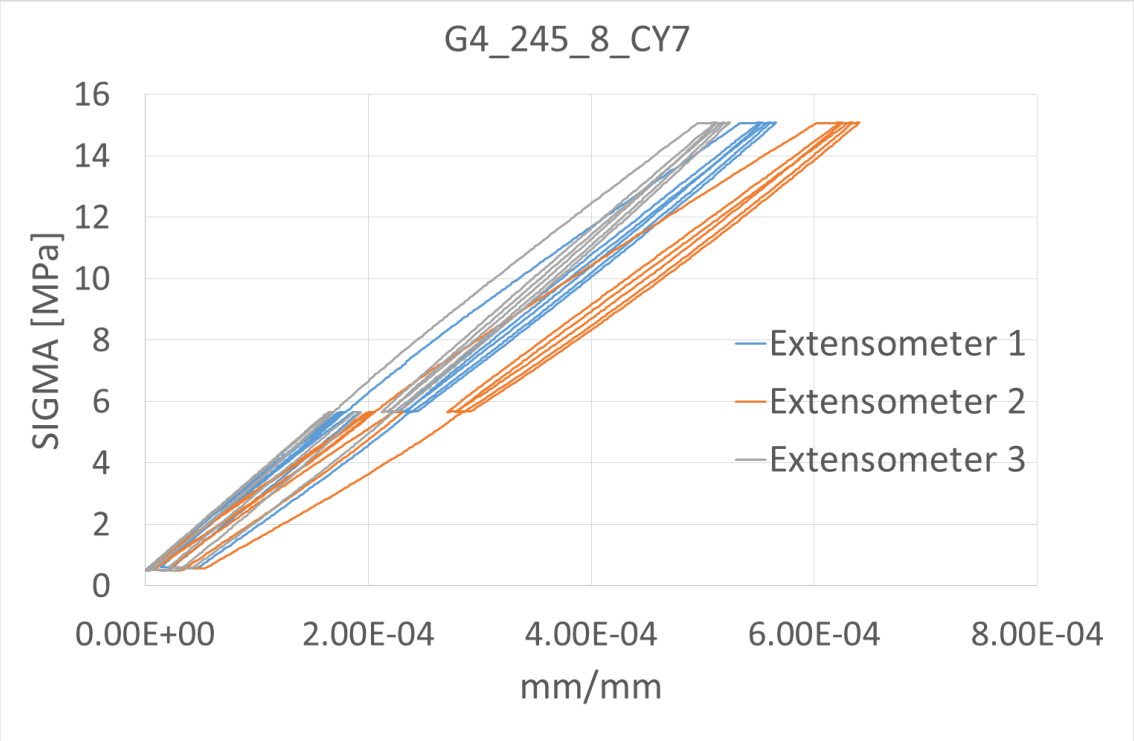

Figure 3.40-Elastic module *G4_245_8_CY7*

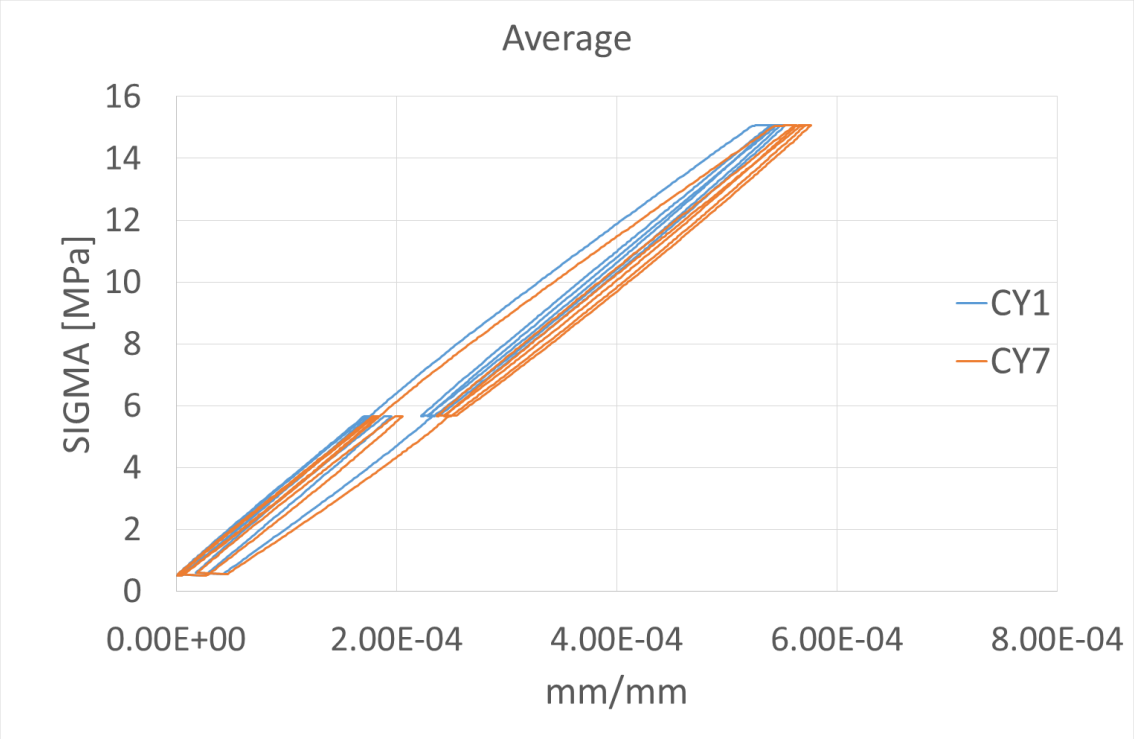

Figure 3.41-Average of the *G4_245_8_CY1* and *G4_245_8_CY7*

The load cycling of each specimen are shown in figure 3.41 and 3.42.

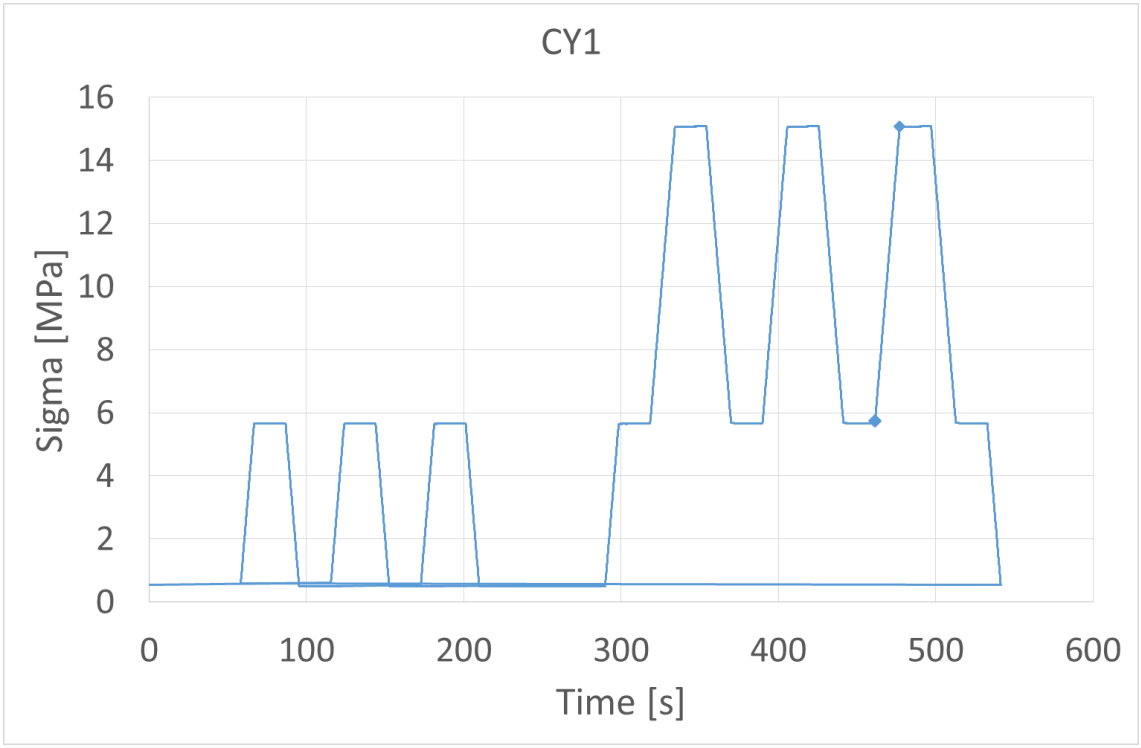

Figure 3.42-Load cycling CY1

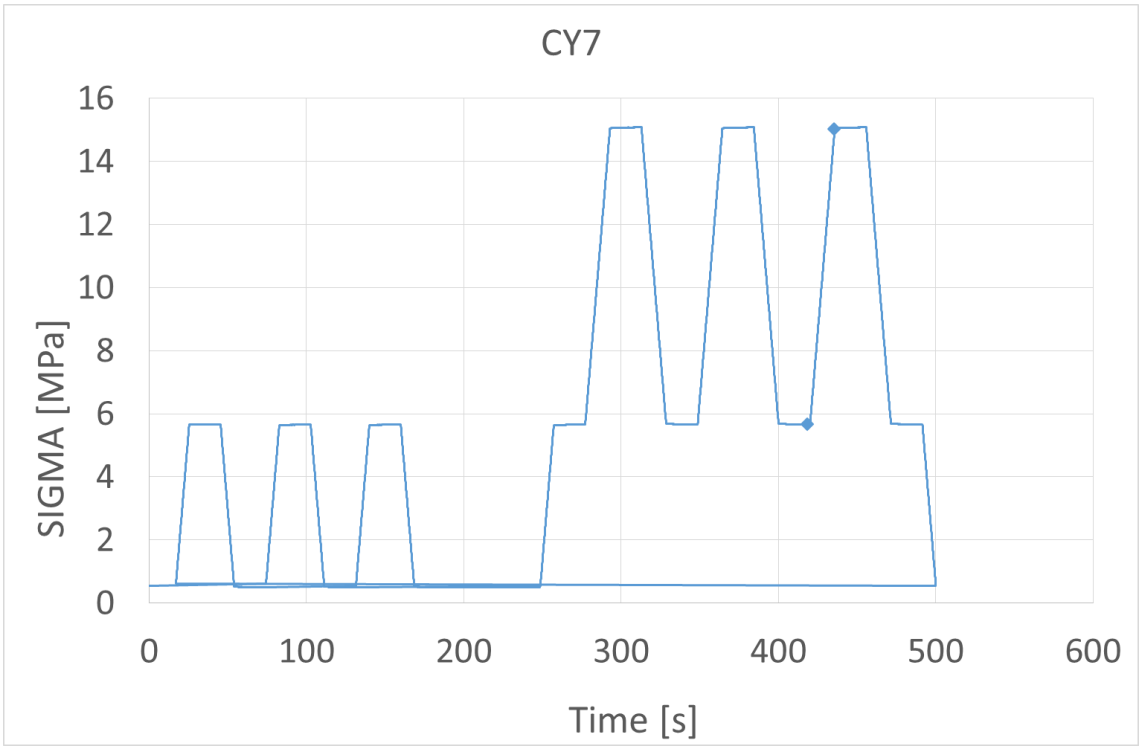

Figure 3.43-Load cycling CY7

The stabilized secant modulus of elasticity $E_{c,s}$ is defined as:

$$E_{C,S} = \frac{\Delta\sigma}{\Delta\varepsilon_S} = \frac{\sigma_a^m - \sigma_b^m}{\varepsilon_{a,3} - \varepsilon_{b,2}}$$

Results for *G4_245_8_CY1*.

		Extensometer 1	Extensometer 2	Extensometer 3
σa [MPa]	15.0619729	0.00051608	0.000567284	0.000553028
σb [MPa]	5.72076342	0.000229604	0.000237825	0.000223734

Table 3.12- Results for G4_245_8_CY1

E1	32607.3233	MPa
E2	28353.1787	MPa
E3	28367.3535	MPa
Em	29775.9518	MPa

Table 3.13-Elastic modulus of G4_245_8_CY1

Results for *G4_245_8_CY7*.

		Extensometer 1	Extensometer 2	Extensometer 3
σa [MPa]	15.0129072	0.000554866	0.0006281	0.00051439
σb [MPa]	5.66009753	0.000233273	0.00027928	0.00021832

Table 3.14-Results for G4_245_8_CY7

E1	29082.6798	MPa
E2	26812.6454	MPa
E3	31589.8942	MPa
Em	29161.7398	MPa

Table 3.15-Elastic modulus of G4_245_8_CY7

The medium elastic module for the material is 29469 MPa.

4. Measuring instruments and machines used

This chapter is dedicated to the description of the characteristics and functioning of the servo-hydraulic machine used for the test campaign object of the present work and present in the CIRI (Interdepartmental Center for Industrial Research - Building and Construction) of the University of Bologna. In addition, the measuring instruments that interface with the test system will be described.

4.1 MTS LANDMARK SERVOHYDRAULIC TEST SYSTEM

The test machine in the CIRI laboratory is produced by the MTS Company and is part of Landmark's test system solutions. It is a high-performance hydraulic servo system used for the execution of both static tests and highly precise and repeatable dynamic tests on materials and components.

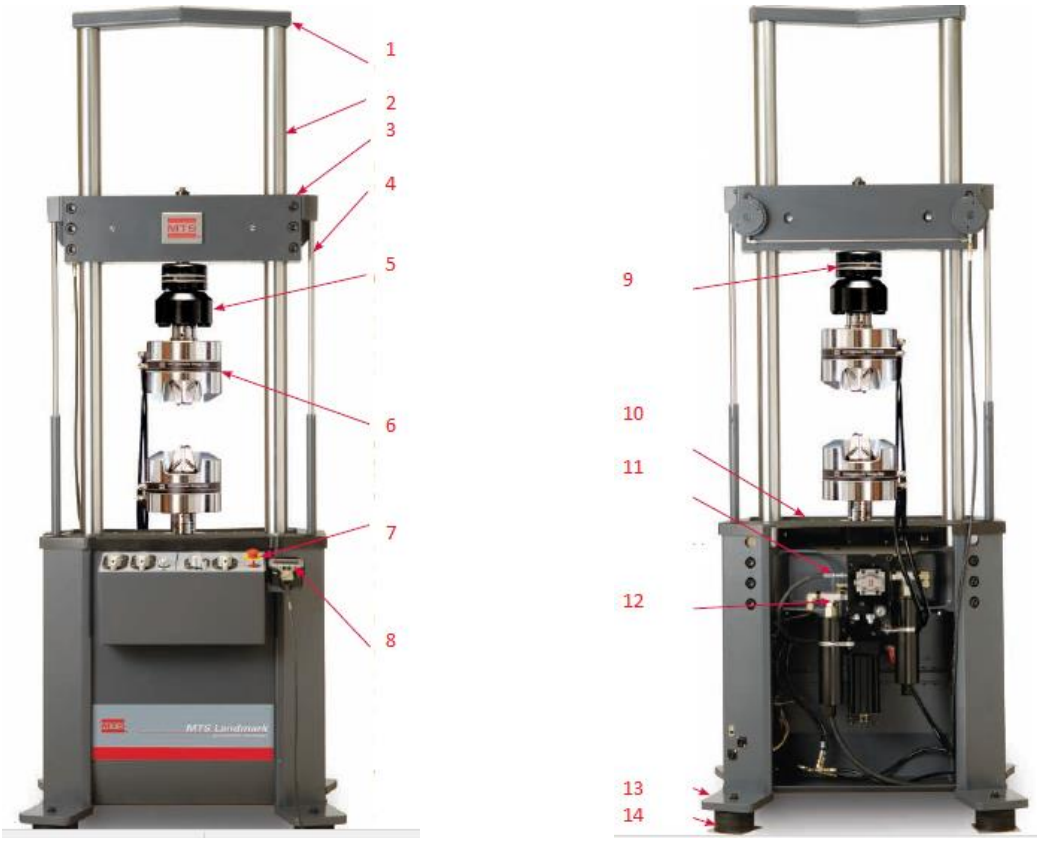

Figure 4.1-Floor-standing MTS Landmark systems feature

1. Optional Tie Bar
2. Precision-Machined Columns
3. Extremely Stiff, Lightweight Crosshead
4. Optional Hydraulically-Powered Crosshead Positioning
    - Conveniently positioned system controls
    - Duouble-Acting Hydraulic Cylinders
    - Optional Powered Crosddhead Locks
5. 611 Load Cell
    - High output, fully fatigue-rated
    - Noise-reducing wiring
    - Temperature compensation
    - Low hysteresis and long-term stability
    - Accommodates all MTS grips, fixtures and platens.
6. MTS Accessories
    - Grips, fixtures, extensometers and test environments for fatigue, thermal mechanical fatigue, fracture, high temperature, component and environmental testing.
7. Intuitive, Centralized Controls
    - Easy-to-turn handles
    - Clear, universal labeling
    - Actuator Velocity Limiting Switch
8. Optional Control Features
    - Crosshead Positioning Controls
    - Specimen Gripping Controls
    - Ergonomic Handset
9. Optional alignment Fixture
10. Large, Durable Work Surface
11. Wide Variety of Fatigue-Rated , Integrated Actuator Beams
    - Piloted End-caps
    - Direct Actuator Step Bearings
    - Low-friction Annular Step Bearings
    - Coaxial-mounted Linar Variable Differential Transducer (LVDT)

12. Broad Selection of Smooth-Ramping, Hydraulic Service Manifolds
    - Acturar Velocitiy Limiting Circuit
    - Five-Port Servovalves
    - Protective Guard
    - Optional Close-Coupled Accumulators
    - Optional Local Filter
13. Wide, Stable Footprint
14. Optional Pneumatic/Elastomeric

The model used is 370.50 and its characteristics are shown in the figure

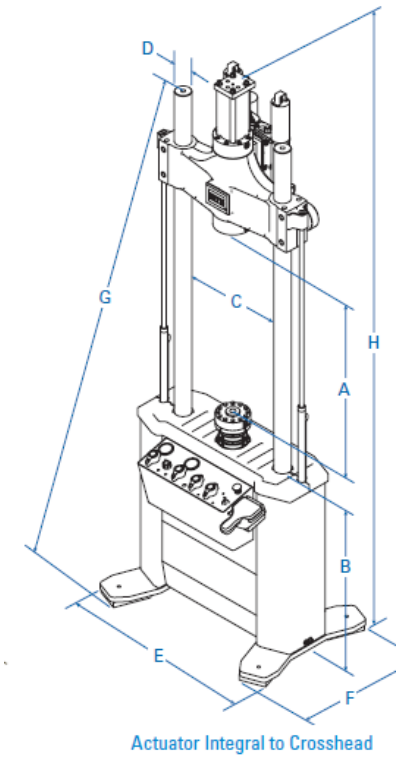

Load Frame Specifications[1]	Diagram Detail	Units	MODEL 370.10		370.25		370.50	
			Actuator integral to Base	Actuator integral to Crosshead	Actuator integral to Base	Actuator integral to Crosshead	Actuator integral to Base	Actuator integral to Crosshead
Force capacity (rated dynamic force)		kN (kip)	100 (22)	100 (22)	250 (55)	250 (55)	500 (110)	500, (110)
Available actuator ratings[1] (nominal)		kN (kip)	15, 25, 50, **100** (3.3, 5.5, 11, **22**)	15, 25, 50, **100** (3.3, 5.5, 11, **22**)	100, **250** (22 , **55**)	100, **250** (22, **55**)	250 , **500** (55 , **110**)	250, **500** (55 , **110**)
Actuator dynamic stroke[1]		mm (in)	100, **150**, 250 (4, **6**, 10)	100, **150**, 250 (4, **6**, 10)	**150**, 250 (**6**, 10)	**150**, 250 (**6**, 10)	**150** (**6**)	**150** (**6**)
Min vertical test space - standard height[2]	A	mm (in)	140 (5.5)	70 (2.8)	231 (9.1)	159 (6.3)	427 (16.8)	345 (13.6)
Max vertical test space - standard height[3]	A	mm (in)	1283 (50.5)	1213 (47.8)	1621 (63.8)	1549 (61.0)	2085 (82.1)	2002 (78.8)
Min vertical test space - extended height[2]	A	mm (in)	363 (14.3)	292 (11.5)	485 (19.1)	413 (16.3)	NA NA	NA NA
Max vertical test space - extended height[3]	A	mm (in)	1753 (69.0)	1683 (66.3)	2129 (83.8)	2058 (81.0)	NA NA	NA NA
Working height[4]	B	mm (in)	$922_{8, 15}$ (36.3)	922_{15} (36.3)	$922_{8, 15}$ (36.3)	922_{15} (36.3)	922_{15} (36.3)	922_{15} (36.3)
Column spacing (test space width)	C	mm (in)	533 (21.0)	533 (21.0)	635 (25.0)	635 (25.0)	762 (30.0)	762 (30.0)
Column diameter	D	mm (in)	76.2 (3.00)	76.2 (3.00)	76.2 (3.00)	76.2 (3.00)	101.6 (4.00)	101.6 (4.00)
Base width	E	mm (in)	1018 (40.1)	1018 (40.1)	1112 (43.8)	1112 (43.8)	1351 (53.2)	1351 (53.2)
Base depth	F	mm (in)	698 (27.5)	698 (27.5)	737 (29.0)	737 (29.0)	896 (35.3)	896 (35.3)
Diagonal clearance - standard height[5]	G	mm (in)	$2580_{8, 11, 15}$ (101.6)	$2649_{11, 15}$ (104.3)	$3084_{8, 11, 15}$ (121.4)	$3155_{11, 15}$ (124.2)	$3629_{11, 15}$ (142.9)	$3699_{11, 15}$ (145.6)
Diagonal clearance - extended height[5]	G	mm (in)	$3084_{8, 11, 15}$ (121.4)	$3153_{11, 15}$ (124.1)	$3589_{8, 11, 15}$ (141.3)	$3660_{11, 15}$ (144.1)	NA NA	NA NA
Overall height - standard height[6]	H	mm (in)	$2588_{8, 12, 15}$ (101.9)	$3028_{9, 15}$ (119.2)	$3095_{8, 14, 15}$ (121.8)	$3490_{10, 15}$ (137.4)	3688 (145.2)	3961 (155.9)
Overall height - extended height[6]	H	N/m (in)	$3058_{8, 13, 15}$ (120.4)	$3498_{9, 15}$ (137.7)	$3603_{8, 14, 15}$ (141.8)	$3998_{10, 15}$ (157.4)	NA NA	NA NA
Stiffness[7]		N/m (lbf/in)	467×10^6 (2.66×10^6)	467×10^6 (2.66×10^6)	473×10^6 (2.7×10^6)	473×10^6 (2.7×10^6)	777×10^6 (4.44×10^6)	777×10^6 (4.44×10^6)
Weight		kg (lb)	635 (1400)	820 (1800)	875 (1925)	1095 (2410)	1570 (3455)	1760 (3875)

Figure 4.2-Floor-Standing Load Frame Specifications MTS 370.50

4.2 MEASURING INSTRUMENTS

4.2.1 Strain gauge

Extensimetry is the method used for the experimental analysis of deformations. The device capable of measuring the deformation of the object on which it is positioned is called a strain gauge. There are different types of strain gages with different characteristics and operating principles. Among the most common are the electrical strain gauges (strain gauges). hey consist of a wire grid applied on a plastic support. When it is glued in the surface of the material under examination, deformations occurs and this causes a variation in the electrical resistance of the wire; by measuring this variation, one can go back to the extent of the deformation. Obviously, the measurement of the deformation is never punctual, but it is however an average measure in a stretch equal to the useful length of the extensometer.

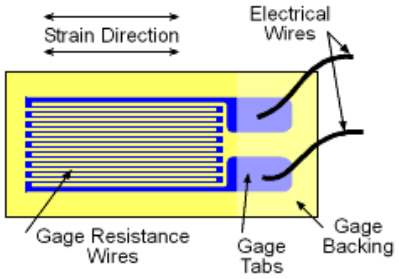

Figure 4.3-Diferents parts of a strain gauge

Usually, the deformation is evaluated from the measurement of a variation of tension rather than a variation of resistance. This is done through the Wheatstone bridge, which is an electrical device that allows signal amplification to provide more precise deformation measurements. The Wheatstone bridge is formed by four connected resistors. A voltage generator is connected between two opposite vertices, while a voltmeter is inserted between of them. Through it is possible to measure the output voltage which is the most interesting quantity. The properties of the strain gauge are shown in table 4.1.

Strain gauge PL-60-11	
Gauge length	60 mm
Gauge resistance	120 ± 0.3 Ω
Gauge factor	2.07 ± 1 %
Temperature compensation	$11*10^{-6}$ /ºC
Transverse sensitivity	0.7%

Table 4.1-Properties Strain gauge PL-60-10

4.2.2 Clip-on transducers gages

The Clip-on gages transducers are extensometers designed to detect the opening of the notch. For this reason, they have been used both in the tensile tests and in the flexural tests in order to monitor the crack opening and also allow the control, as already seen, of the tensile test in terms of CODMax and CODm and of the bending test in terms of CODMin.

Figure 4.4-Clip-on gage transducer for measuring the crack opening.

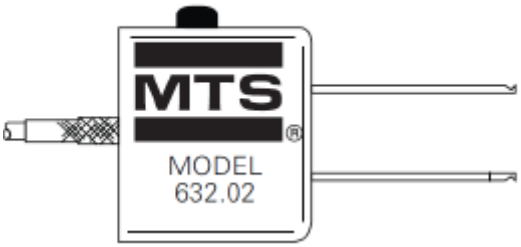

Figure 4.5-Transducer representation Gage Clip-on model MTS 632.02

The transducer is positioned on the specimen thanks to its two metal arms. Through these two arms, the Clip-on Gage sensor can measure the dimensional variation that occurs in the specimen during the execution of a test. The Gages Clip-on transducers use electrical resistance strain gauges glued to a metal element to form a Wheatstone bridge circuit. Any dilation or contraction of the specimen causes movement in the transducer arms. These moments change the resistance of the strain gauge. The variation in the Wheatstone bridge balance produces an electrical output that is proportional to the displacement of the transducer arms.

4.2.3 LVDT

LVDT, Linear Variable Differential Transducer, are used for creep measurements. Two different models of LVDT are used, in total 21. For its use, a previous calibration is necessary, this consists of taking several measurements and seeing the voltage it gives. With this, a function will be built and the slope of the line is find. In the following figures it shown the process used. In the following tables 4.2 and 4.3 and in the figure 4.6 it shown the process used, for the smallest LVDT. For the larger ones the process is shown in table 4.4 and 4.5 and figure 4.7.

Data	27/04/2018
Serial	193627
Sensitivy	161.2
Model	GT 2500RA

Table 4.2- Characteristics LVDT 193627

[mm]	Comparator	SCXI
0	0	-0.0006
-0.5	-0.501	-0.4963
-1	-1.001	-0.9931
-1.5	-1.502	-1.4899
-2.5	-2.502	-2.4695
-1	-0.999	-0.9906
-0.5	-0.502	-0.4985
0	0	-0.001
0.5	0.5	0.4945
1	1.002	0.9894
1.5	1.501	1.4801
2.5	2.501	2.448
1.5	1.501	1.4805
1	1.003	0.9902
0.5	0.501	0.4951
0	-0.001	-0.0022

Table 4.3-Measures LVDT and comparator

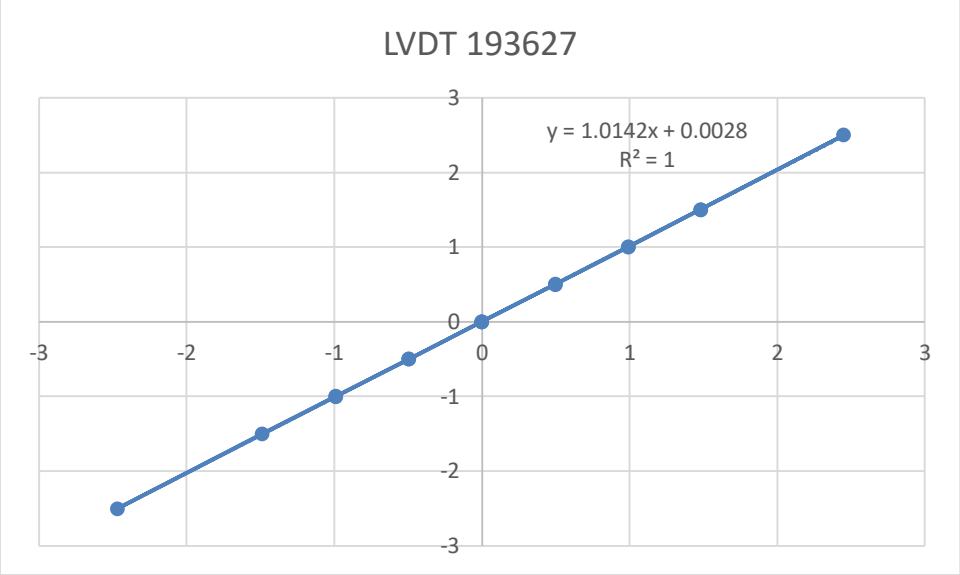

Figure 4.6-Calibration line

Data	07/05/2018
Serial	92010042
Sensitivy	8
Model	WA/10

Table 4.4-Characteristics LVDT 92010042

[mm]	Comparator	SCXI
0	0	-0.001
2	2	1.6462
4	4	3.3572
6	6	5.1314
8	8.001	6.9636
10	10.001	8.8083
8	8.001	6.9635
6	6	5.1322
4	4	3.3584
2	2	1.6479
0	0	0.004

Table 4.5-Measures LVDT and comparator

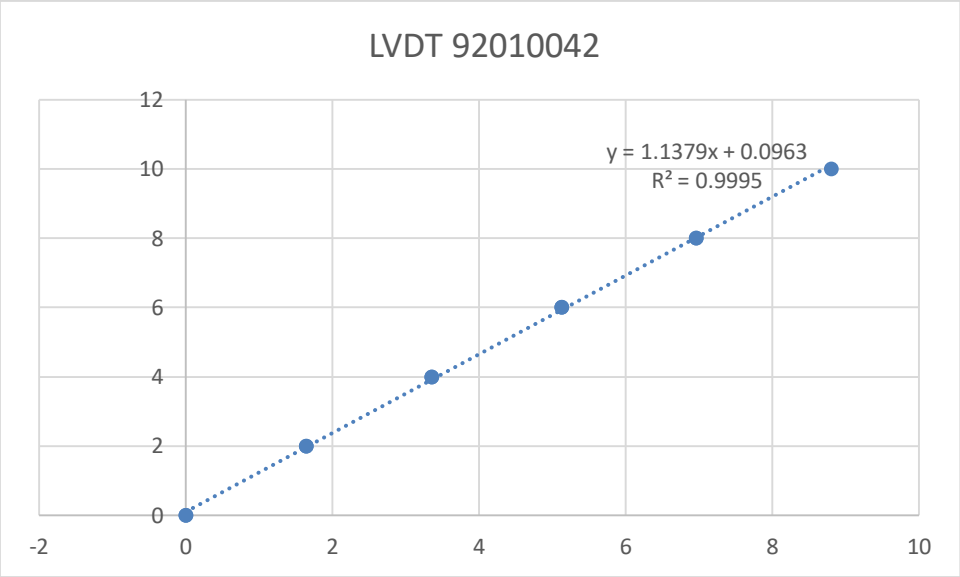

Figure 4.7-Calibration line LVDT 92010042

In the table 4.6 it can see a summary of the LVDT.

Serial	Sensitivity	Coefficient
193626	161.03	1004
193870	158.44	1008
203456	159.27	1014
203458	158.63	1004
203453	157.77	1005
203457	159.99	1010
193627	161.2	1014
193625	158.47	1005
193628	159.44	1004
193871	160.11	1011
193872	162.02	1013
193629	163.99	1016
203460	160.31	1009
92810135	8	1127
165010124	8	1116
92010042	8	1138
92810133	8	1128
91910175	8	1120
165010129	8	1122
165010130	8	1128
91910173	8	1151

Table 4.6-Summary of the LVDT

4.3 ROOM WITH CONTROLLED TEMPERATURE AND HUMIDITY

In order to carry out the long-term test, a garage or room with controlled temperature and humidity it used. In it, environmental condition can be measured and maintained. During the first fifty days the temperature will be 20º with a relative humidity of 55%. Then the temperature will be increased to 30º. Although it is not included in this thesis, the temperature will continue to increase to evaluate the behaviour of FRC.

Figure 4.8-Room with controlled temperature and humidity

5. Compression creep test on cylindrical specimens

This chapter describes how compression creep test has been performed and the results obtained. For its realization, it is necessary to examine isolated cylinders to be able to evaluate the phenomenon of shrinkage.

5.1 CONTROL OF THE TEST

5.1.1 Shrinkage

The phenomenon of shrinkage causes volumetric damage in the concrete as a result of water shocks. This phenomenon is therefore independent of the load and is influenced by the geometry of the specimen and the external environment in which it is positioned.

In this test, the impregnated samples are two thrown cylinders, they too have been fitted with two strain gauges positioned at an angular distance of 180º. The test was conducted leaving the samples free of load inside the cell seen in predation and continuous monitoring of the deformations.

5.1.2 Compression creep

In the compression test, the deformation is measured where one part is the viscosity and the other the shrinkage, so it is necessary to evaluate the shrinkage separate in order to know the real value of the viscosity. As in the previous case we will have two strain gauges positioned at an angular distance of 180º.

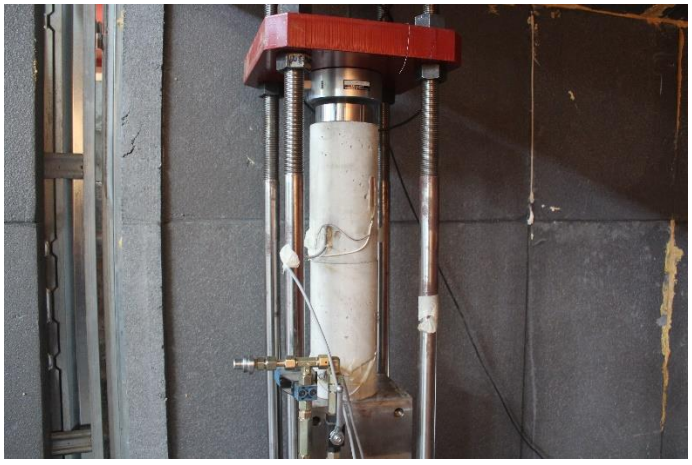

Figure 5.1-Compression creep test

5.2 RESULTS

5.2.1 Shrinkage

Two cylindrical specimens are tested *CY1* and *CY2*. The figure 5.2 shown the graphic deformation-time of the two cylinders. However due to a problem, the strain gauge of the cylinder *CY2* has not read correctly so it has been deleted.

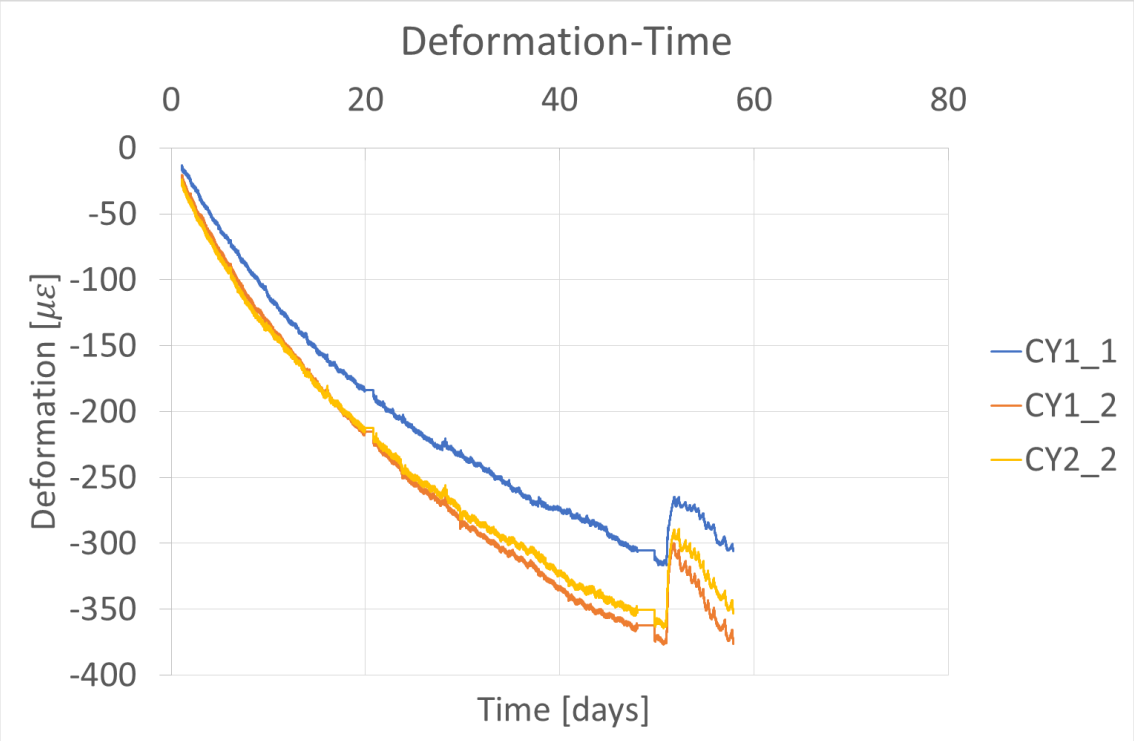

Figure 5.2-Deformation-time cylindrical specimens in shrinkage

5.2.2 Compression creep

As it has seen before, two cylinders are used *CY3* and *CY4.* Although by a failure in the strain gauge, only the cylinder CY3 could be plotted figure 5.3.

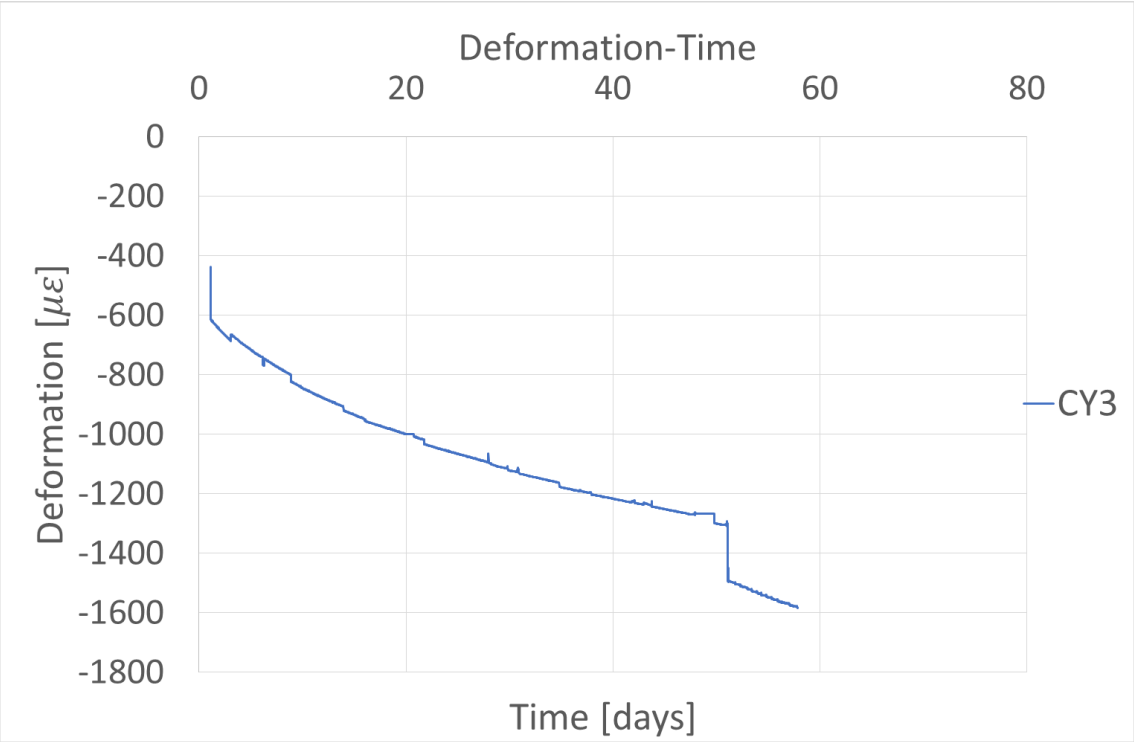

Figure 5.3-Deformation-Time compression creep cylinder CY3

6. Bending creep test on cracked notched beams

This chapter describes how the flexion test has been performed and the results obtained. For its realization, it is necessary to carry out two processes, first a pre-cracking of the notch with a test of three-point deflection, after this three notched beams will be chosen and will be testes to creep.

6.1 CONTROL OF THE TEST

6.1.1 Three-point deflection test

The three-point deflection test it is controlled by measuring the opening at the mouth of the notch (Crack Mouth Opening Displacement, CMOD), with the signal of the Clip-on Gage transducer. So a CMOD-Force curve is obtained from this test. This test is used to characterize fibro-reinforce material and to know their performance, measuring their CMOD to 3.5 mm. In our case to evaluate the viscosity, it is necessary to stop the test before, in order to simulate what happens if it crack opens under conditions of use, so we will take the opening of the fissure to 0.5 mm. This test would end here with the beams with a CMOD residue.

Figure 6.1-Three point test in beam specimen

6.1.2 Long-term bending test

Long-term bending tests were carried out on loading frames that allow to tests up to three specimens at the same time, using a four-point bending setup, required in order to have lateral stability of the specimens. Loads were applied to the topmost prim, using a lever mechanism and transferred to the lower prisms using a series of steel plates with cylindrical supports. The lever multiplication factor was measured with a load cell before the tests. The load was not monitored during the long-term tests. During the tests, the CMOD was monitored using a displacement transducer. (Buratti & Mazzotti, 2016).

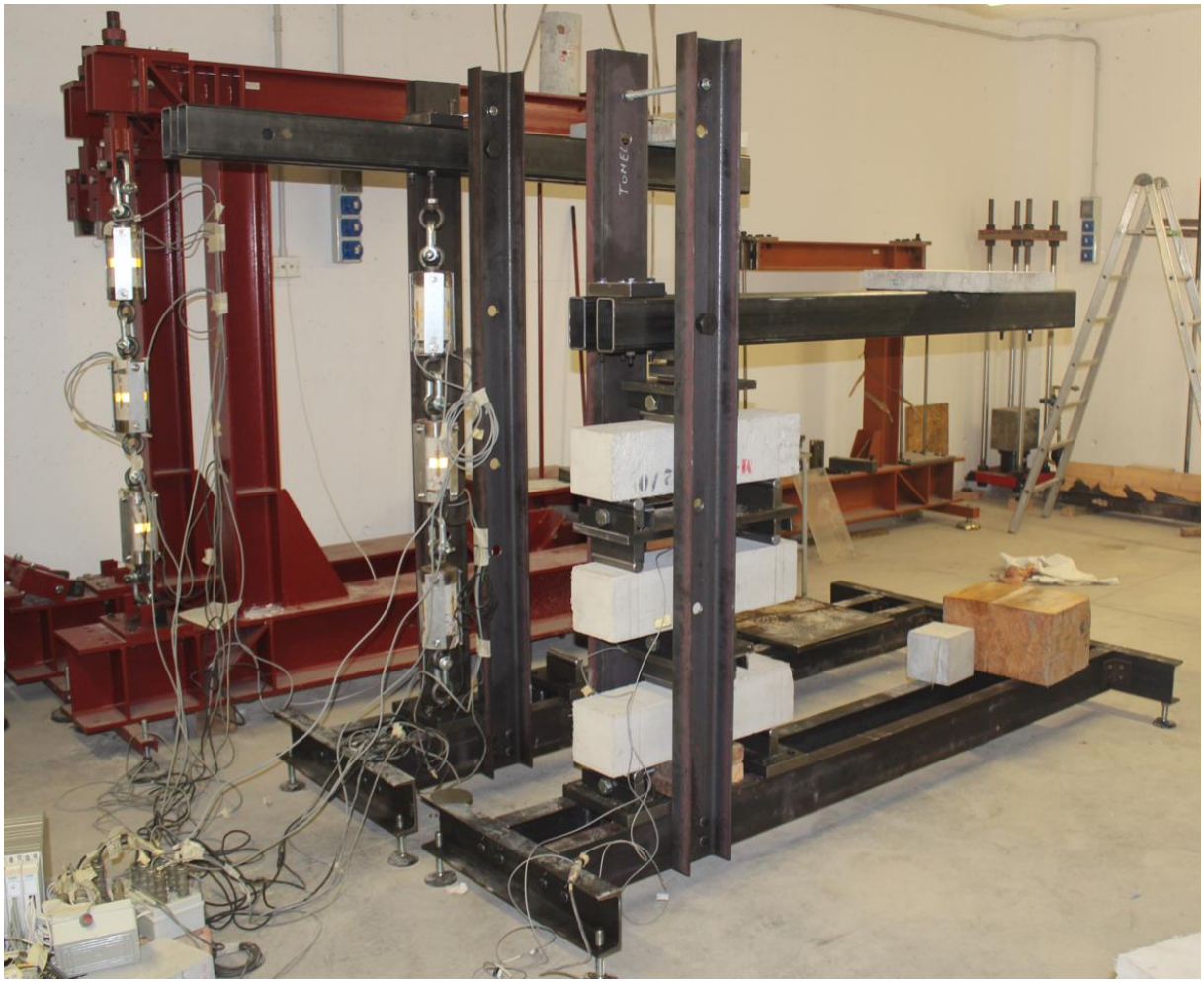

Figure 6.2-Test of the beams in creep, frame on the right

6.2 RESULTS

6.2.1 Three point deflection test

In this part, eight beams are tested:

- *G3_254_8_T1*
- *G3_254_8_T2*
- *G3_254_8_T3*
- *G3_254_8_T4*
- *G3_254_8_T5*
- *G3_254_8_T6*
- *G3_254_8_T7*
- *G3_254_8_T8*

In the figure, 6.3 and 6.4 the graphics of Load-CMOD and Stress-CMOD are shown.

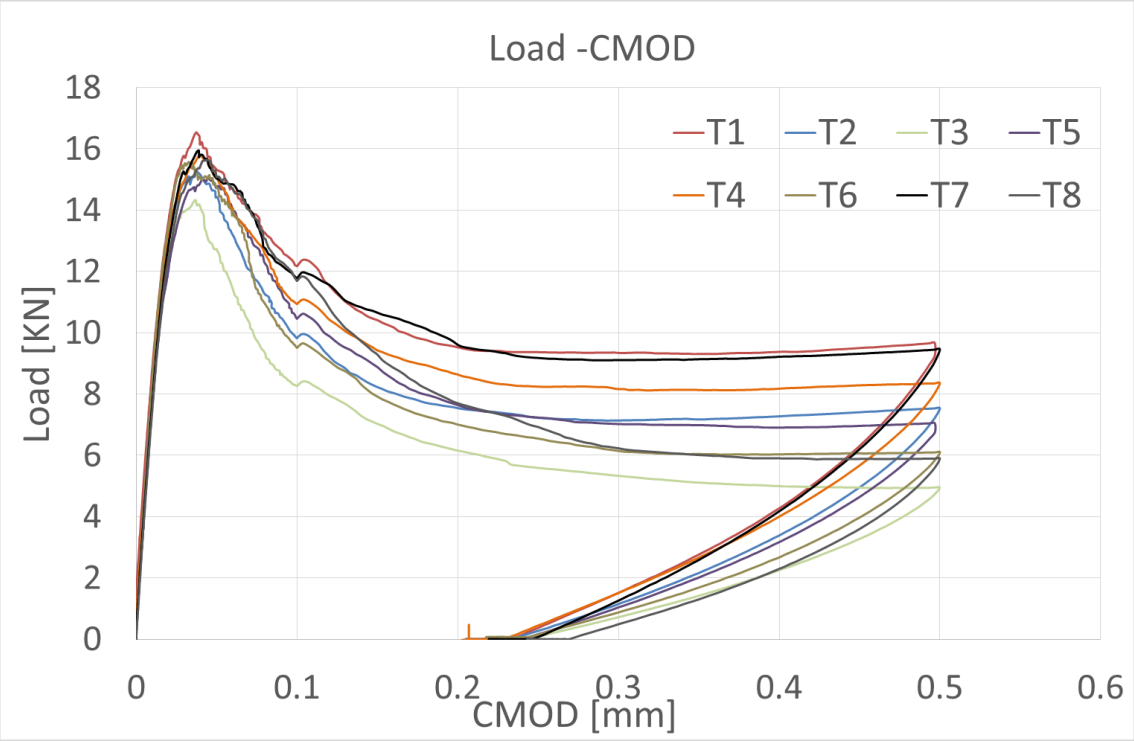

Figure 6.3-Load-CMOD beams specimens

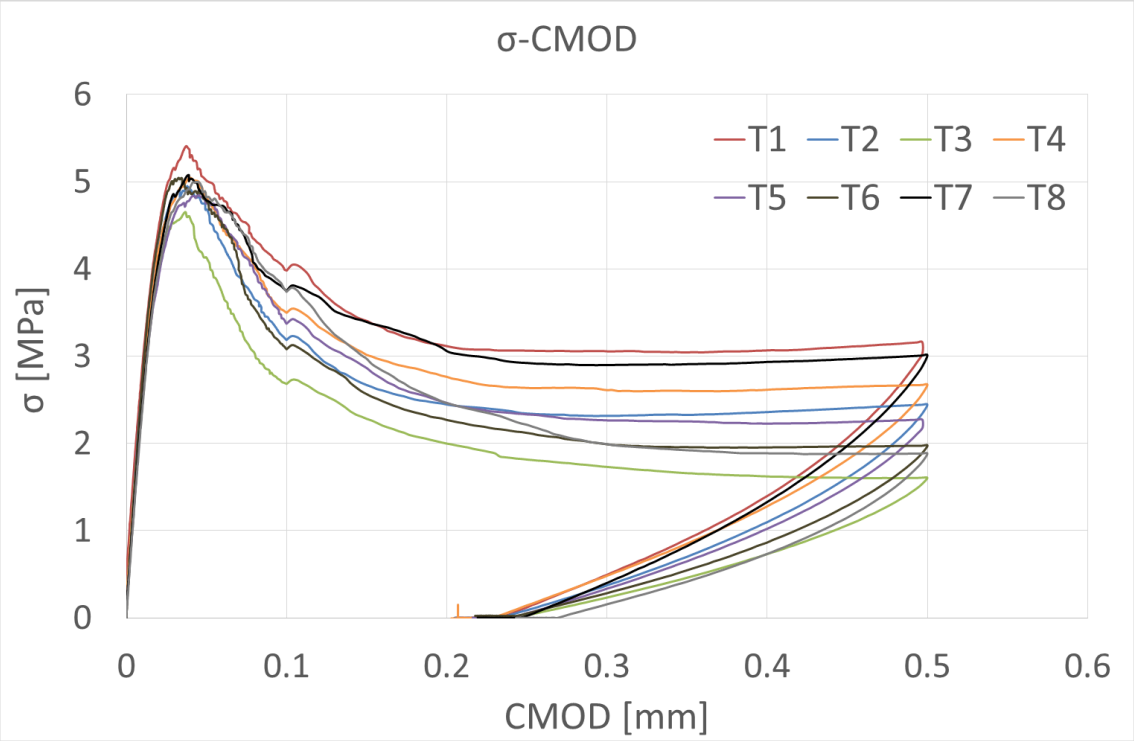

Figure 6.4-σ-CMOD beam specimens

Data of the graphs are summarized in the table 6.1.

Beam	F [kN]	CMOD [mm]	σ [MPa]
1	9.662	0.497	3.160
2	7.534	0.500	2.444
3	4.946	0.500	1.606
4	8.357	0.500	2.673
5	7.049	0.497	2.273
6	6.102	0.500	1.977
7	9.457	0.500	3.011
8	5.894	0.500	1.884

Table 6.1-Summary of pre-cracking test

To perform the creep test, the three with the highest sigma will be selected, in this case *G3_254_8_T1*, *G3_254_8_T4* and *G3_254_8_T7*.

6.2.2 Load beams

In order to known the loads of the beams in creep, the table 6.2 and 6.3 are made.

Code	F Precrack (KN)	L	M	M Creep	L'	F Creep
T4	8.357	500	1045	522	150	6.964
T7	9.457	500	1182	591	150	7.881
T1	9.662	500	1208	604	150	8.052

Table 6.2-Load beams for creep test

Code	Order	Weigth above	Load frame	Load	Relationship	Load ratio
T4	Above	0.19	6.91	7.1	**1.020**	0.51
T7	Middle	0.801	6.91	7.71	**0.978**	0.49
T1	Below	1.302	6.91	8.21	**1.020**	0.51

Table 6.3-Load beams for creep test II

6.2.3 Creep test

The results of the long-term tests are referred to the beams selected *G3_254_8_T1*, *G3_254_8_T4* and *G3_254_8_T7*.

The measurement of time and CMOD starts before the beams are loaded, so it is needed search for time zero as seen in the figure 6.5.

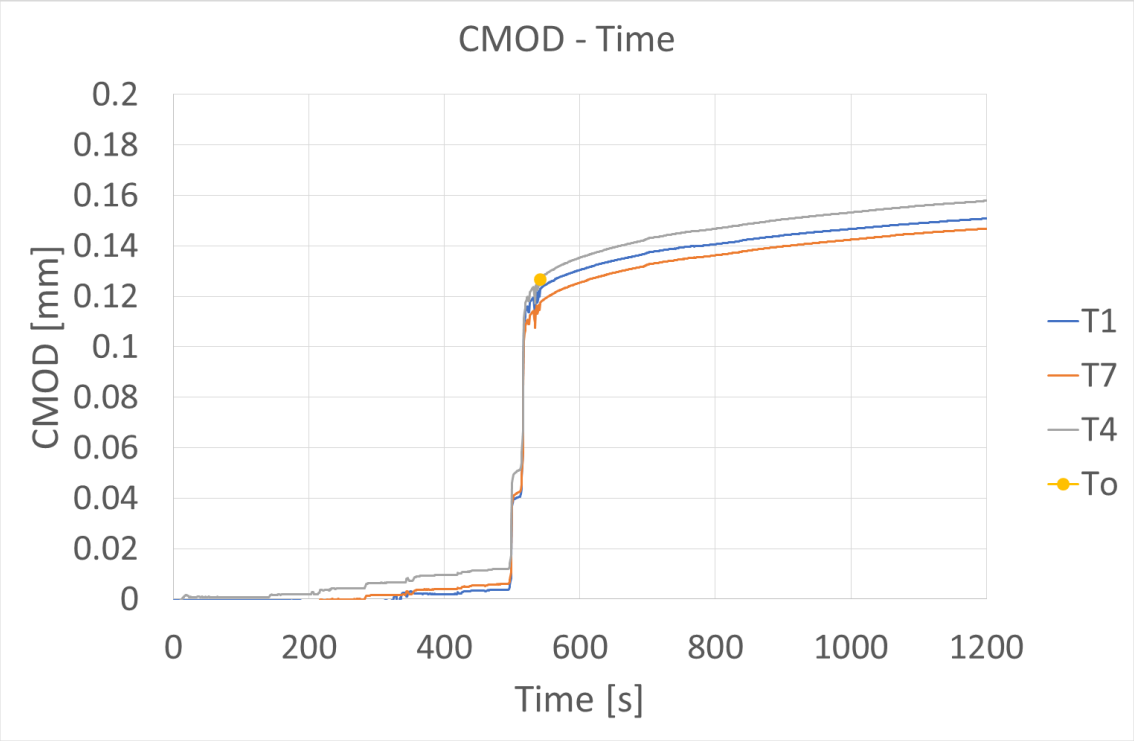

Figure 6.5-CMOD-time for the beams at the start of the test

Once the time zero is defined, the following graphs are made CMOD-time figure 6.6, where it possible to see the how the Crack Mouth Opening Displacement growth versus the time. In the figure 6.7 viscosity coefficient-time, the viscosity coefficient is calculated in the following way:

$$\varphi = \frac{CMODt - CMOD_0}{CMOD_0}$$

Where:

- CMODt, Crack Mouth Opening Displacement in the time t
- $CMOD_0$ Crack Mouth Opening Displacement in the time 0

The figure 6.8 shown the rate of increase of viscosity- time. The rate of increase of viscosity is calculated as the slop of the line between two points, it will be calculated each 6 hours for the first day, each 12 hours for the first 7 days and then for each week.

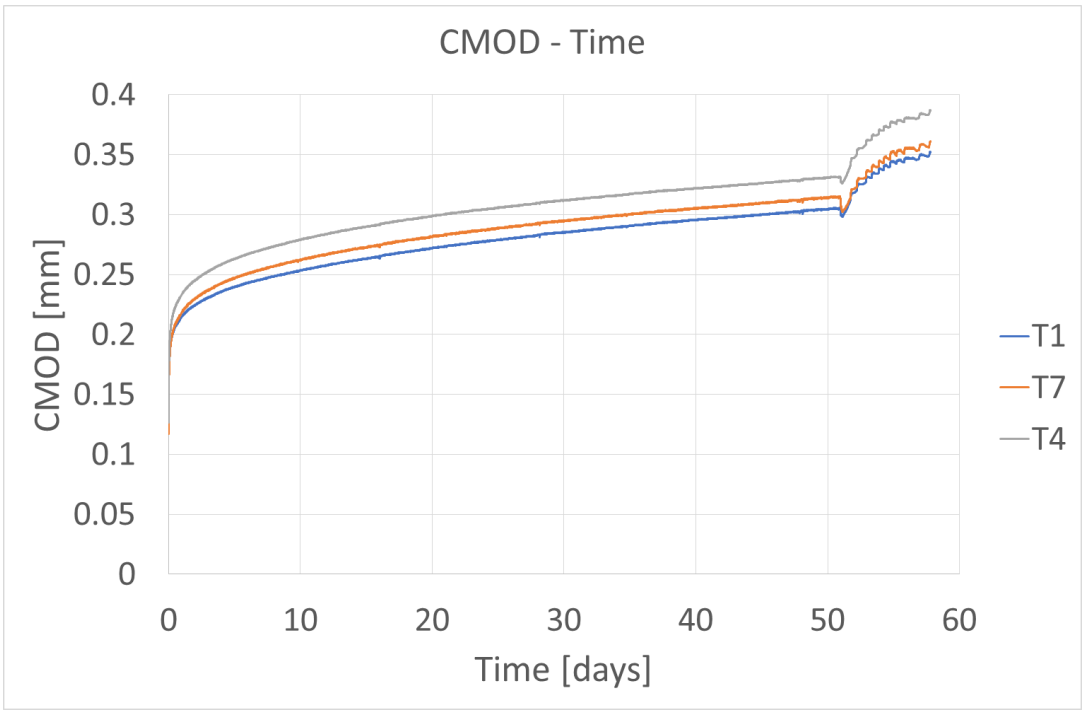

Figure 6.6-CMOD-Time beams T1, T7 and T4.

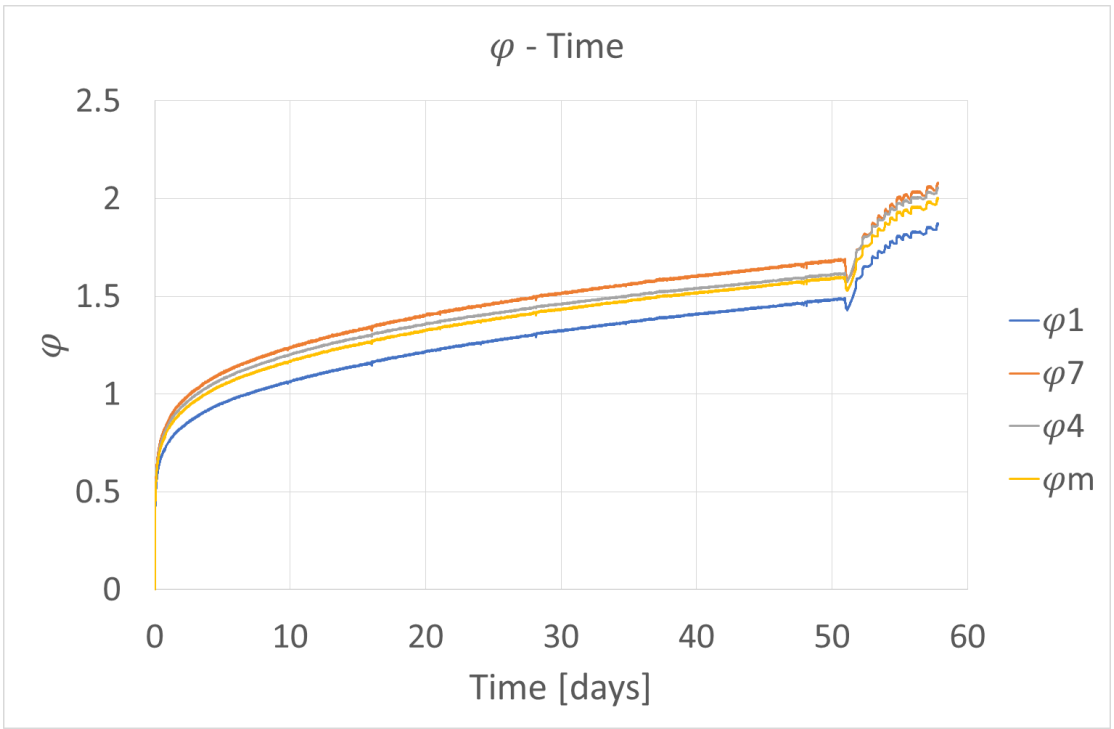

Figure 6.7- φ-Time for beams T1, T7 and T4

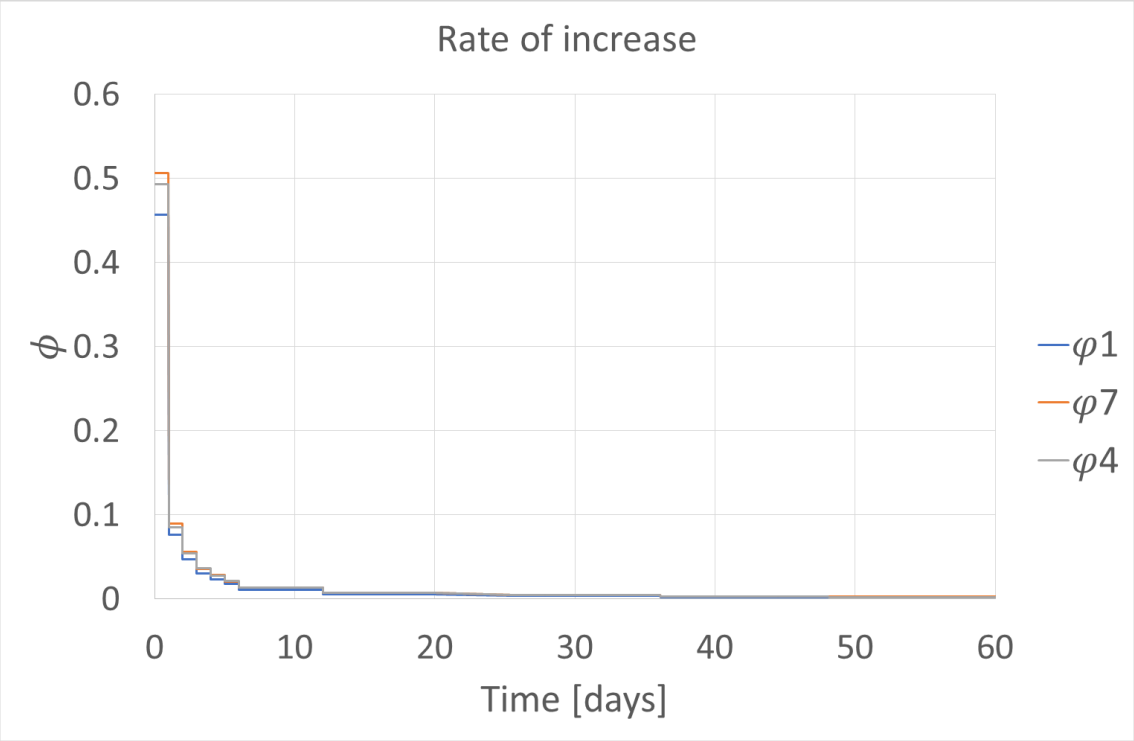

Figure 6.8-Rate of increase-Time for beams T1,T7 and T4

7. Uniaxial tensile creep test on cracked cores

This chapter describes how the uniaxial tensile creep test has been performed and the results obtained. For its realization, as in bending test, it is necessary to carry out two processes, first a pre-cracked of the core with uniaxial tensile test, after this three cylindrical specimens will be chosen and will be testes to creep.

7.1 CONTROL OF THE TEST

7.1.1 Uniaxial test

This test will be carried out measuring the opening of crack (indicated with the terminology Crack Opening Displacement - COD), based on the signals of the Clip-on Gage transducers. In particular, the check was performed on the maximum slot opening, CODMax, and average, CODm. The control, carried out starting from the CODMax and CODm signals, guarantees the stability of the execution of the tests carried out on materials, like fibre-reinforced concretes, which can present a softening behaviour. The CODmax will be controlled until it reaches 0.05 mm. Then, the CODm will be controlled up to a value of 0.2 mm, once the value is reached, test stops. A uniform opening is needed for later carry out the test in creep.

Figure 7.1-Uniaxial test on cylindrical specimens

7.1.2 Creep test on cracked cores

Uniaxial tension tests were carried out using the same loading frames used for bending tests, which were designed in order to accommodate the two different tests setups by modifying the position of the lever. As for bending, a series of three specimens were tested, they were connected using shackles and eyebolts, which were screwed to the steel plates glued at the ends of the cylinders. It is worth noticing that in this setup the ends of the cylinders are free to rotate.

The crack opening displacement was measured on three points around the circumference (120°). To do so strain gauges were applied on the specimens maintaining their central portion (the one crossing the notch) detached. The strains measured were compared with Clip On Displacement transducer measurements in order to calibrate the system. (Buratti & Mazzotti, 2016)

Figure 7.2-Setups long-term uniaxial tension tests

7.2 RESULTS

7.2.1 Short-term

In this part, 12 cylindrical specimens are tested:

- *G4_T2A*
- *G4_T4A*
- *G4_T1C*
- *G4_T1A*
- *G4_T3C*
- *G4_T5B*
- *G4_T4C*
- *G4_T5A*
- *G4_T1B*
- *G4_T2B*
- *G4_T4B*

In the table 7.1 shows those that have had a uniform crack opening, which are marked with OK, those which do not have a homogeneous cracked opening are marked with NO.

Code	Result
G4_T2A	NO
G4_T4A	OK
G4_T1C	NO
G4_T1A	NO
G4_T3C	OK
G4_T5B	NO
G4_T3A	OK
G4_T4C	NO
G4_T5A	OK
G4_T1B	NO
G4_T2B	OK
G4_T4B	OK

Table 7.1-Cylindrial specimens with uniform crack opening

The figures 7.3, 7.4, 7.5, 7.6, 7.8 and 7.9 shown the Load-COD graphs of each selected cylinder.

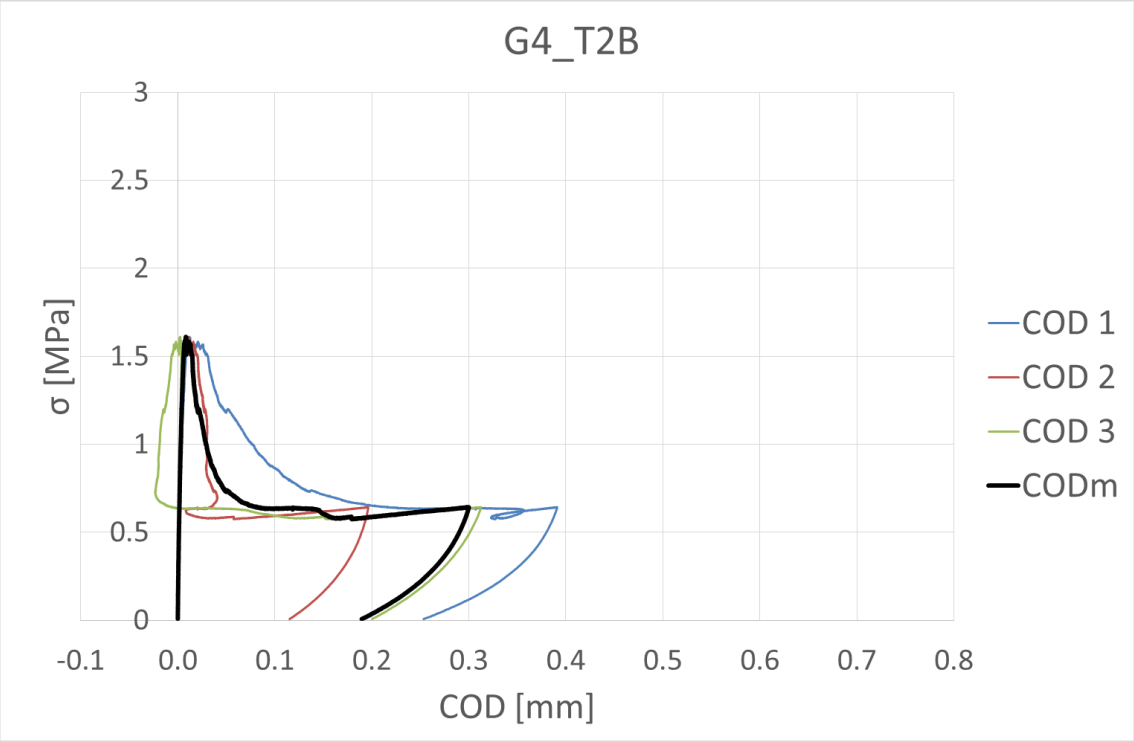

Figure 7.3- σ-COD *G4_T2B*

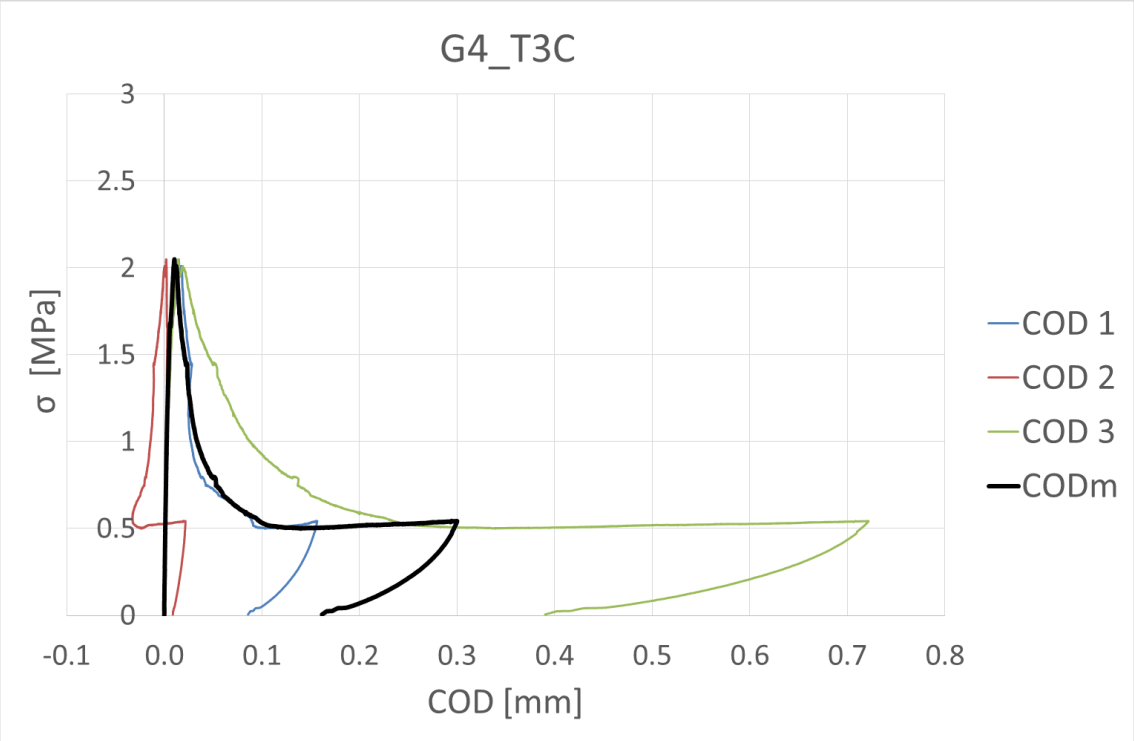

Figure 7.4- σ-COD *G4_T3C*

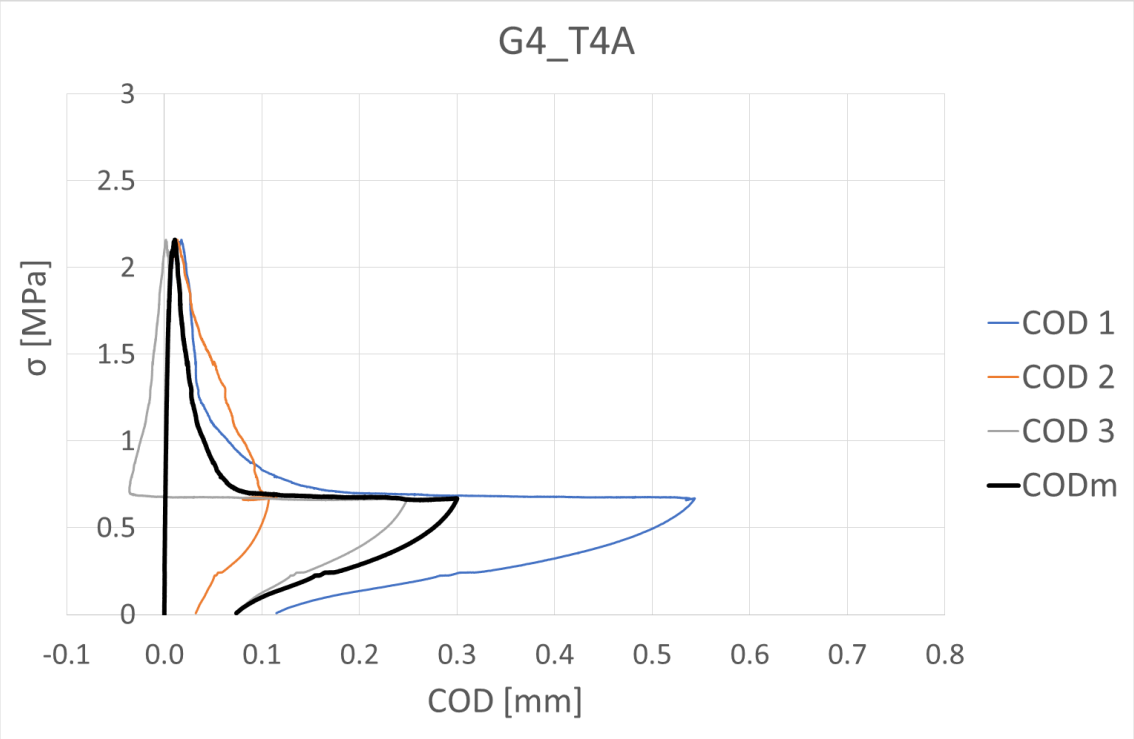

Figure 7.5- σ-COD *G4_T4A*

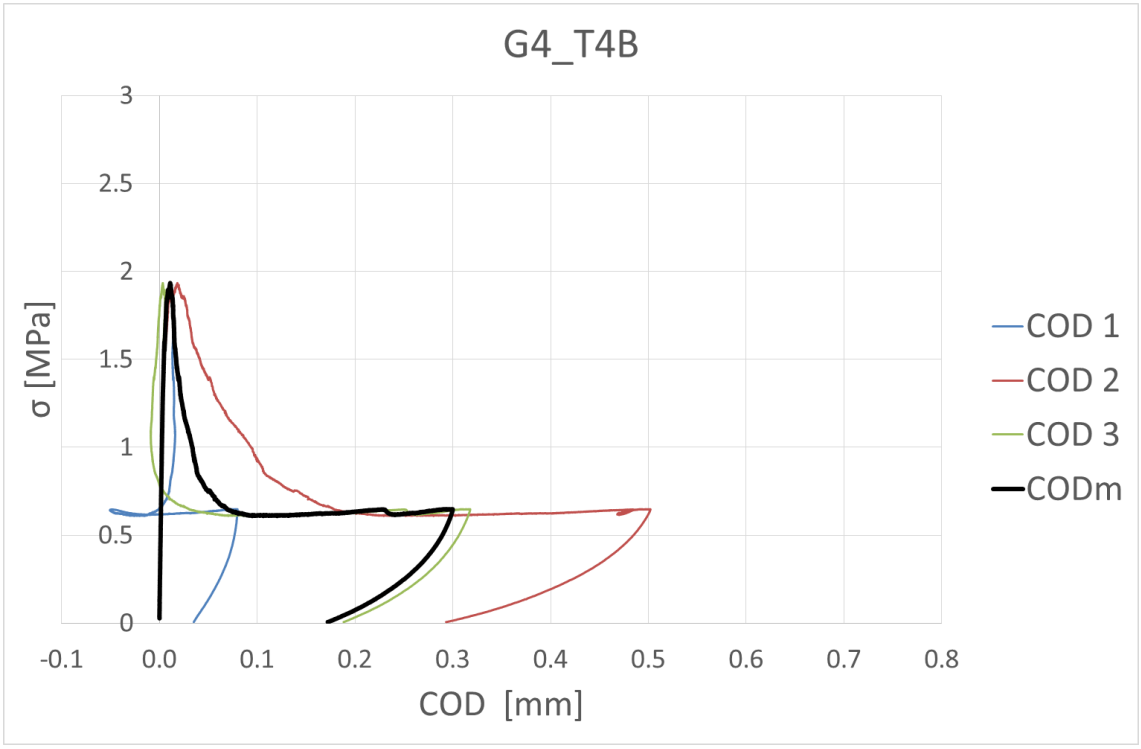

Figure 7.6- σ-COD *G4_T4B*

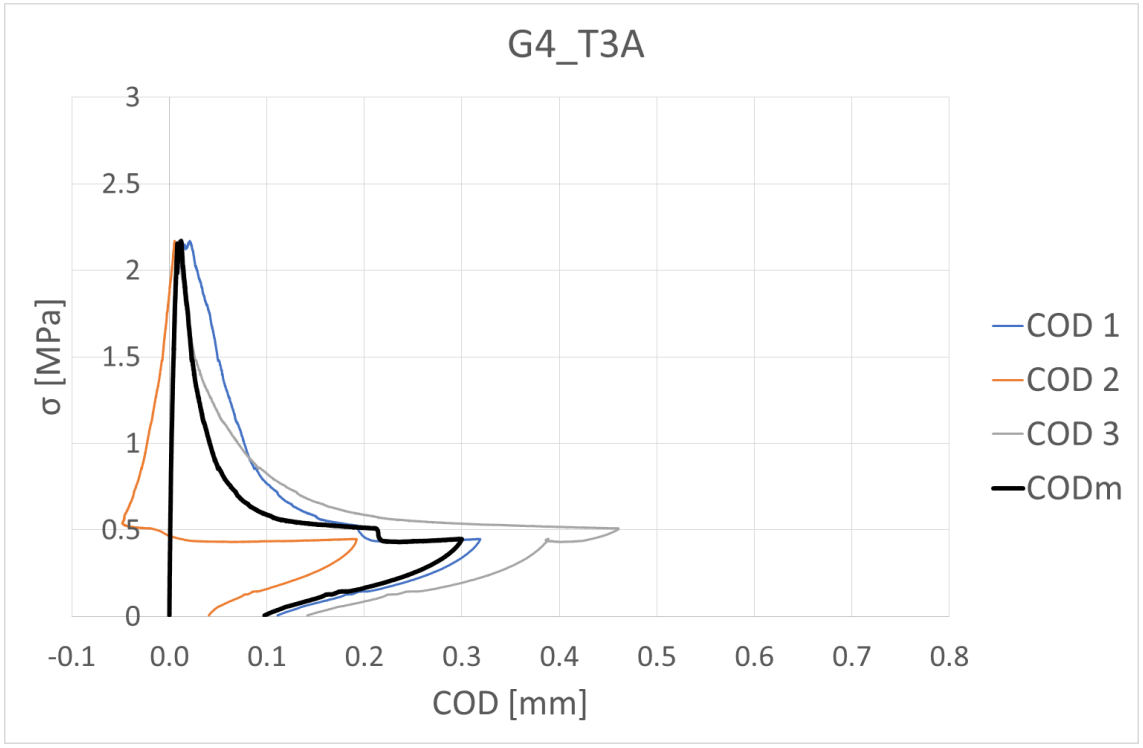

Figure 7.7- σ -COD *G4_T3A*

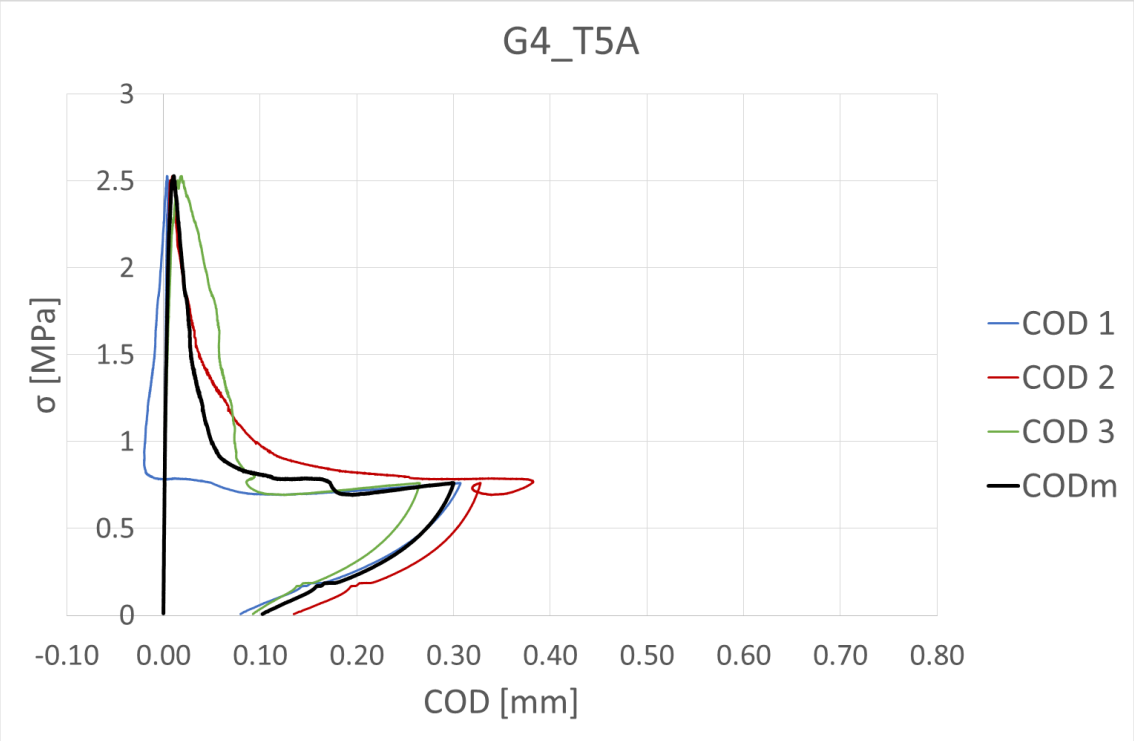

Figure 7.8- σ-COD *G4_T5A*

7.2.2 Load cylinders

Of the cylinders whose crack opening is uniform, we must select three. The table 7.2 shown the COD of the cylinders and the position on the frame. Those cylinders that have undergone almost pure traction have been selected and therefore open the cracks without inflection.

Code	COD1	COD1	COD3	F	CODm	COV COD	Position
G4_T5A	0.30714725	0.32785622	0.26497507	7.93079297	0.29999285	10.68%	Above
G4_T2B	0.39099983	0.19623835	0.312572	6.35831299	0.29993673	32.67%	
G4_T3A	0.31885091	0.19208493	0.38890415	4.56013721	0.29994667	33.26%	Middle
G4_T4B	0.07979696	0.50206837	0.3177812	6.38746484	0.29988218	70.60%	
G4_T4A	0.5436996	0.10719679	0.24917041	6.93710352	0.30002226	74.21%	
G4_T3C	0.15663457	0.02169378	0.72172727	5.37605713	0.30001854	123.79%	Below

Table 7.2- Summary of cylindres and position on the frame

7.2.3 Long-term

The results of the long-term tests are referred to the cylinders selected *G4_T5A*, *G4_T3A* and *G4_T3C*.

The figures 7.9, 7.10 and 7.11 shown the evolution of COD over the time for each cylinder and 7.12 the average of all of them. The figures 7.13, 7.14 and 7.15 viscosity coefficient-time for each cylinder and 7.16 for the average, and figures 7.17, 7.18 and 7.19 the increasing of viscosity- time for each cylinder and 7.20 for the average.

In figures referred to cylinder *T3A*, two averages can be seen; one is referred to three COD, as for the other cylinders, and another one is only referred to the COD1 and COD2 because COD3 instead of opening is closed.

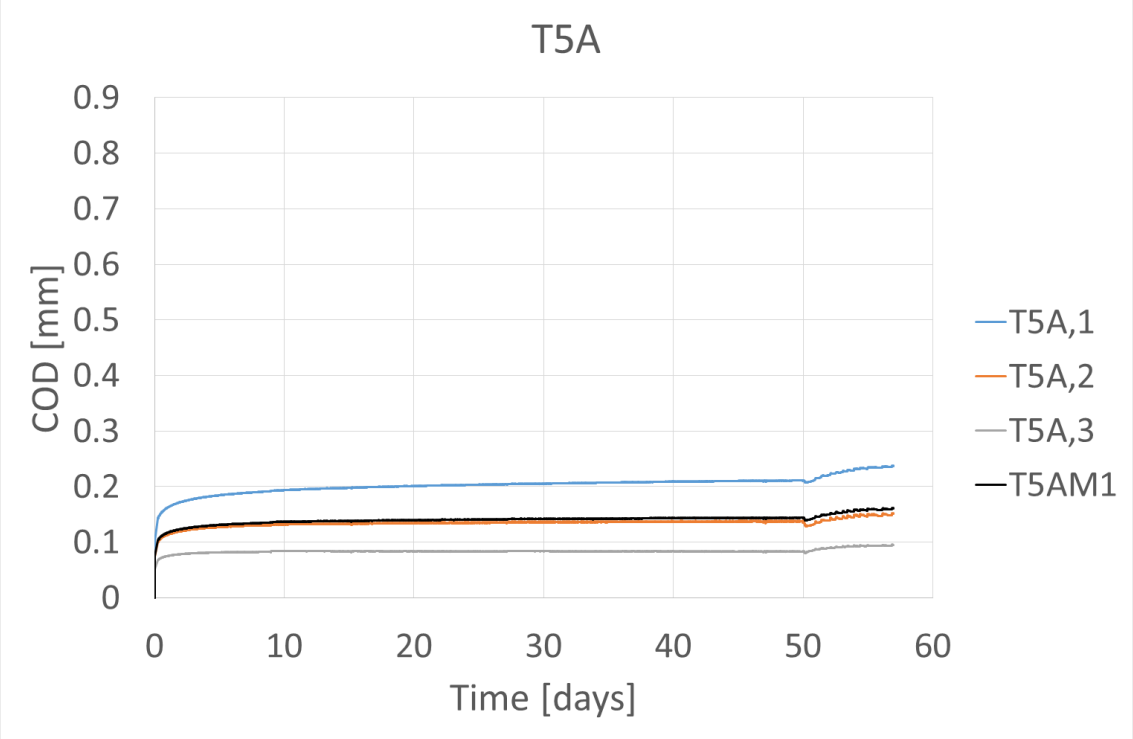

Figure 7.9-COD-time cylinder T5A

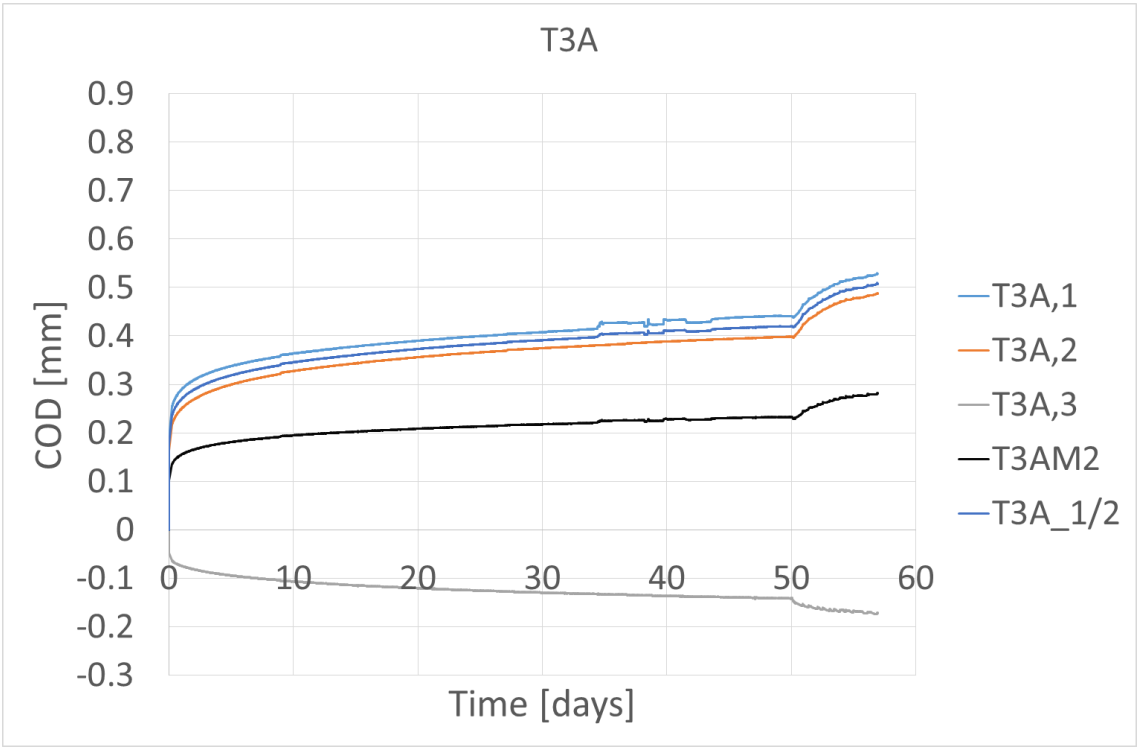

Figure 7.10-COD-time cylinder T3

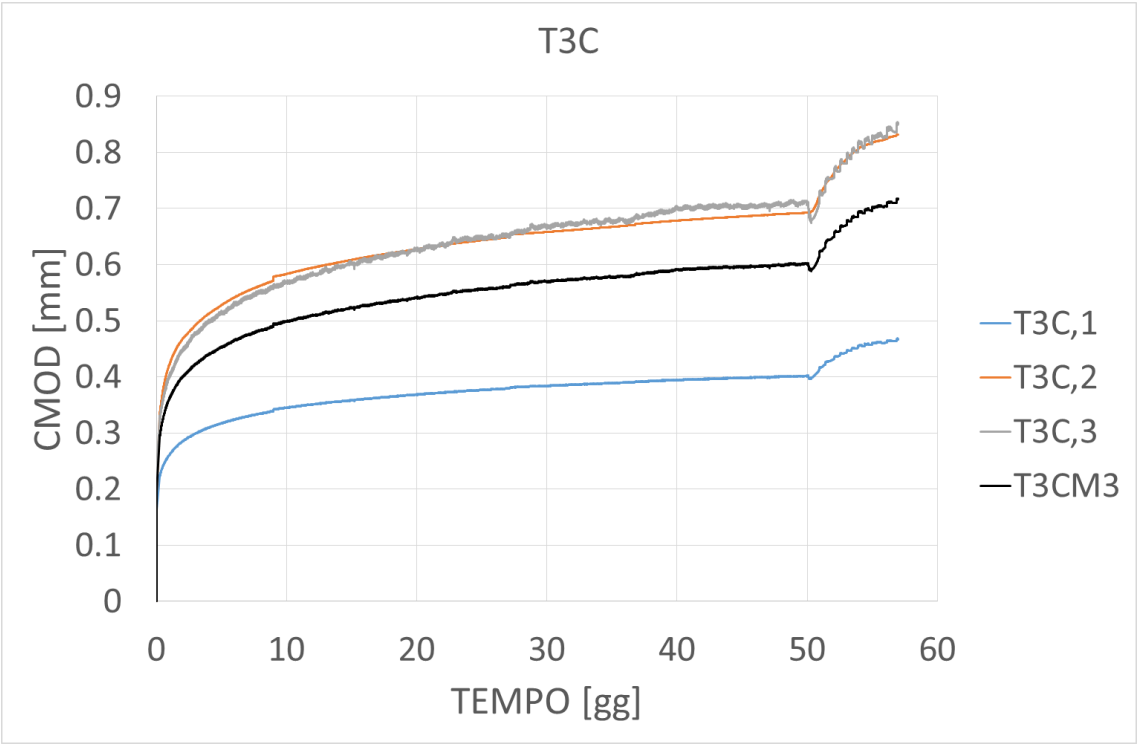

Figure 7.11-COD-time cylinder T3C

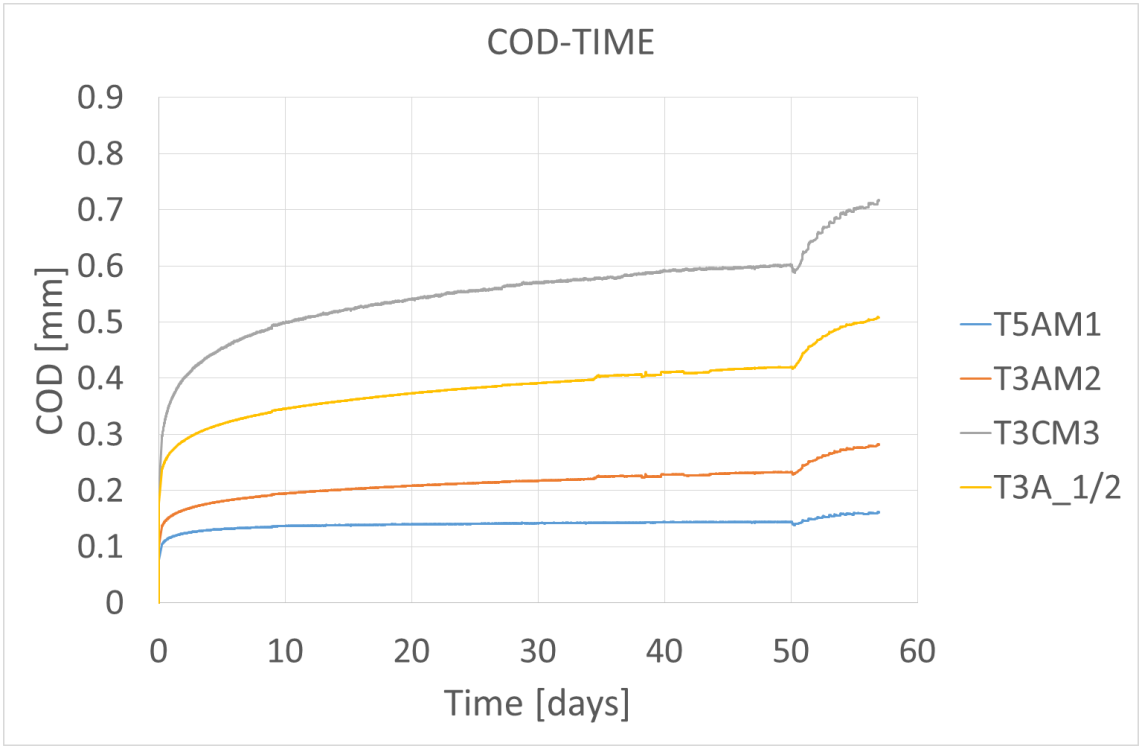

Figure 7.12-COD-time of the average of the cylinders

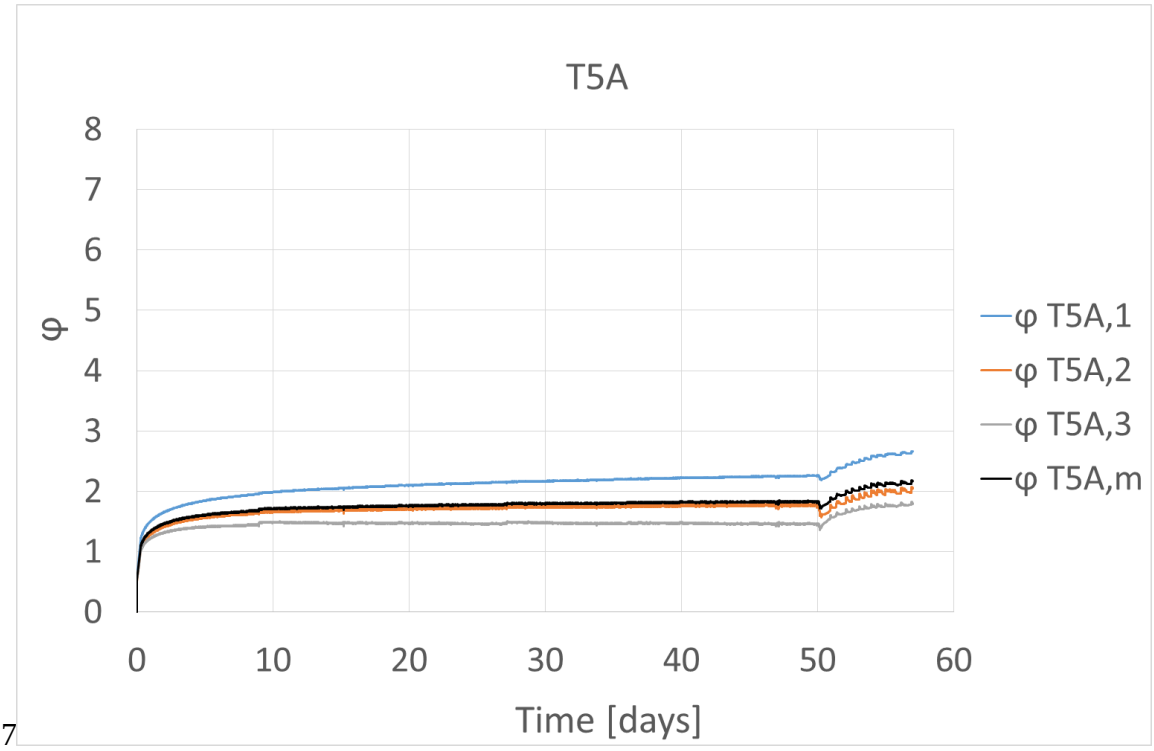

7

Figure 7.13-φ-Time cylinder T5A

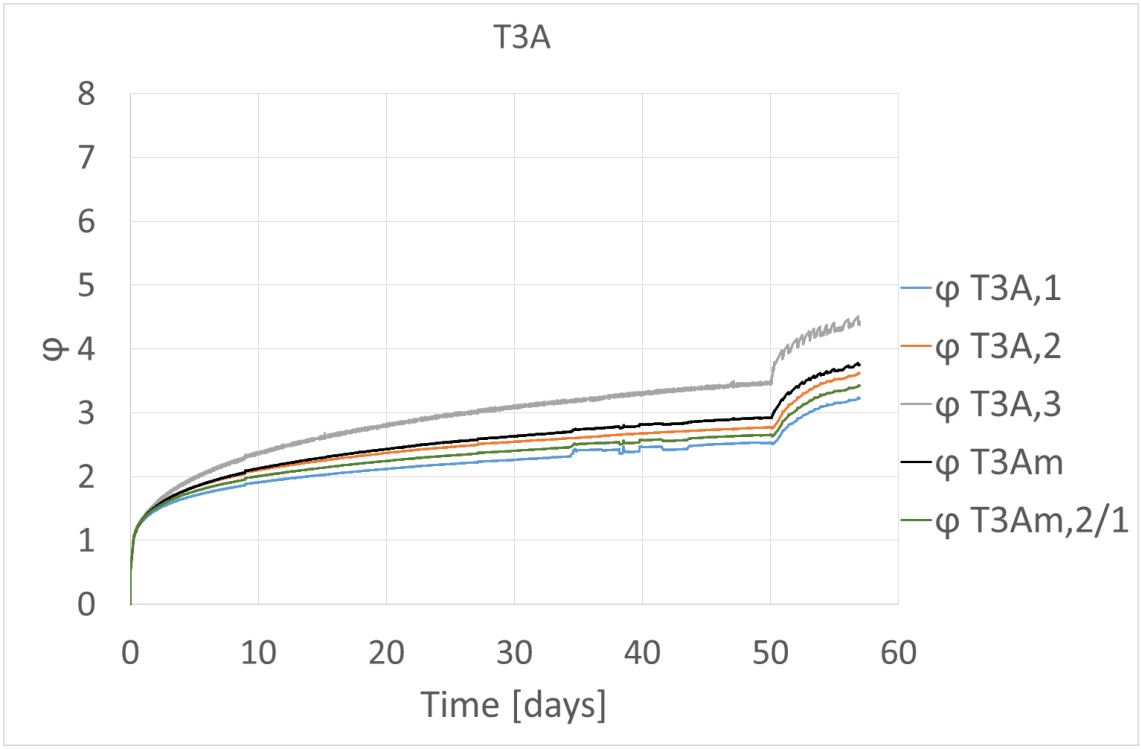

Figure 7.14-φ-Time cylinder T3A

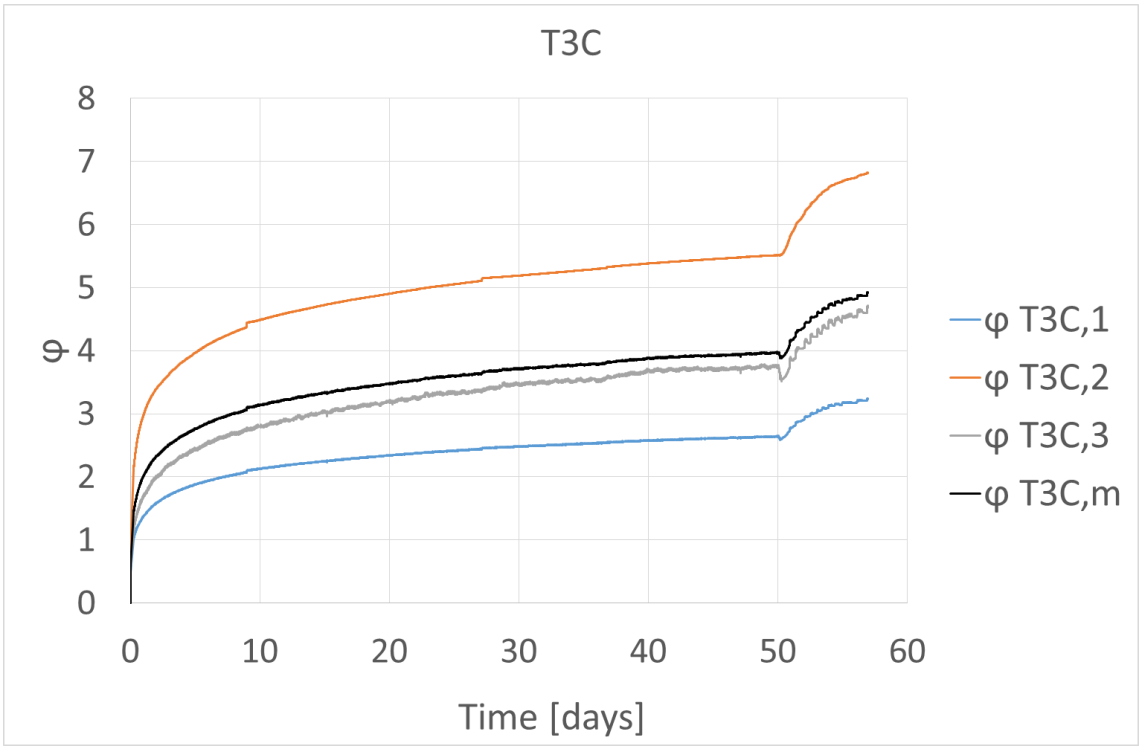

Figure 7.15-φ-Time cylinder T3C

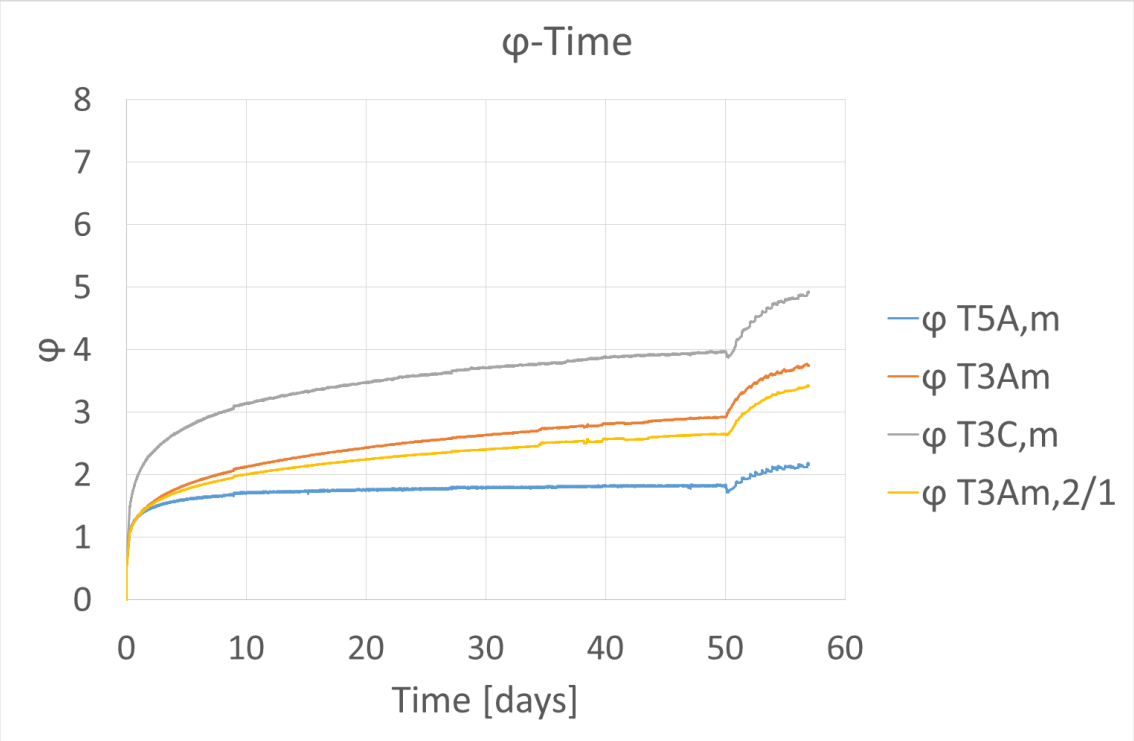

Figure 7.16-φ-Time of the average of the cylinders

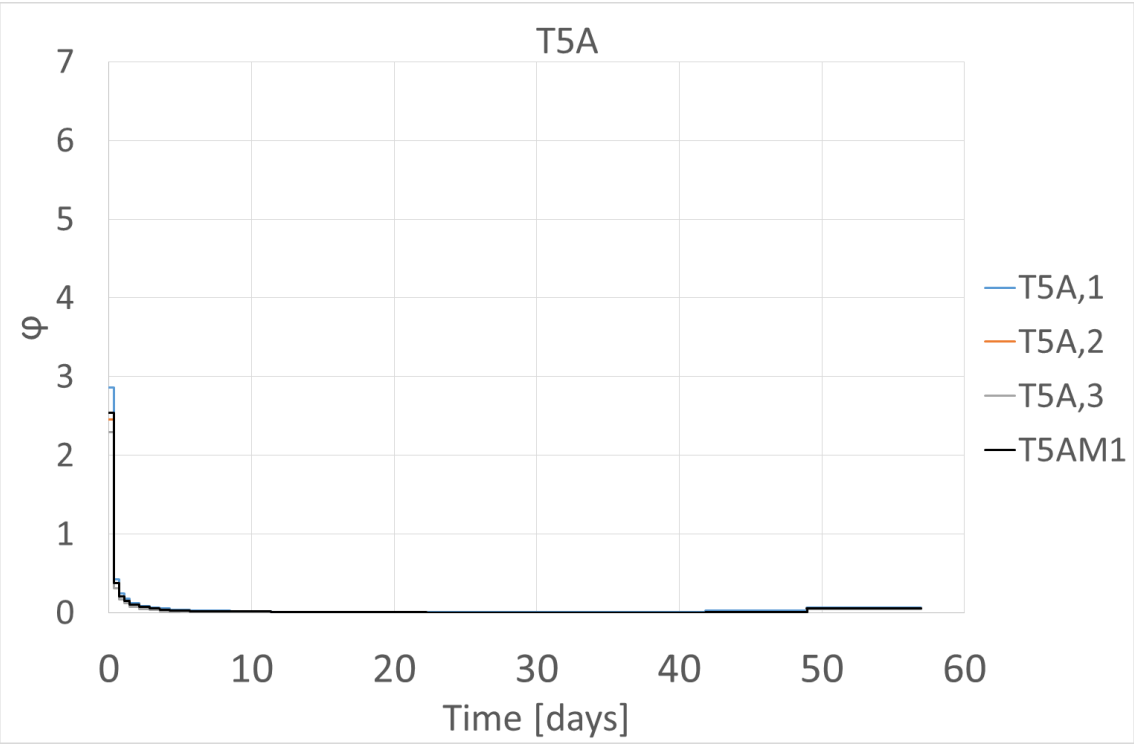

Figure 7.17-Rate of increase-Time T5A

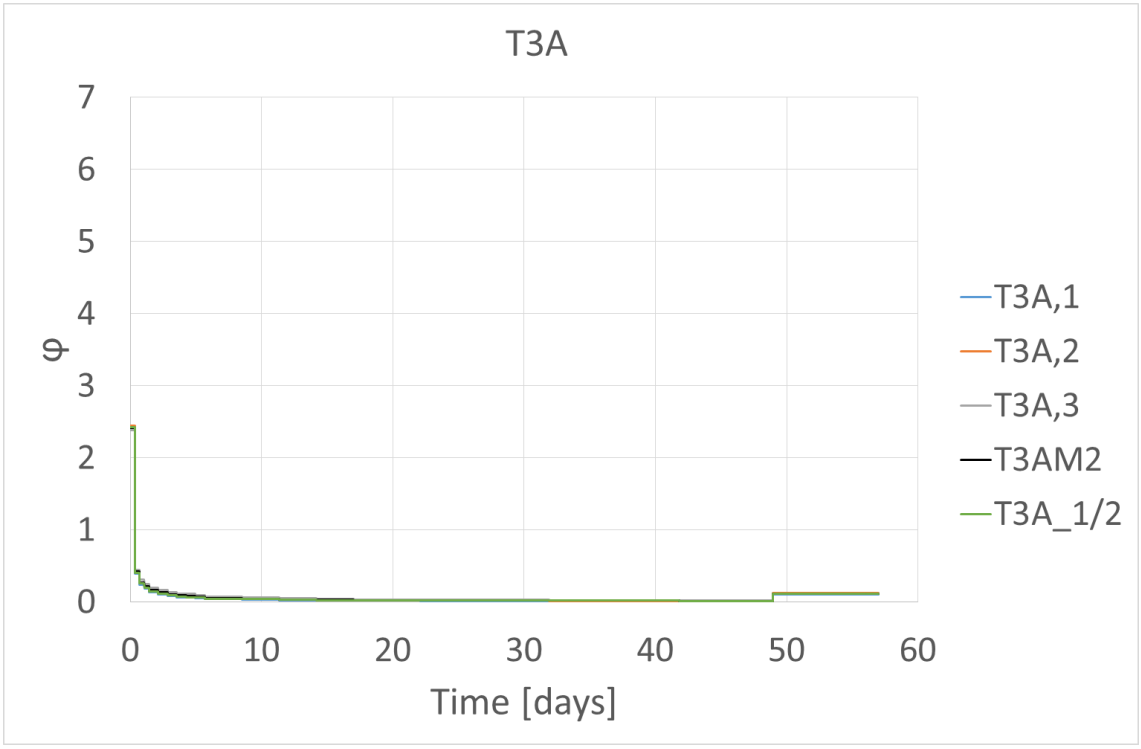

Figure 7.18-Rate of increase-Time T3A

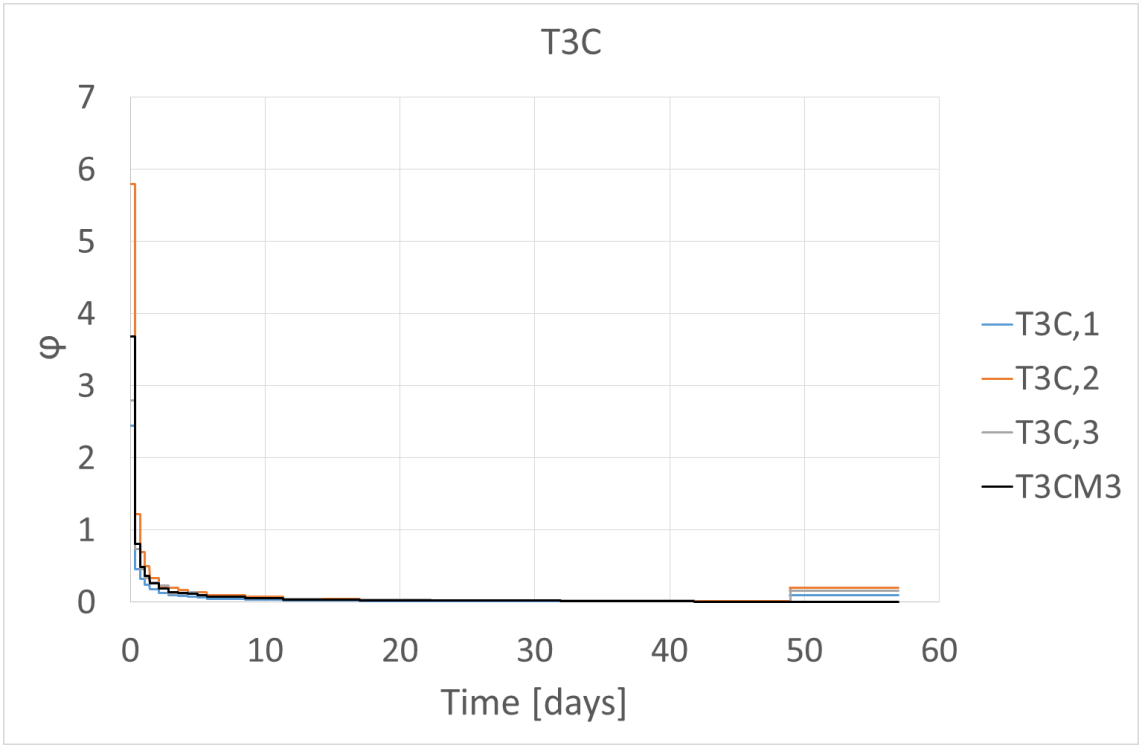

Figure 7.19-Rate of increase-Time T3C

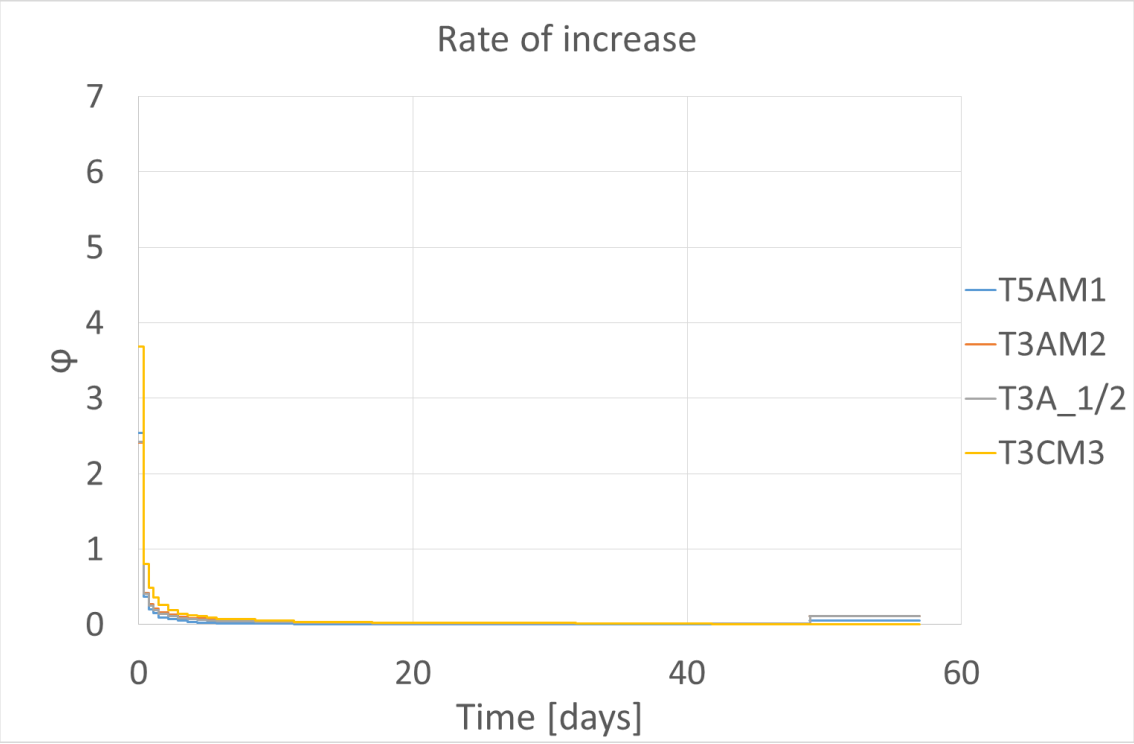

Figure 7.20-Rate of increase-Time of the average of cylinders

8. Direct tensile test on single fibres

This chapter describes how tensile test has been performed and the results obtained. There will be two test, one in short-term and a second one in long-term. Finally, the results obtained are shown.

8.1 CONTOL OF THE TEST

8.1.1 Short-term

The MTS Landmark 500 machine is used to carry out the test. In order to execute the test, the ends of the fibres were mechanically clamped of the aluminum plates, mediated bolting. In particular, a system composed of lower plates, fibre and superior plate was created.

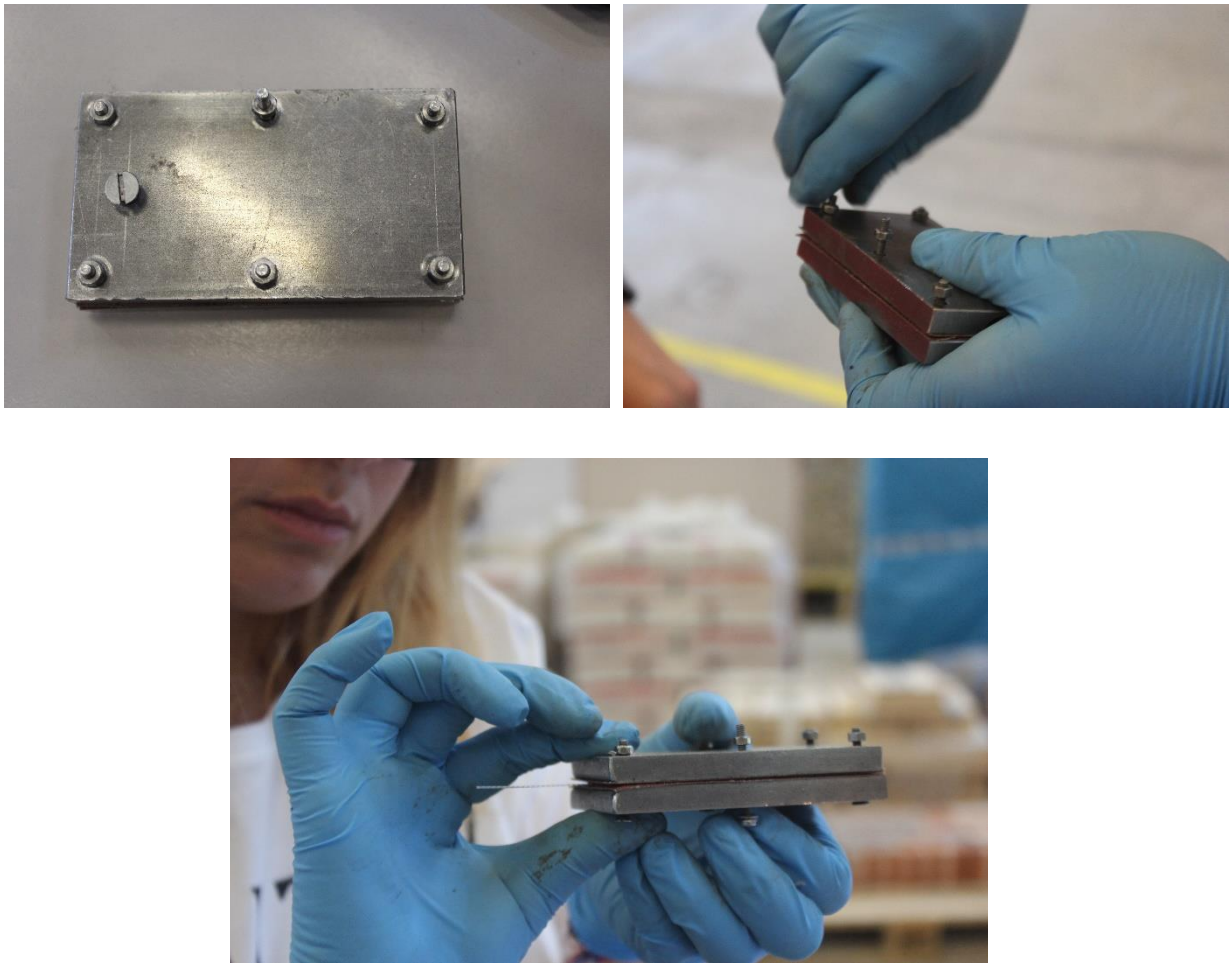

Figure 8.1-System of plates for short-term test of single fibres

The test was performed with a machine control based on the movement of the actuator. The figure 8.2 shows the moment in which the test was performed.

Figure 8.2- Machine control of tensile test

Figure 8.3-Tensile test on single fibre

8.1.2 Long-term

For the long-term test the frame of figure 8.4 is used. The fibre is glued with X60 at both ends 1.5 cm. Two LVDTs will be used to measure their elongation. The fibres are loaded to 20%.

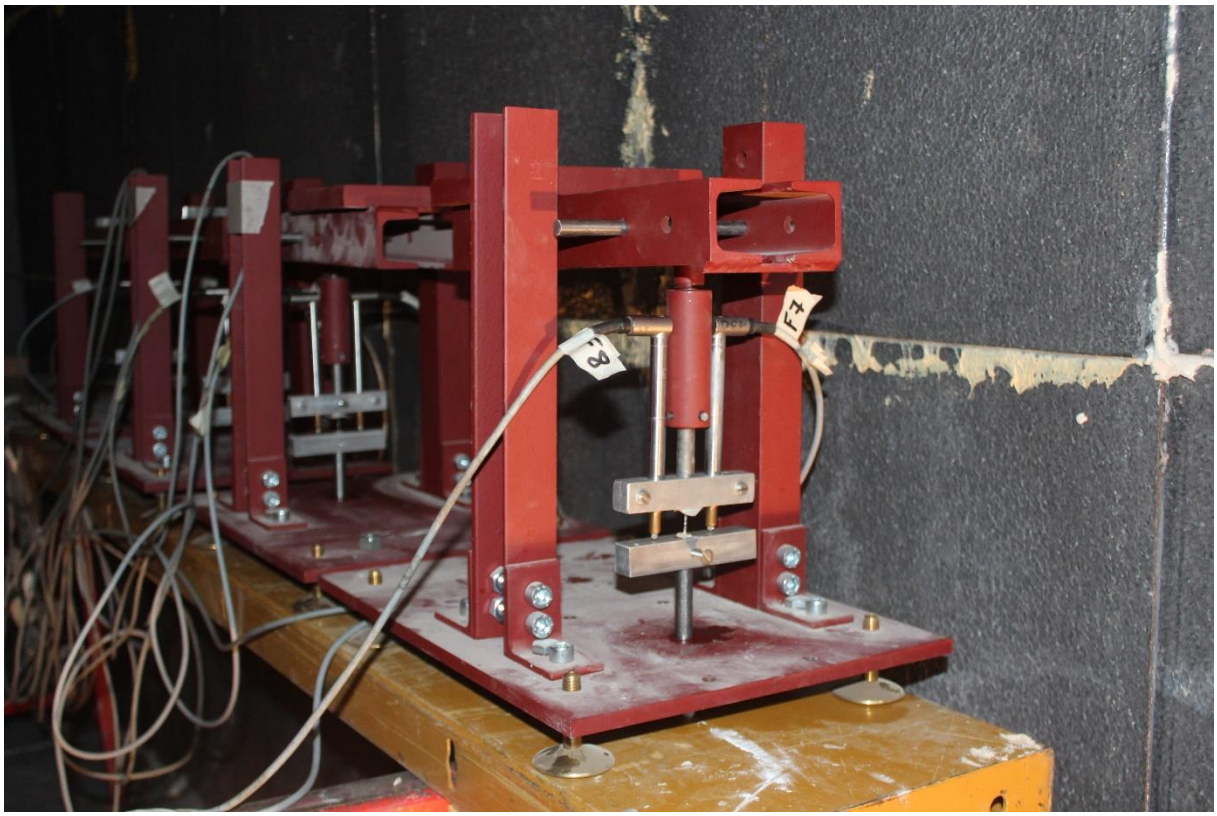

Figure 8.4-Tensile long-term test

8.2 RESULTS

8.2.1 Short-term

In this part, eleven fibres are tested:

- *BASF_B1*
- *BASF_B2*
- *BASF_B3*
- *BASF_B4*
- *BASF_B5*
- *BASF_B6*
- *BASF_B7*
- *BASF_B8*
- *BASF_B9*
- *BASF_B10*
- *BASF_B11*

The table 8.1 summarizes the test carried out and the figures 8.5 and 8.6 Load-Displacement and the Stress-Displacement of each fibres. The fibres are loaded at 30%, which is 9.75 kg.

Code	Area (mm2)	Peak Force (KN)	Peak resistance (MPa)	Peak resistance (Kg)
BASF_B1	0.515299735	0.2176	422.2785	21.76
BASF_B2	0.515299735	0.2056	398.9911	20.56
BASF_B3	0.515299735	0.2226	431.9816	22.26
BASF_B4	0.515299735	0.2691	522.2203	26.91
BASF_B5	0.515299735	0.2436	472.7346	24.36
BASF_B6	0.515299735	0.2351	456.2393	23.51
BASF_B7	0.515299735	0.2786	540.6562	27.86
BASF_B8	0.515299735	0.2536	492.1408	25.36
BASF_B9	0.515299735	0.2691	522.2203	26.91
BASF_B10	0.515299735	0.2606	505.7251	26.06
BASF_B11	0.515299735	0.2244	435.4747	22.44
Average		0.2436	472.7875	24.363

Table 8.1-Summary of tensile of fibres

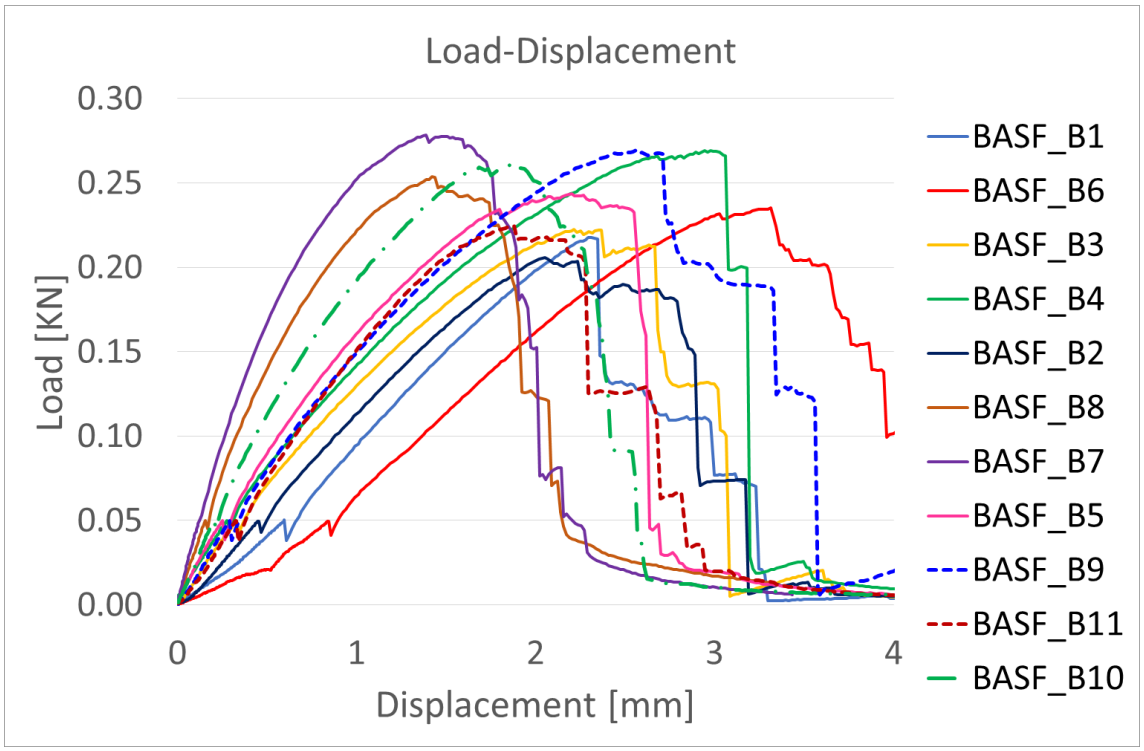

Figure 8.5-Load-Displacement of each fibres

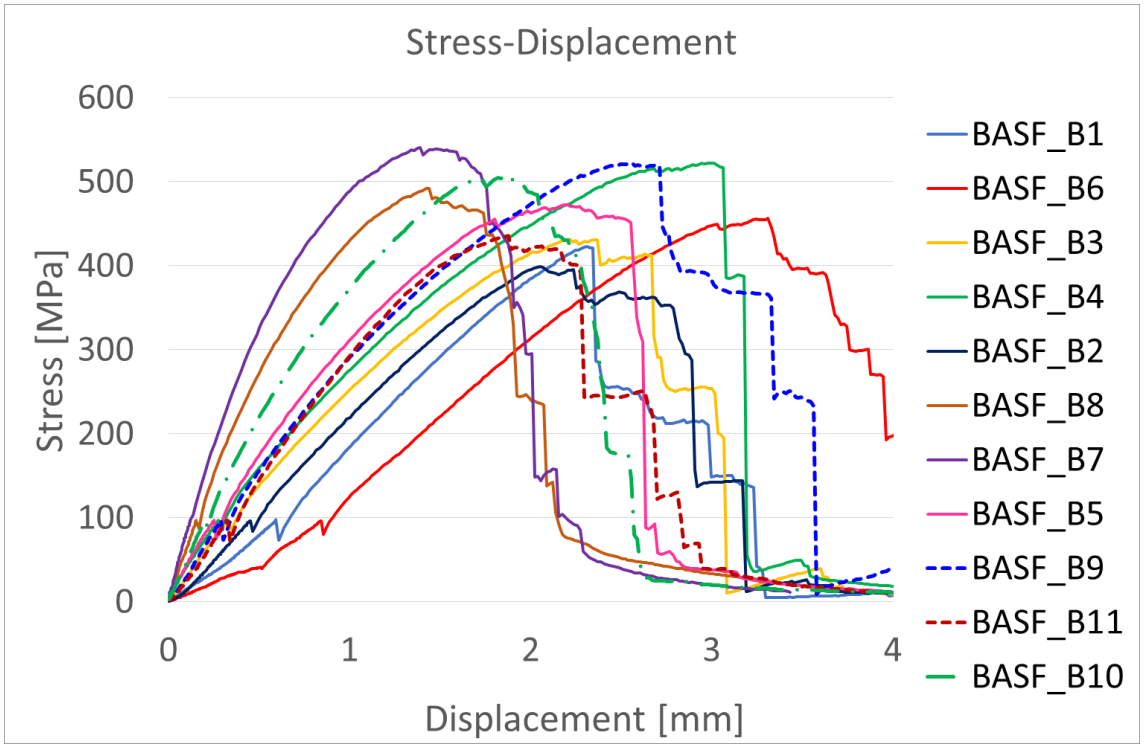

Figure 8.6-Stress- Displacement of each fibres

8.2.2 Long-term

For these tests two fibres, called F1 and F2, loaded at 20% were used. As mentioned above, two LVDTs are used for the measurement. The figures 8.7, 8.8 and 8.9 shown the Deformation-Time, φ-Time and Rate of increase-Time of the fibre 1. The figures 8.10, 8.11 and 8.12 shown the Deformation-Time, φ-Time and Rate of increase-Time of the fibre 2. The figures 8.13, 8.14 and 8.14 shown the Deformation-Time, φ-Time and Rate of increase-Time of the average of the fibres.

For the F2 fibre in Figure 8.10 it can be seen that the LVDT1 grows and the LVDT2 decreases, this is due to a rotation of the fibre.

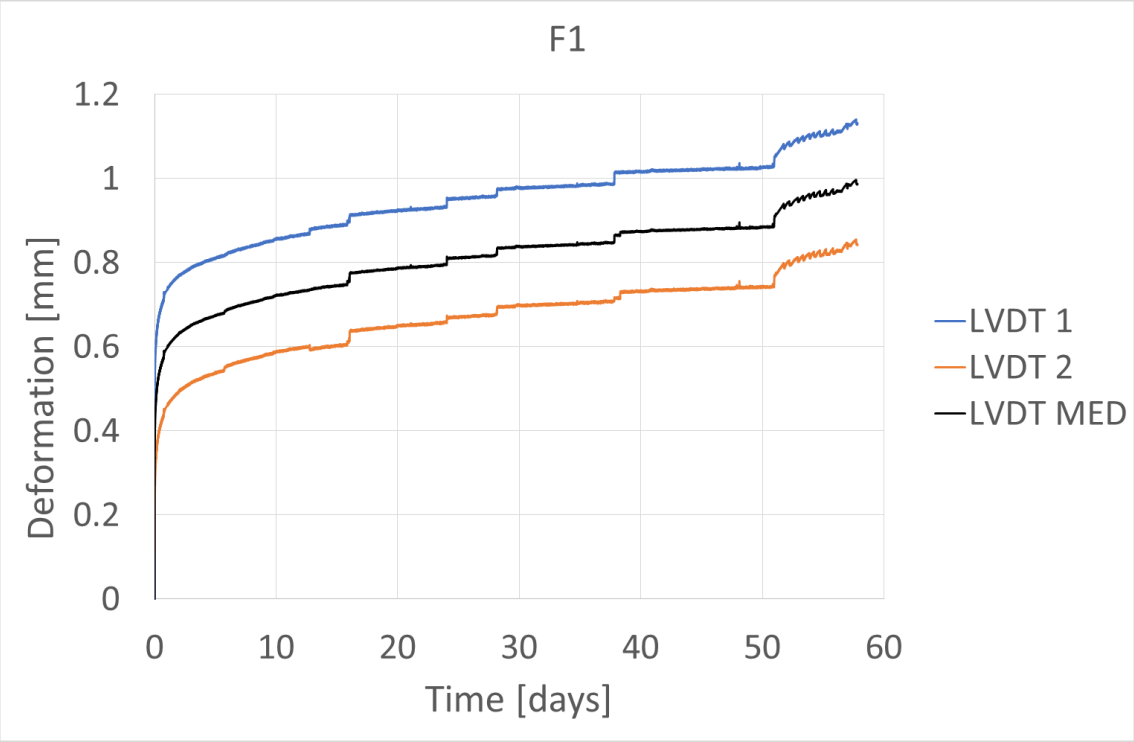

Figure 8.7-Deformation-Time F1

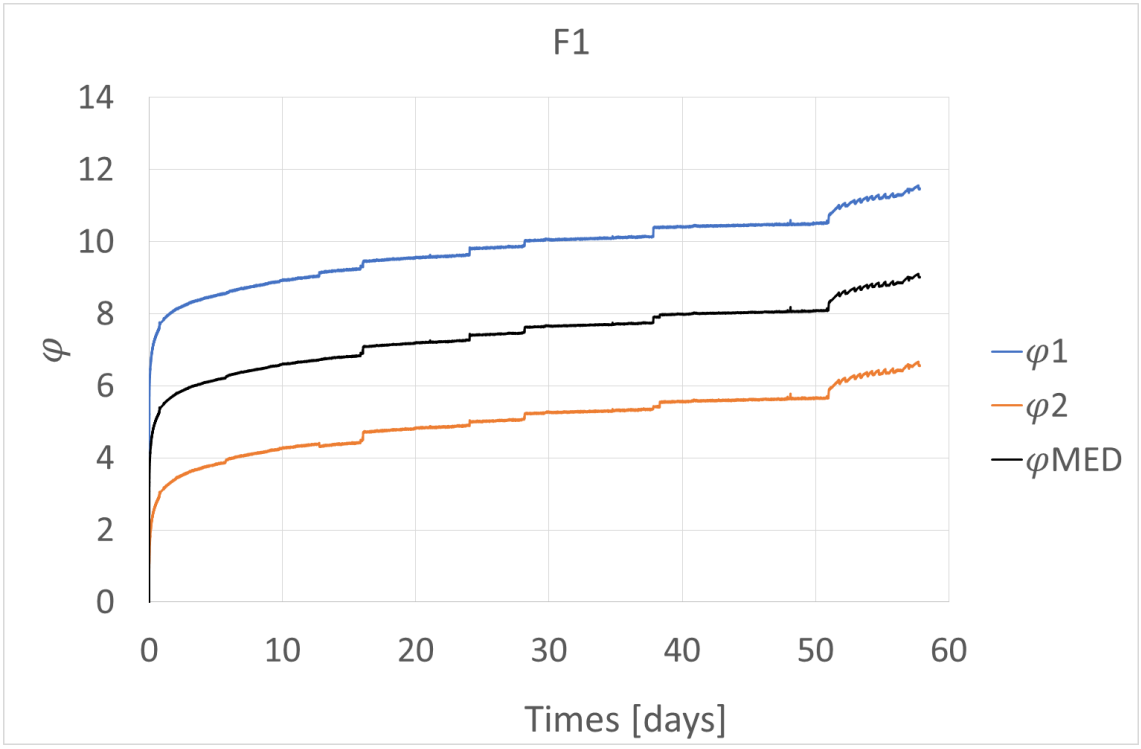

Figure 8.8-φ-Time F1

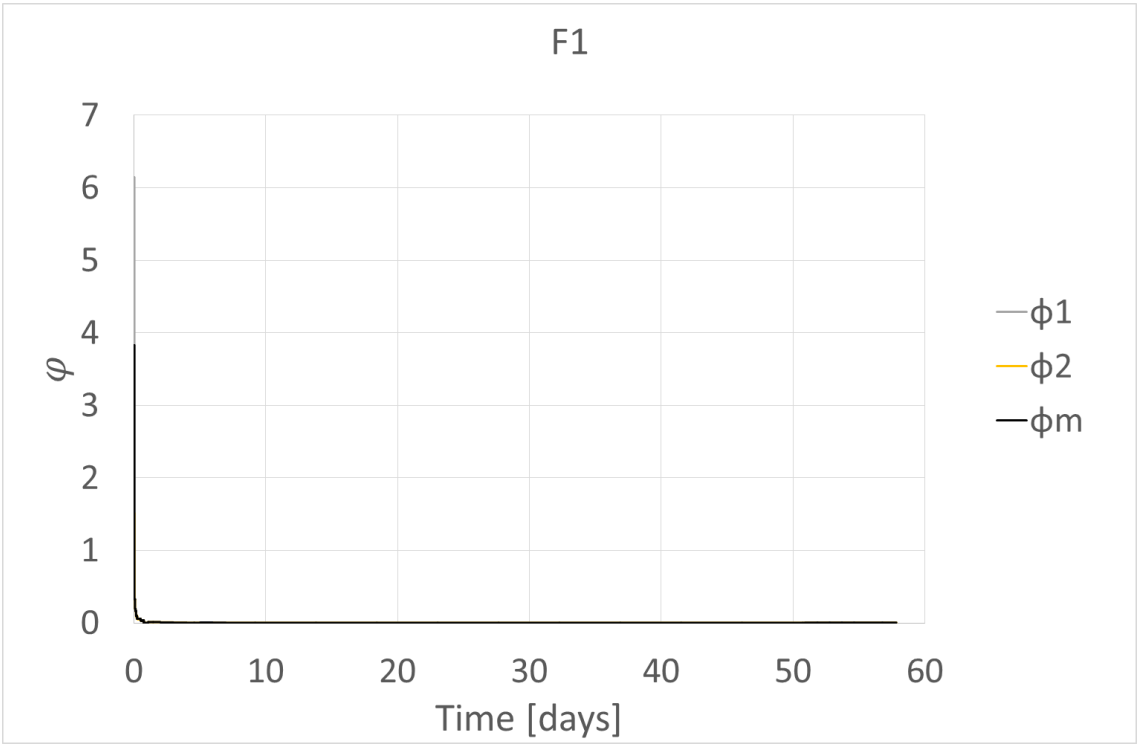

Figure 8.9-Rate of increase-Time F1

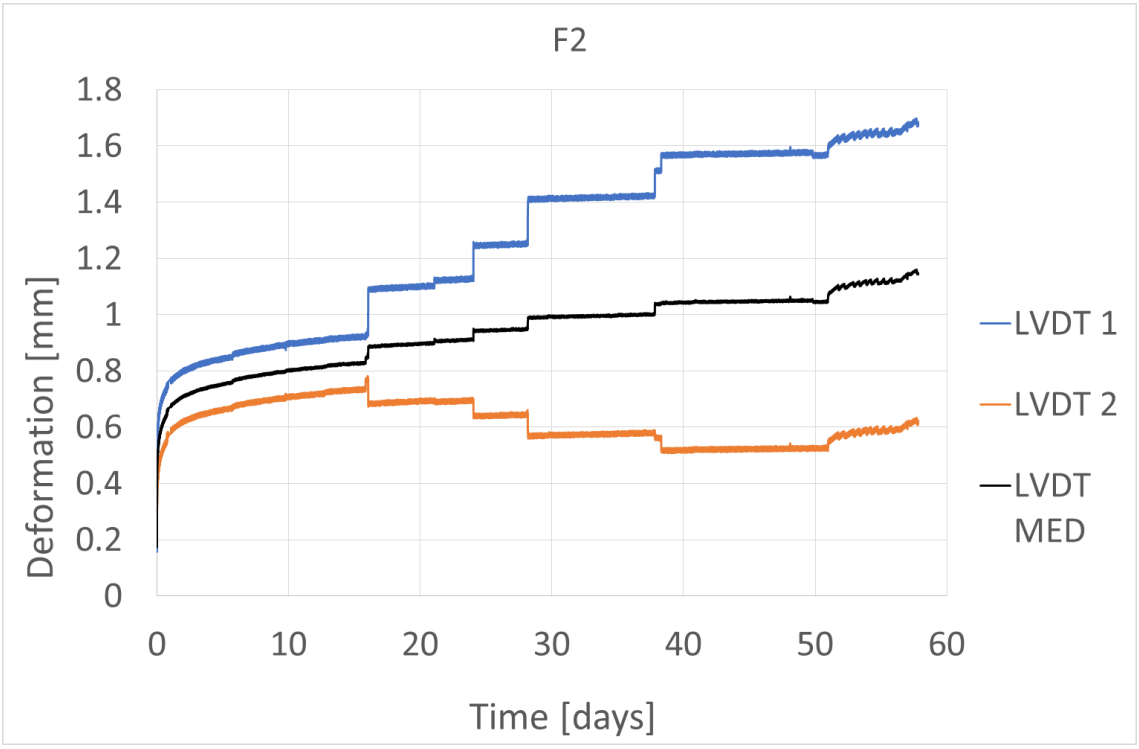

Figure 8.10-Deformation-time F2

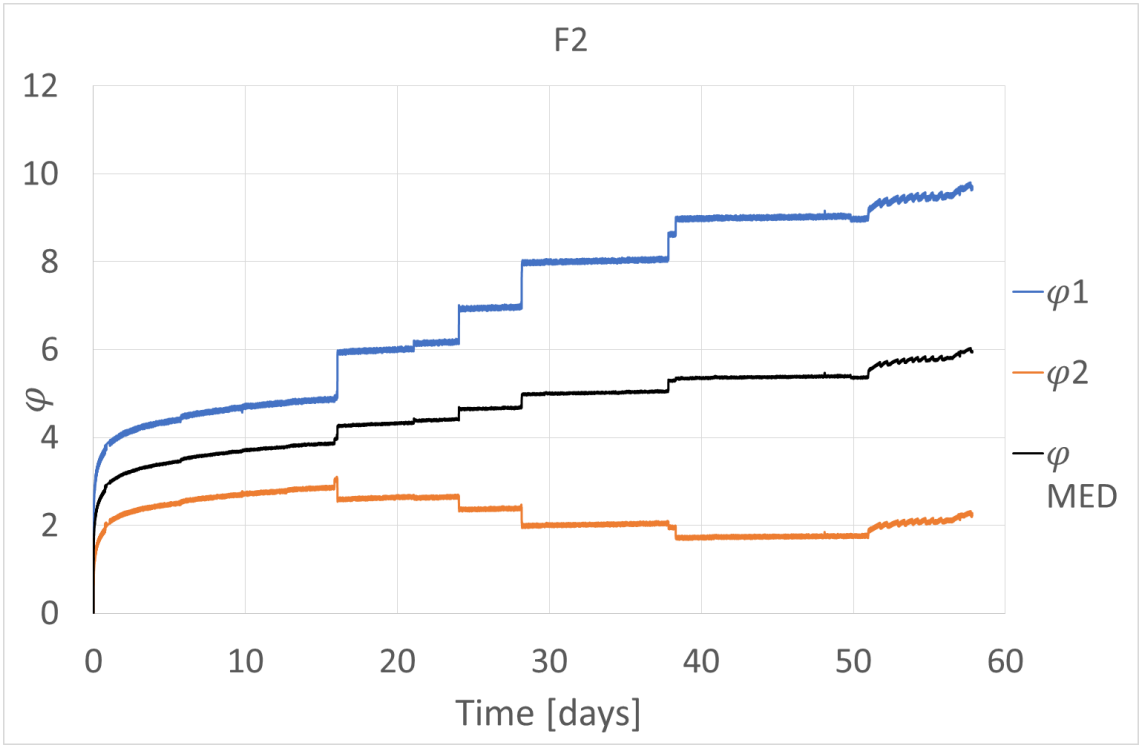

Figure 8.11- φ-Time F2

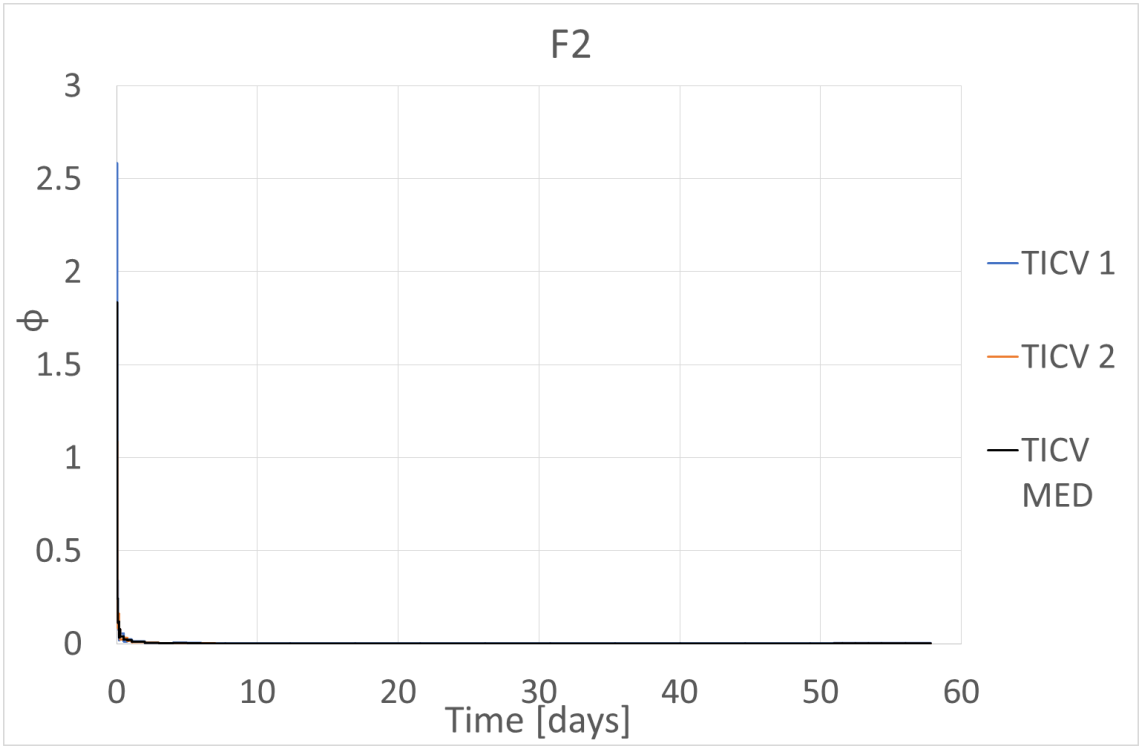

Figure 8.12-Rate of increase-Time F2

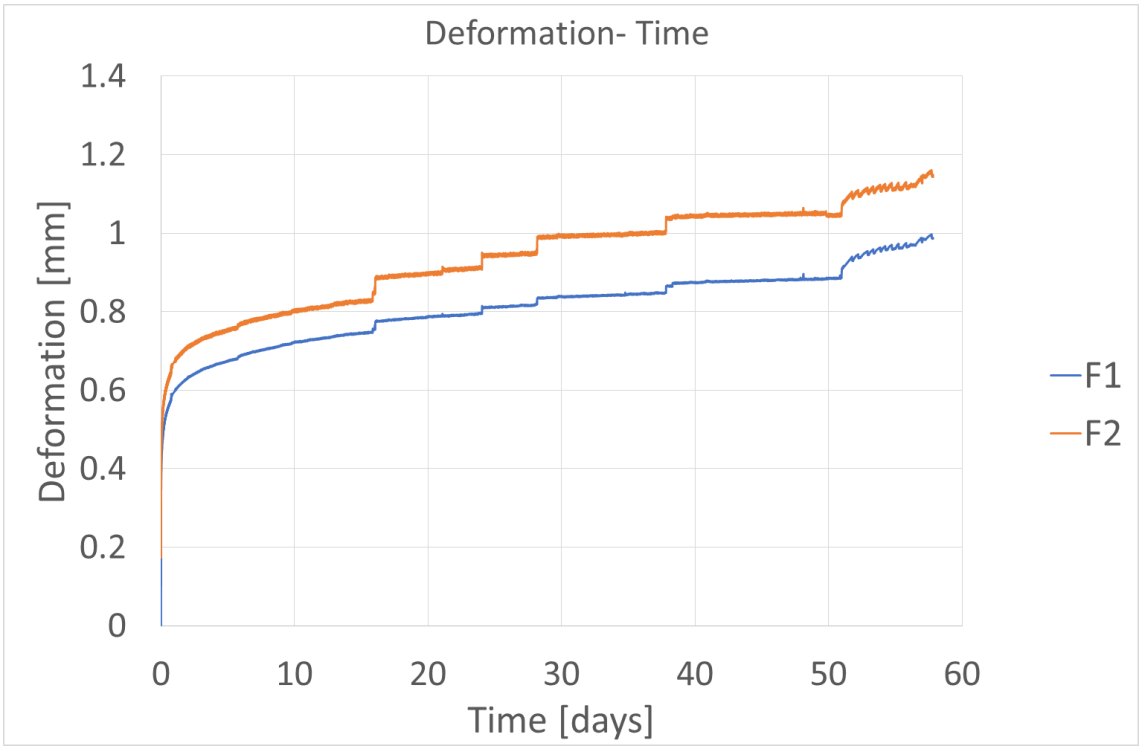

Figure 8.13-Deformation-Time of the average of the fibres

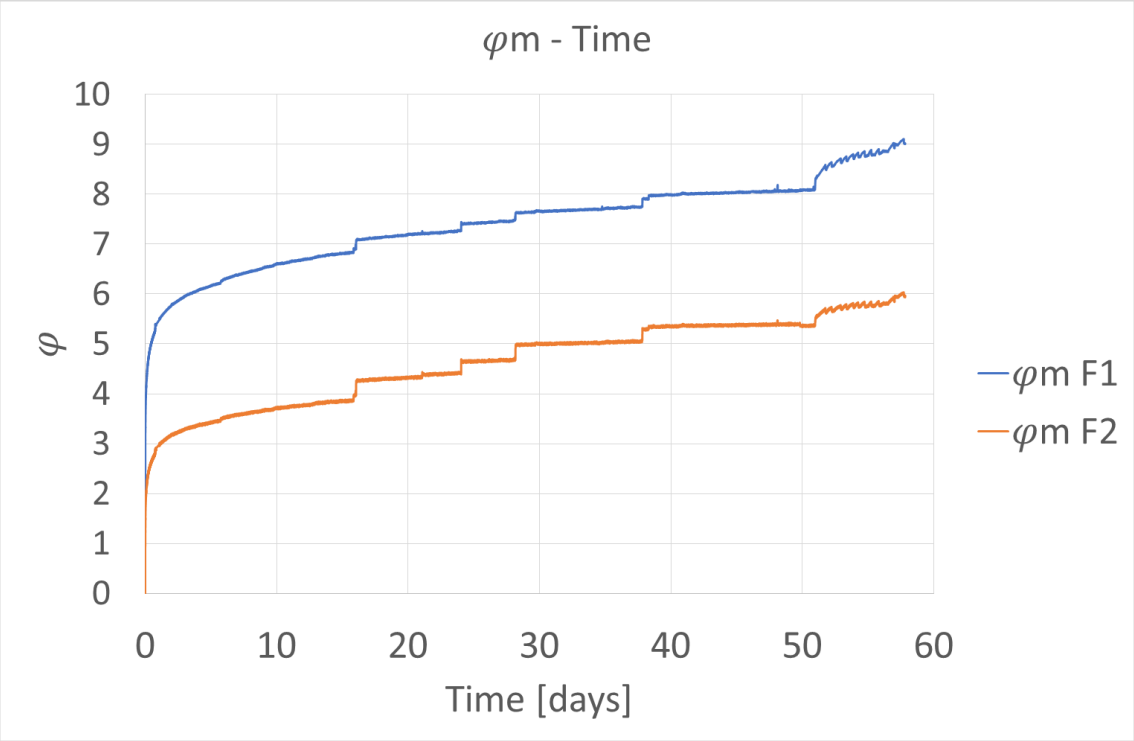

Figure 8.14-φ-Time of the average of the fibres

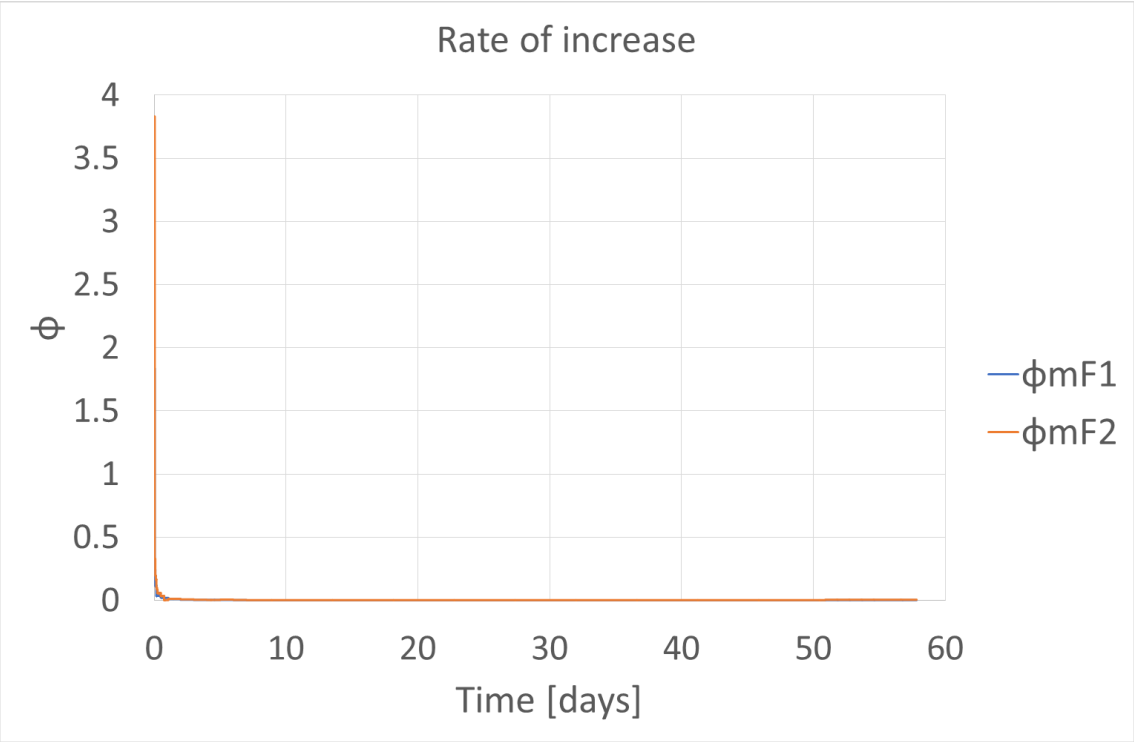

Figure 8.15-Rate of increase-Time of the average of the fibres

Finally, the elastic modulus of both fibres are calculated in the table 8.2.

	ΔL [mm]	ε	σ 20% [MPa]	E[MPa]
Fibre 1	0.4	0.02	89	4450
Fibre 2	0.5	0.025	89	3560

Table 8.2-Elastic modulus for fibres in long-term

9. Conclusions

A significant deal of research has been focused, in recent years, on the characterization the long-term behaviour of FRC elements in cracked conditions. Even if different researchers are converging on similar testing protocols the following main conclusions can be drawn from the literature review presented by the present thesis:

- Creep can be visible both on the whole material and on the single fibres as polymers.
- Analyzing the creep coefficient it possible say that increase over time and it has a significant increasing when the temperature is higher.
- Standard testing protocols, and relationship among main deformation parameters, need to be developed in order to allow an easier comparison of results and to facilitate discussion among researchers.
- The extent to which parameters such as creep load ratio, crack opening at the beginning of the long-term test, temperature and relative humidity influence the behaviour of FRCs has not yet been fully defined.
- Chemical, physical and mechanical phenomena governing creep of FRCs in cracked conditions have no yet been fully understood.
- Inverse analysis procedures are most probably required for the interpretation of long-term bending tests.
- Prediction models for FRC creep in cracked conditions and in particular for tensile creep are not yet available but are needed if these phenomena are to be included in design.
- In order to include the characterization of the FRC in the standard, a greater number of tests must be carried out.

10.References

(2000). *116R-90: Cement and Concrete Terminology.*

544, A. C. (2010). *Report on the Physical Properties and Durability of Fibre-Reinforced Concrete.*

544.1R, A. (1996). *State-of-the-Art Report on Fibre Reinforced Concret* . Farmington Hills, MI.

Arango, S., Serna, P., Martí-Vargas, J., & García-Taengua, E. (2011). *A Test Method to Characterize Flexural Creep Behaviour of Pre-cracked FRC Specimens.*

Babafemi, A. J. (2015). *Tensile Creep of Cracked Macro Synthetic Fibre Reinforced Concrete.*

Babafemi, A., & Boshoff, W. (2015). *Tensile creep of macro-synthetic fibre reinforced concrete (MSFRC) under uni-axial tensile loading.*

Bayasi, M. Z., & Soroushian, P. (1992). *Effect of Steel Fibre-Reinforcement on Fresh Mix Properties of Concrete.* ACI Materials Journal.

Báyszko, J. (2017). *Comparative analysis of creep in standard and fibre reinforced oncretes under different load conditions.* Szczecin: West Pomeranian University of Technology Szczecin.

Bentur, A., & Mindess, S. (2007). *Fibre reinforced cementitious composites.*

Buratti, N., & Mazzoti, C. (2016). *Creep Testing Methodologies and Results Interpretation.* Valencia.

Buratti, N., & Mazzotti, C. (2016). *Experimental tests on the long-term behaviour of SFRC and MSFRC in bending and direct tension.* Vancouver.

Collepardi, M., & Coppola, L. (1996). *Materiali Innovativi per Calcestruzzi Speciali.* Editore Enco.

di Prisco, M., Plizzari, G., & Vandewalle, L. (2009). *Fibre reinforced concrete new design perspectives. Journal of Materials and Structures.*

EFNARC. (2002). *Specification and guidelines for self-compacting concrete. Surrey, UK: European Federation of Suppliers of Specialist Construction Chemicals.*

Fall, D. (2014). *Steel Fibres in Reinforced Concrete Structures.* Gothenburg: CHALMERS UNIVERSITY OF TECHNOLOGY.

Fibre Reinforced Concrete Asociation. (03 de 05 de 2018). Obtenido de http://fibrereinforcedconcrete.org/fibre-reinforced-concrete/applications/

Hughes, B., & Fattuhi, N. (1976). *Workability of Steel Fibre Reinforced Concrete.* Magazine of Concrete.

Istruzioni per la Progettazione, l'Esecuzione ed il Controllo di Strutture di Calcestruzzo Fibrorinforzato. (Febbraio de 2008). Roma.

Kormeling, H. A., Reinhardt, H. W., & and Shah, S. P. (1980). *Static and Fatigue Properties of Concrete Beams Reinforced with Continuous Bars and with Fibres.* ACI JOURNAL.

Kurtz, S., & Balaguru, P. (s.f.). *Postcrack creep of polymeric fibre-reinforced concrete in flexure.*

Lau, A., & Anson, M. (2006). Effect of high temperatures on high performance steel fibre reinfoced concrete.

Löfgren, I. S. (2005). *Fracture properties of FRC determined through inverse analysis of wedge splitting and three-point bending tests.*

MacKay, J., & Trottier, J. (s.f.). *Post-crack creep behaviour of steel and synthetic FRC under flexural loading.*

Mangat, P. S., & Azari, M. M. (s.f.). *Compression creep behaviour of steel fibre reinforced cement composites.* Marischal College, Aberdeen, U.K. : Department of Engineering, University of Aberdeen, .

Mangat, P. S., & Swamy, R. (1974). *Compactibility of Steel Fibre-Reinforced Concrete.*

Mansour, A., Srebic, J., & and Burley, B. J. (2007). Developement of Straw-Cement Composite Sustainbale Buiding Material for Low-Cost Housing in Egypt. 1571-1580.

Naaman, A. E., Wongtanakitcharoen, T., & Hauser, G. (2005). *Influence of Different Fibres on Plastic Shrinkage Cracking of Concrete.*

Parveen, A. S. (2013). *Structural Behaviour of Fibrous Concrete Polypropylene Fibres.*

PS, M., & M, M. (1986). *Compression creep behaviour of steel fibre reinforced cement composites.*

Ramakrishna, G., & Sundararajan, T. (2005). *Studies on the durability of natural fibres and the effect of corroded fibres on the strength of mortar.*

Ramakrishnan, V., Gollapudi, S., & and Zellers, R. (1987). *Performance Characteristics and Fatigue of Polypropylene Fibre Reinforced Concrete.* Detroit: American Concrete Institute.

Richardson, A., & Ovington, R. (2017). Performance of fibre concrete with regard to temperature.

The constructor . (30 de 06 de 2018). Obtenido de https://theconstructor.org/concrete/rheology-of-concrete/15319/

UNE-EN. (2006). *Fibras para el hormigón.*

van Mier, J., & van Vliet, M. (2002). Uniaxial tension test for the determination of fracture parameters of concrete: state of the art. 1195–1206.

Wafa, F. F. (1990). *Properties and Applications of Fibre Reinforced Concrete.*

Zerbino, R., Monetti, D., & Giaccio, G. (s.f.). *Creep behaviour of cracked steel and macromacrosynthetic.*